OXIDATIVE STRESS EFFECTS OF AN INDIGENOUS TOBACCO PRODUCT (*TUIBUR*): *AN IN VITRO STUDY*

A THESIS SUBMITTED IN PARTIAL FULFILLMENT OF THE REQUIREMENTS FOR THE DEGREE OF DOCTOR OF PHILOSOPHY

LALRINHLUPUII

MZU REGISTRATION NO. : 1506941

Ph.D. REGISTRATION NO. : MZU/Ph.D./1007 OF 15.05.2017

DEPARTMENT OF CHEMISTRY

SCHOOL OF PHYSICAL SCIENCES

FEBRUARY, 2025

OXIDATIVE STRESS EFFECTS OF AN INDIGENOUS TOBACCO PRODUCT (*TUIBUR*): *AN IN VITRO STUDY*

BY

LALRINHLUPUII

Department of Chemistry

Under the supervision of

Prof. MUTHUKUMARAN R.

and joint-supervision of

Prof. G. GURUSUBRAMANIAN

Department of Zoology

Submitted

In partial fulfillment of the requirement of the Degree of Doctor of Philosophy in Chemistry of Mizoram University, Aizawl.

MIZORAM UNIVERSITY

Department of Chemistry

Thesis Certificate

This is hereby certified that the research work for the dissertation entitled "**Oxidative Stress Effects of an Indigenous Tobacco Product (*Tuibur*): An *in vitro* study**" submitted by ***Ms. Lalrinhlupuii*** to Mizoram University, Tanhril, Aizawl, for the award of the Degree of Doctor of Philosophy in Chemistry is *bona fide* record of the research work carried by under my supervision. The contents of this dissertation, in full or in parts, have not been submitted to any other Institute or University for the award of any degree or diploma.

Tanhril, Aizawl-04
Date:

Prof. Muthukumaran R.
Department of Chemistry
Supervisor

Prof. Gurusubramanian
Department of Zoology
Joint-Supervisor

Tanhril Campus, Aizawl 796 004. Phone: 94363 52161
Fax: (0389) 233 0834 E-mail: rsic15@gmail.com

Declaration of the Candidate

Mizoram University

February, 2025

I, **Lalrinhlupuii**, hereby declare that the subject matter of this thesis is the record of work done by me, that the contents of this thesis did not form basis of the award of any previous degree to me or to do the best of my knowledge to anybody else, and that the thesis has not been submitted by me for any research degree in any other University/ Institute.

This is being submitted to the Mizoram University for the degree of Doctor of Philosophy in Chemistry.

(LALRINHLUPUII)
Candidate

(Prof. N. MOHONDAS SINGH)
Head

(Prof. MUTHUKUMARAN R.)
Supervisor

(Prof. G.GURUSUBRAMANIAN)
Joint Supervisor

DEDICATION

To my grandmother.

ACKNOWLEDGEMENT

To my revered supervisor, ***Prof. Muthukumaran R.***, Professor, Department of Chemistry, Mizoram University, Tanhril, Aizawl, I extend my heartfelt gratitude. His visionary guidance, profound knowledge, and unwavering commitment have been pivotal to the conception and realization of this research. His mentorship, characterized by dedication, protectiveness, and an inspiring zest for life, has left an indelible mark on both my academic and personal growth. The traits he embodies are truly admirable and qualities I aspire to emulate.

I also wish to express my appreciation to ***Prof. Suman Rai***, Dean, School of Physical Sciences, Mizoram University. His invaluable encouragement and support have greatly contributed to the successful culmination of my research endeavors within the School.

To the esteemed teaching faculty of the Department of Chemistry, Mizoram University, including ***Prof. N. Mohondas Singh,*** Head of Department, ***Prof. Diwakar Tiwari, Dr. Zodinpuia Pachuau, Dr. A. Bimolini Devi***, ***Dr. Lalrempuia, Dr. Joydeep Das, Dr. Manjeet Singh, Dr. G Rajendra Kumar*** and non-teaching staff, I extend my profound thanks or their unwavering assistance throughout my research journey. I am equally grateful to my joint supervisor ***Prof. G. Gurusubramanian***, Department of Zoology, Mizoram University, for his invaluable contributions to my work.

I am profoundly indebted to ***Prof. Mu-Rong Chao*** and his team of researchers, Department of Occupational Safety and Health, Chung Shan Medical University, Taichung; ***Dr. Dulal Senapati*** and his scholars, Chemical Sciences Division, Saha Institute of Nuclear Physics, Kolkata; ***Dr. Pritha Battacharjee*** and her team, Department of Environmental Science, University of Calcutta, Kolkata; and ***Prof. N. Senthil Kumar***, Department of Biotechnology, Mizoram University, for

their indispensable guidance, expert opinions, and access to research facilities, which significantly enriched the quality of my work. My sincere appreciation also extends to ***Mr. Lalbiaktluanga*** and ***Prof. Hranghmingthanga***, Department of Physics Mizoram University for their cooperation, I am truly appreciative.

To my lab-mates, ***Rammawia, Ananya***, ***Nanaua, Bomngam***, ***Mesti*** and ***Nikrang***, I am immeasurably grateful for their camaraderie, support and encouragement. Their friendship and reassurance lightened the burdens of the challenges encountered during this journey. Sharing this path with them has been a privilege. I am equally indebted to my fellow research scholars of the Department of Chemistry for their cooperation and support.

I acknowledge with gratitude the financial assistance provided by Department of Biotechnology (DBT), New Delhi and Mizoram University through research funding and fellowship, which were instrumental in facilitating this work .

With immense joy and humility, I express my deep gratitude to **my family and my dear friends** for their enduring love, prayers, and unwavering faith in me. Their support has been my greatest source of strength and inspiration, and I am forever indebted to them for their profound impact on my life and achievements.

To God Almighty, I humbly express my profound gratitude for His boundless blessings: the priceless gift of health, the wisdom to endure with resilience, and the steadfast support system that has sustained me throughout this journey.

(LALRINHLUPUII)

TABLE OF CONTENTS

Title of the Thesis

Certificate

Declaration of the Candidate

Dedication

Acknowledgement v

Table of Contents vii

List of Tables x

List of Figures xi

Abbreviations xiv

CHAPTER 1

1. INTRODUCTION AND REVIEW OF LITERATURE.

1.1. An account on Smokeless Tobacco Products (SLT). 1

1.2. Indigenous tobacco products of Mizoram – Tuibur. 5

1.3. The Tobacco plant. 8

1.3.1.Some tobacco alkaloids. 12

1.3.2. Other chemical components of interest**.** 18

1.4. Consequences of the tobacco industry. 23

1.5. Oxidative stress. 25

1.6. Spectroscopic and analytical techniques. 30

1.7. Cell lines as model systems. 35

1.8. Bioactivity Assays. 38

CHAPTER 2

2. MATERILAS AND METHODS.

2.1. Tuibur manufacturing. 47

2.2. Sample Collection. 51

2.3. Chemical analysis using ATR-FTIR. 52

2.3.1. Standard Samples. 53

2.3.2. Sample Preparation. 53

2.2.3. ATR - FTIR Spectral measurement. 53

2.3.4. Multivariate Analysis using Chemometrics. 54
2.3.5. Standard Solution Calibration and Validation models. 54
2.4. Nicotine characterization using SERS. 55
2.4.1. Synthesis of spherical-shaped gold nanoparticle. 55
2.4.2. Sample preparation and spectral data collection. 55
2.4.3. Statistical Analysis. 56
2.5. Alkaloid concentration estimation using LC-MS/MS. 56
2.5.1. Sample preparation and LC-MS/MS analysis. 57
2.5.2. Statistical analysis. 57
2.6. Assessment of oxidative stress effects of Tuibur. 58
2.6.1. Micronucleus assay on buccal epithelial cells. 58
2.6.1 (a). Sample collection, preparation and dual staining. 58
2.6.1 (b). Statistical analysis. 58
2.6.2. Choosing cell line as a model system. 59
2.6.3. Cell seeding. 60
2.6.4. MTT Assay for Cell Viability. 60
2.6.4 (a). Cell viability. 61
2.6.4 (b). Statistical analysis. 62
2.6.5. ELISA for oxidative stress assessment. 62
2.6.5 (a) Cell Lysate Preparation. 62
2.6.5 (b) Total Antioxidant Capacity (TAC) Assay. 62
2.6.6. DCFDA (ROS generation) Assay. 64
2.6.7. Griess Assay for Nitrite determination. 64
2.6.8. Acridine Orange/Ethidium Bromide (AO/EB) Staining for Apoptosis. 66

CHAPTER 3

2. CHEMICAL CHARACTERIZATION AND OXIDATIVE STRESS RELATED BIOLOGICAL ACTIVITY OF TUIBUR.

3A. Chemical characterization of Tuibur. 67
3A.1. pH. 67
3A.2. Characterization of different grades of Tuibur samples using FT-IR. 68

3A.2.1. Identification of significant region of the ATR-FTIR spectra for analysis. 72
3A.2.2. Calibration models for quantitative analysis of nicotine, hydroquinone and benzoquinone. 73
3.A.2.3. Chemical analysis of tuibur samples using PLS model. 74
3A.3. Nicotine characterization using SERS. 75
3A.4. LC- MS/MS quantification of tobacco specific alkaloids in tuibur. 80
3A.5. Discussion. 83
3B. Biological Activity of Tuibur. 92
3B.1. Tuibur oxidative stress biomarker assessment. 92
3B.2. *In vitro* cytotoxicity screening via MTT assay. 95
3B.2.1. Tuibur cytotoxicity. 95
3B.2.2. Nicotine cytotoxicity. 97
3B.2.3. Hydroquinone cytotoxicity. 99
3B.2.4. Potassium Nitrate (KNO_3) cytotoxicity. 101
3B.2.5. Sodium Nitrite ($NaNO_2$) cytotoxicity. 103
3B.3. Effect of tuibur exposure on Total Antioxidant Capacity (TAC). 105
3B.4. Effect of tuibur treatment on intracellular ROS production. 106
3B.5. Effect of tuibur treatment on cellular NO_x level in AGS cell line. 108
3B.6. Tuibur treatment induced apoptosis. 109
3B.7. Discussion. 111

CHAPTER 4

4. SUMMARY AND CONCLUSION. 123
REFERENCES 131
Bio Data
List of Publications
Conferences and Symposiums
Particulars of the Candidate

LISTS OF TABLES

Table	Title	Page
1.1.	List of Smokeless Tobacco Products (SLT).	2
2.1.	List of tuibur samples collected.	52
2.2.	Trolox standard solution preparation.	63
2.3.	Nitrite standard solution preparation.	65
3.1.	pH of grades of tuibur samples collected at different production sites in Mizoram, India.	67
3.2.	ATR-FTIR spectral data of nicotine, hydroquinone, benzoquinone and tuibur.	71
3.3.	R^2– values for PLS models using different spectral regions of chemical standard spectra.	72
3.4.	Chemometric analysis of chemicals using significant spectral regions.	73
3.5.	Outcome of the predicted concentration in tuibur samples using standard chemical calibration models.	74
3.6.	Pearson's correlation of pH vs. Peak Intensity of tuibur sample.	79
3.7.	Pearson's Correlation of Peak Intensity vs. Concentration of tuibur samples.	79
3.8.	Concentration of tobacco specific alkaloids – Nicotine and Cotinine, in tuibur (T1 – T10).	80
3.9.	Pearson's correlation between amount of tobacco used and concentration of alkaloids (LC-MS/MS).	82
3.10.	Calculated unprotonated nicotine concentration of tuibur samples.	83
3.11.	Characteristics of the three groups under study.	93
3.12.	Mean micronuclei count in the three study groups.	93
3.13.	Multiple comparisons of mean MN in the three study groups.	94
3.14.	AGS cell scoring for normal, early-stage and late-stage apoptosis, n=1000 cells/well. The data is presented as mean ± SD, n=3.	110

LISTS OF FIGURES

Fig. No.	Title	Page
1.1.	Native American Tobago pipe.	1
1.2.	Vintage Snuff boxes.	1
1.3.	(a) Vaibel; (b) Zozial.	5
1.4.	Tuibur (waterpipe).	6
1.5.	(a) *Nicotiana tabacum;* (b) *Nicotiana rustica.*	9
1.6.	Cured tobacco leaves.	10
1.7.	S (-) – Nicotine.	13
1.8.	Cotinine.	15
1.9.	Nornicotine.	16
1.10.	Metabolism of nicotine to cotinine and nornicotine.	18
1.11.	Tobacco specific nitrosamines (TSNAs).	20
1.12.	Hydroquinone to p-benzoquinone conversion with intermediate.	21
1.13.	Types of adherent cells. (a) Epithelial; (b) Endothelial; (c) Neuronal; and (d) Fibroblast.	36
1.14.	Reduction of MTT tetrazolium salt to MTT formazan crystal.	39
1.15.	Schematic representation of types of ELISA.	41
1.16.	Jablonski diagram.	43
2.1.	Tuibur Manufacturing setup.	48
2.2.	Ching al preparation.	49
2.3.	(a) Smouldering tobacco stalk inside tuibur lu; (b) Tuibur manufacturing apparatus; (c) Water source; (d) Tuibur factory; (e) Bottled Tuibur.	50
2.4.	Collected Tuibur samples.	51
3.1.	ATR-FTIR spectra of Nicotine, Hydroquinone and Benzoquinone standard (neat) samples.	69
3.2.	ATR-FTIR spectra of 10 tuibur samples of different grades.	70
3.3.	PLS calibration model plots of (a) Nicotine, (b) Hydroquinone and (c) Benzoquinone.	73
3.4.	SERS spectrum of nicotine standard solution.	76
3.5.	SERS spectra of tuibur samples with AuNP colloidal solution.	77
3.6.	Peak Intensity at 1030 cm^{-1} of nicotine standard and tuibur solutions.	78

List of figures (continued)

3.7. (a)Linear regression plot for Amount of tobacco vs. Nicotine. 81

3.7. (b)Linear regression plot for Amount of tobacco vs. Cotinine. 81

3.8. Structure of (a) unprotonated nicotine, (b) mono-protonated nicotine, and (c) di-protonated nicotine. 84

3.9. (a)Normal buccal epithelial cell; (b) Buccal epithelial cell with micronucleus. 93

3.10. Comparison of MN frequency in control and smokeless tobacco user populations. 93

3.11. Cytotoxicity of tuibur on AGS cell line. Cells were exposed to tuibur in concentration ranging from 0 to160 µg/µL for 24, 48 and 72 hrs. Cell viability was determined using MTT assay. The data presented are shown as mean ± S.E, n = 3. 95

3.12. Kinetics plot of tuibur treated AGS cells. Data presented as log[tuibur] vs. % absorbance for evaluating IC_{50}. 96

3.13. Effect of incubation time on IC_{50} (µg/µL) values of tuibur exposed AGS cells after 24, 48, and 72 h, respectively, in cell counting assay. 96

3.14. Cytotoxicity of nicotine on AGS cell line. AGS cells viability after 24, 48 and 72 h treatment with the dosage of nicotine ranged from 0 to 0.0032 µg/µL. The data were presented as mean ± S.E, n = 3. 97

3.15. Kinetics of nicotine cytotoxicity on AGS cells. Cells were observed by relative absorbance and IC_{50} value for nicotine was calculated. The data are presented as mean ± S.E, n = 3. 98

3.16. Time evolution of IC_{50} (µg/µL) values of nicotine in AGS cells with increasing incubation times (24, 48 and 72 h). Bars represent mean±SEM for 3 replicates. 98

3.17. Cytotoxicity of hydroquinone on AGS cell line. The cells were exposed to hydroquinone doses ranged between 0 to 0.16 µg/µL for 24, 48 and 72 h, respectively. Cell viability was measured using MTT assay. The data presented are mean ± S.E, n = 3. 99

List of figures (continued)

3.18. Concentration-response curve for hydroquinone exposure to AGS cells after 24, 48 and 72 h incubation, respectively. The data are presented as mean ± S.E, n = 3. 100

3.19. The histogram depicting the time evolution of IC_{50} values of hydroquinone in AGS cells. MTT Assay was applied to measure the proliferation inhibition rate of hydroquinone. Bars represent mean±SEM for 3 replicates. 100

3.20. Dose-response curve for the growth inhibition activity of potassium nitrate at various incubation times (24, 48, and 72 h) with increasing concentrations of KNO_3. Growth inhibition of AGS cells was assessed by MTT assay. The data presented are depicted as mean ± S.E, n = 3. 101

3.21. Dose-response curve of potassium nitrate exposure to AGS cells with varying incubation periods (24, 48, and 72 h). The data are presented as mean ± S.E, n = 3. 102

3.22. Effect of incubation time on IC_{50} values of KNO_3 exposure to AGS cells after 24, 48 and 72 h and MTT assay was applied for calculating the growth inhibition rate of KNO_3. Bars represent mean ± SEM for 3 replicates. 102

3.23. Dose-response curve for the putative cytotoxic effects of $NaNO_2$ on AGS cells using MTT assay. The resulting growth inhibition data is represented as mean ± S.E, n = 3. 103

3.24. Growth altering effects of $NaNO_2$ with AGS cells on exposure to increasing concentrations of $NaNO_2$. Growth modulation(s) were assessed by MTT assay and IC_{50} values were calculated. The data are represented as mean ± S.E, n = 3. 104

3.25. Effect of incubation time on IC_{50} (µg/µL) values of $NaNO_2$ exposure to AGS cells using MTT assay. Bars represent mean ± SEM for 3 replicates. 104

3.26. Total Antioxidant capacity of tuibur, nicotine, hydroquinone and potassium nitrate treated AGS cell line. the data are presented as mean±S.D, n=3. 105

List of figures (continued)

3.27. Fluorescence intensity change in DCFDA stained cells using FACS; (a) % ROS in H_2O_2 treated cells; (b) % ROS in tuibur treated cells; (c) % ROS in nicotine treated cells; (d) % ROS in hydroquinone treated cells; (e) % ROS in KNO_3 treated cells. (Black indicates unstained control cells, red indicates stained control cells and green indicates stained chemical treated cells). 107

3.28. Degree of % change in intracellular ROS production in control and treated AGS cells. The data is presented as mean ± S.D., n=2. 107

3.29. Comparison of NO_x levels in AGS cells exposed to tobacco smoke components. NO_x species levels as nitrite ion content was determine by Greiss Assay. The data are presented as mean ± S.D., n = 3. 108

3.30. (a) Normal AGS cells, (b) early-stage apoptotic (white arrows) and late -stage apoptotic (orange-red arrows) AGS cells. Cells magnified to 16X. 110

3.31. Frequency of apoptosis in control and treatment groups of AGS cell line. 110

3.32. Percentage apoptotic index (AI) in control and treatment groups of AGS cell line. 110

ABBREVIATIONS

8-OHdG	8-oxo-2′-deoxyguanosine
AAS	Atomic absorption spectrometry
AGS	Human Gastric Adenocarcinoma
A_{max}	Absorbance maximum
ANOVA	Analysis of variance
AO	Acridine orange
ATP	Adenosine triphosphate
ATR	Attenuated Total Reflectance
ATR-FTIR	Attenuated Fourier Transform Infrared spectroscopy
AuNP	Gold nanoparticle
BCA	Bicinchoninic acid
BCL-2	B-cell lymphoma 2

BSA	Bovine serum albumin
CAT	Catalase
CB	Coomassie brilliant blue G-250
CNS	Central Nervous System
CSF	Cerebrospinal fluid
DAMPs	Damage-associated molecular patterns
DCFH-DA/DCFDA	2',7'- dichlorofluorescin-diacetate
DMF	Dimethyl formamide
DMSO	Dimethyl sulfoxide
DHR123	Dihydrorhodamine 123
EB	Ethidium bromide
ELISA	Enzyme-linked immunosorbent assays
eNOS	endothelial nitric oxide synthase
EPR	Electron paramagnetic resonance
FACS	Fluorescence-activated cell sorter or Flow-activated cell sorting
FBS	Fetal Bovine Serum
FC	Flow cytometry
FCS	Fluorescence correlation spectroscopy
FID	Flame ionization detector
FISH	Fluorescent in situ hybridization
FLIM	Fluorescence lifetime imaging
FLOCK	Flow clustering without K
FRAP	Ferric ion reducing antioxidant power
FRAP	Fluorescence recovery after photobleaching
FRET	Fluorescence resonance energy transfer
FSC	Forward scattering of light
FT-IR	Fourier transform infrared spectroscopy
GABA	γ-aminobutyric acid
GATS	Global adult tobacco survey
GEC	Gingival epithelial cells
GPx	Glutathione peroxidase

GR	Glutathione reductase
GSH	Glutathione S-transferases
GST	Glutathione S-transferase genes
GTS	Green tobacco sickness
HDBRG	Havel Dee Bouxo Rio Grande
Hela	Henrietta Lacks cell line
HepG2	Human liver cancer
hGF	Human gingival fibroblast
HPLC	High-performance liquid chromatography
HR	hazard ratio
HSD	Honestly Significant Difference
HT29	Human colorectal adenocarcinoma
HTS	High throughput screening
HUAECs	Human umbilical artery endothelial cells
IARC	International Agency for Research on Cancer
IC_{50}	Half maximal inhibition concentration
ICMR-NCDIR	Indian Council of Medical Research – National Centre for Disease Informatics and Research
ICP-AES	Inductively-coupled plasma atomic emission spectroscopy
ICP-MS	Inductively-coupled plasma mass spectroscopy
IPA	Isopropanol
IR	Infrared
ISTDs	Stable isotope-labelled internal standards
K562	Chronic myelogenous leukemia cell line
KNO_3	Potassium nitrate
MCR5	Human diploid lung tissue
MDA	Malondialdehyde
MN	Micronuclei
MRM	Multiple reaction monitoring
MS	Mass spectrometry
mtDNA	mitochondrial deoxyribonucleic acid

MTS	3-(4,5-dimethylthiazol-2-yl)–5-(3-carboxymethoxyphenyl)-2-(4-sulfophenyl)-2H-tetrazolium
MTT	3-(4,5-dimethylthiazol-2-yl)-2,5-diphenyl tetrazolium bromide
m/z	Mass to charge ratio
NAA	Neutron activation analysis
NAB	N-nitrosoanabasine
nAChRs	Nicotinic acetylcholine receptors
NADPH	Nicotinamide adenine dinucleotide phosphate
$NaNO_2$	Sodium nitrite
NAT	2,3-naphthotriazole
NAT	N-nitrosoanatabine
NED/NEDA	N-naphthyl-ethylenediamine
NB4	Acute promyelocytic leukemia cell line
NCCS	National Centre for Cell Science
NCDIR	National Centre for Disease Informatics and Research
NCs	Synthesized trypsin-Cu nanoclusters
NCI-H292	Human adenocarcinoma lung epithelial cells
NED/NEDA	N-naphthyl-ethylenediamine
NFSHRb	Non-familial sporadic heritable retinoblastoma
NIR	Near infrared
NNAL	N-nitrosoanatabine (NAT) and 4-(methylnitrosamino)-1-(3-pyridyl)-1-butanol
NNK	4-(methyl nitrosamino)-1-(3-pyridyl)-1-butanone
NND	*N*-demethylase
NNN	N-nitrosonornicotine
NO	Nitric oxide
NO_2	Nitrogen dioxide
NO_3-N	Nitrate nitrogen
NOS	Nitric oxide synthase
NO_x	Nitrogen oxide

NSAR	N-nitrososarcosine
Nuli1	Human epithelial normal bronchial cells
O.D.	Optical density
$ONOO^-$	Peroxynitrite
OR	Odds ratio
ORAC	Oxygen radical antioxidant capacity
OSRDs	Oxidative stress related diseases
PABA	Para-aminobenzoic acid
PAHs	Poly aromatic hydrocarbons
PBS	Phosphate buffer saline
PCA	Principal component analysis
PLS	Partial Least Square
PUFAs	Polyunsaturated fatty acids
QH	Semiquinone
QH_2	Hydroquinone
RAJI	Human B lymphoblastoid cell line
RAW 264.7	Mouse macrophage-like cell line
RIPA	Radioimmunoprecipitation assay
RNA	Ribonucleic acid
RNS	Reactive nitrogen species
ROA	Raman Optical Activity
ROS	Reactive oxygen species
RTK	Receptor tyrosine kinase
S.D.	Standard deviation
SDS	Sodium dodecyl sulphate or sodium lauryl sulphate
SEAR	South-East Asia Region
S.E./SEM	Standard error mean
SEC	Standard error of calibration
SEP	Standard error of prediction
SERS	Surface enhanced Raman Spectroscopy
SLT	Smokeless Tobacco Products
SOD	Superoxide dismutase

SPADE	Spanning-tree progression analysis of density-normalized events
SSC	Side scattering
TAC	Total antioxidant capacity
TEAC	trolox equivalence antioxidant capacity
TID	Thermal ionization detector
TIRF	Total internal reflection fluorescence
TPM	Total particulate matter
TSC	Trisodium citrate
TSNA	Tobacco-specific nitrosamines
tSNE	t-Distributed Stochastic Neighbor Embedding
U-937	Pro-monocytic cell line
USEPA	United States Environmental Protection Agency
Uv-vis	Ultraviolet-visble
WHO	World Health Organization
WST-1	Water-soluble tetrazolium salt
XTT	2,3-bis-(2-methoxy-4-nitro-5-sulphenyl)-(2H)-tetrazolium-5-carboxanilide

CHAPTER 1

INTRODUCTION

AND

REVIEW OF LITERATURE

CHAPTER 1

INTRODUCTION AND REVIEW OF LITERATURE

1.1. An account on Smokeless Tobacco Products (SLT).

Prior to the arrival of Columbus and his crew of sailors to America in fifteenth century, tobacco chewing was a common practice among the native Americans. A Y-shaped pipe called "Tobago/Tobaca" (Figure 1.1.), was used by the indigenous Americans to inhale powdered tobacco. Different tribes of the native Americans also chewed green as well as dried tobacco to subdue hunger, relieve toothache, quench thirst and to suppress fatigue. Lime or burned finely powdered molluscs were also mixed with chewing tobacco. British naval sailors used to chew tobacco in their vessels when smoking was forbidden. During the early to mid-1900s, chewing tobacco became vastly popular in the United States of America in the form of a twist, sweet plug and snuff (International Agency for Research on Cancer, 2007a).

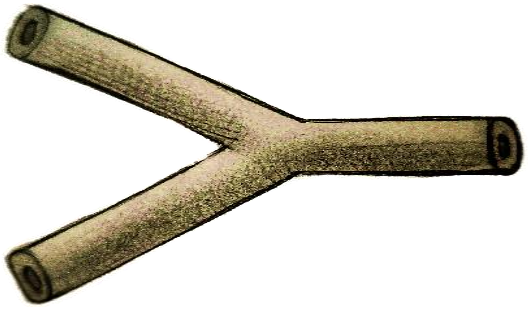

Figure 1.1. Native American Tobago pipe.

"Snuff" was first known to be used by the native Brazilians though the Dutch were responsible for naming it. By the first half of the 1600s, the use of snuff had become widespread throughout Africa, Japan, China and South America. In the 1650s, the use of snuff spread out across Japan and China in the Ching Dynasty. Snuff use was also prevalent in France, England, Ireland and Scotland. In Europe, among the many varieties of snuff products, Scotch snuff (dry), Maccaboy (moist) and Rapee or French snuff (dry) were the three major types during the 1800s (Figure 1.2) (Encyclopedia Britannica, 2018; Sanchez-Ramos, 2020).

Figure 1.2.Vintage Snuff boxes.
(Photo Credit: Smithsonian Museum.)

With the introduction of tobacco into South Asia, it gradually morphed into different forms of products besides smoking. Tobacco also became an added ingredient of pan (chewing betel quid), a 2000-year long practise that existed in South Asia and straddling the South Pacific Islands. As of 2021, India ranked second worldwide with 757.51 thousand metric tons in tobacco production trailing behind China which is leading the global tobacco production by 2127.6 thousand metric tons (Shahbandeh, 2023). By virtue of ever-expanding consumer base, the tobacco industry is a lucrative business with an interminable market. Presently, the use of smokeless tobacco (SLT) have evolved tremendously catering to the needs of its users across the globe. Various products including the previously mentioned snuff and pan, such as zarda, mishri, gutkha, snus, khaini, plug, toombak, khiwam, loose-leaf, iq'mik etc. are available for purchase including more modern forms like dissolvable tobacco products (Table 1.1.). These SLTs are usually used orally by sucking or chewing as well as employing other forms of oral intake besides consumption using the nasal passage.

Table 1.1. List of Smokeless Tobacco Products (SLT).

Type	**Name**	**Description**	**Mode of use**
SLT without additives	Plug	Burley tobacco and bright or cigar tobacco immersed in sweetener (liquorice or sugar) covered by a wrapper leaf	Chewed, spat or swallowed
	Loose leaf	Air-cured tobacco, loosely packed strips of shredded tobacco	Chewed or held in place between the lower lip and cheek
	Roll/Twist	Aged tobacco leaves twisted in a similar fashion to a rope	Cut and placed/held between the cheek and gums
	Dry Snuff	Fire-cured, powdered tobacco	Used nasally as well as orally
	Moist/ Creamy Snuff	Aged and fermented tobacco, made into fine particles	A pinch or dip is placed between the cheek and gums
	Snus	Snuff pre-packaged in pouches	The pouch is placed between the cheek and gums
	Mishri	Baked, toasted powered tobacco	Held in the mouth after application on the teeth and gums
	Tuibur	Tobacco-smoke infused water, liquid tobacco product	Held in the mouth and spat out after a few minutes
SLT	Khiwam	Paste made of tobacco leaf extract with spices and other additives e.g., musk	Chewed

	Iq'mik	Fire-cured tobacco, mixed with punk ash	A small amount is pinched and chewed
	Rapee	Dried tobacco leaves flavoured with clove, tonka bean, camphor, cinnamon powder and ash of selected trees	Inhaled nasally
	Gudhakhu	Paste made from powered tobacco and molasses	Applied by finger to the gums and teeth
	Maras	Powdered tobacco, mixed with wood ash (oak, walnut, grapevine)	Placed between the inner lining of the lips and the gums
	Naswar	Sun-dried (partially cured), powdered tobacco mixed with ash, oil colouring agents and other additives like slaked lime, menthol, cardamom etc. rolled into balls.	Placed under the tongue and sucked
	Red tooth powder	Red finely powdered tobacco with an assortment of additives including herbs, camphor etc.	Applied onto the teeth and gums
	Shammah	Powdered tobacco with added oil, ash, lime, black pepper and flavouring ingredients	Placed in the inner lining of the cheeks or lips
	Toombak	Fermented tobacco (1 year) and baking soda at a ratio of 4:1	Rolled into a ball called *saffa,* placed under the tongue, between the gums and lip or cheek
	Chimó	Crushed boiled tobacco leaves mixed with additives like baking soda, brown sugar, vanilla, anisette flavouring and Mamón tree ash	Placed and held between the gums and lip or cheek
	Khaini	Coarsely cut sun-dried or fermented tobacco leaves mixed with slaked lime	Placed between the inner lip lining and gums
	Gul	Powdered tobacco with molasses and other additives	Applied to teeth and gums many times per day
	Zarda	Tobacco flakes flavoured with spices, menthol, saffron, raw khiwam, herbs, silver flakes	Used in pan, chewed alone or with areca nut
SLT with Areca nut	Pan	Betel leaf with areca nut, slaked lime and tobacco (raw, sun-dried or roasted)	Chewed and swallowed
	Gutka	Finely chopped sundried and roasted tobacco and areca nut mixed with slaked lime, catechu and other additives	Sucked and chewed and/or swallowed
	Kharra	Tobacco, areca nut, catechu, lime and other additives	Sucked and chewed
	Dhora	Moist mixture of tobacco with lime, areca nut, catechu, peppermint, cardamom	Sucked and chewed
	Mainpuri	Finely cut areca nut mixed with tobacco, slaked lime, cloves, cardamom, sandalwood and Kewara along with catechu	Sucked and chewed
Others	Dissolvable tobacco products	Tobacco with flavouring and preservatives made in the form of dissolvable pellets, mints, strips, sticks, etc.	Held in the mouth and dissolved

(IARC, 2007b; Lalmuanpuii, 2016; Stanfill et al., 2018, 2011; Stepanov et al., 2015; Muthukrishnan & Warnakulasuriya, 2018)

Accounting for more than 80 lakh deaths per year, the popularity of tobacco rarely seems to decline. More than 80% (~1.3 billion) of tobacco consumers live in lower and middle – income countries which contributes to added poverty due to the diversion of essential living expenses to tobacco (World Health Organisation, 2013). In the year 2000, the World Health Organization (WHO) reported that 32.7% (both sexes combined of adults aged 15 years and over) of the population worldwide were tobacco consumers. A 10.4% decline was seen within 20 years with 22.3% (7.8% of all women; 36.7% of all men) of the global populace still using tobacco in 2020. The global trend in the prevalence of tobacco consumption among adult users peak at the age group between 45 – 54 for men and 55 – 64 for women. The South-East Asia Region (SEAR) has the highest average prevalence rate with 29% of its masses using tobacco in 2020, as compared to other WHO regions. The number of adult male tobacco consumers rose in the past 20 years (2000 – 2020) in four regions under WHO, while the number of adult female users has been declining with a total of 1.298 billion estimated adult tobacco users in 2020 (World Health Organisation, 2021).

The average prevalence of smokeless tobacco consumption among adults (15 years and older) worldwide is estimated at 6.0% (8.5% male and 3.4% female) during the period of 2010 – 20. SEAR contributes the largest group of SLT users. On average, the prevalence rate of SLT in this region is 18.3% (both sexes) with an estimated 266.2 million adult smokeless tobacco users. As such, about 2.6%, which accounts for adolescents aged between 13–15 years, are reported to be currently using SLT products globally. Rate of SLT use is high in the SEAR and Eastern Mediterranean region where 4.7% of adolescent males each along with 2.9% and 3.1%, of adolescent females, respectively consume SLT products (World Health Organisation, 2021).

India being the 7th largest country in the world (largest country in South Asia) with a land area of 32,87,469 km^2 and accommodating the world's largest demography (1.4286 billion as on April, 2023), still ranks 5th place, with a percentage of 21% among the prime consumers of SLT worldwide, trailing behind Palau (51.3%), Myanmar (43.2%), Bangladesh (27.5%) and Marshall Islands (21.6%) (Elfein, 2022). According to the GATS 2 Fact Sheet (2017), India has an overall of 21.4% of current SLT consumers with 29.6% being male and 12.8% being female. The current tobacco

consumers in India comprises of 28.6% of the adult population ranging from age 15 and above which accounts for 266.8 million individuals.

In India, SLT use is widely and highly prevalent among the Northeast Indian populace. Tripura place's first among the Indian states with 48.5% of its population consuming multiple forms of SLTs. Mizoram is a small state in India covering a land area of only 21,081 km^2, housing a population of roughly 10.97 lakh individuals forming a total of 0.09 % of India's population (Census, 2011). Food habits including addition of condiments such as ash-filtered water or *chingal*, fermented pork fat and consumption of smoked meat are commonplace practises (Bhowmick, P., Lalrinhlupuii et al., 2022). Though Mizoram is rather secluded and its population small, it still ranks quite high in the national SLTs consumption rate with 33.5% of its adult population being smokeless tobacco consumers. Mizoram also places first among all Indian states as the highest smoking population with 34.4 % (Global adult tobacco Survey 2, 2017). Moreover, Mizoram ranks second in the prevalence of tobacco use among the states/Ut's in India with 58.7% of its population being under the influence of tobacco. A total of 61.6 % (56.6% urban, 68.5% rural) of the adult female population and 72.9% (69.5% urban, 77.4% rural) of the adult male population of Mizoram use some form of tobacco (NFHS5, 2021). According to National Centre for Disease Informatics and Research (NCDIR), the prevalence of smokeless tobacco use (54.1%) in Mizoram is much higher as compared to that of smoking (43.6%) (Indian Council of Medical Research-National Centre for Disease Informatics and Research, 2022).

1.2. Indigenous tobacco products of Mizoram – Tuibur.

Among the population with the highest prevalence rate of tobacco consumption in the country, tobacco has long been imbedded into the tradition as well as culture of the Mizo tribe. Believed to have originated from Shinlung/Chhinlungsan situated on the banks of Yalung river in China, this tribe migrated SEAR towards their present habitation (Mizoram) in India during the 16th century (Mizoram State E-

Figure 1.3. (a) Vaibel; (b) Zozial.

Governance Society, 2021). The age-old tradition of using tobacco in different indigenous forms has cultural, social and traditional significance. This can be evidently comprehended by the common practice of smoking in any social setting or gathering. Offering tobacco to others was also considered a sign of hospitality. Even in the aspect of marital courtship, a hand-rolled cigare\tte called Zozial [Figure 1.3 (b)], was known to be offered by maidens to their suitors while being courted. Similarly, proficiency in waterpipe smoking was also considered an advantageous trait for potential brides. Vaibel [Figure 1.3 (a)] is likewise a traditional bamboo smoking pipe which was mainly practiced by the men-folk of the Mizo tribal community.

Tuibur, which has two modalities of use (smoking and smokeless), is a distinct form of traditional tobacco use. Tuibur, in the smoking form (Figure 1.4), which bares similarity to the Indian hookah, is a waterpipe made of bamboo and clay comprising five parts connected using housed joints wedged together where the bottom container holds water. The pipe is sucked to allow the smoke to get saturated into the water which is later sipped using bamboo/gourd tubes. The other form of tuibur, which is a liquid SLT, though categorized as a SLT, is unique because of the fact that it is made by infusing tobacco smoke into an alkaline water called *chingal*. The liquid product (tuibur) is sipped, retained in the oral cavity and then spat out after the user no longer tastes the alkalinity of the concoction. This mode of use is repeated several times a day. Tuibur in this liquid form was not only used as an oral tobacco product but also as a remedial means to treat aliments such as toothache and oral diseases along with its use as a pesticide/insecticide during farming. Tuibur was prepared at home with small amounts of tobacco for personal use but at present, it is manufactured in small-scale cottage industries which supply the majority of consumers (E-governance, 2018).

Figure 1.4. Tuibur (waterpipe).

Early toxicological studies on tuibur used the Allium root tissue as a test system. This study demonstrated a dose-dependent reduction of the mitotic index, lagging chromosomes, micronuclei (MN) formation along with tumour formation in

the Allium root even at low-concentration tuibur exposure (Mahanta et al., 1998). An epidemiological study by Phukan et al., (2005) revealed the potential increase in stomach cancer risk among tuibur users of the Mizo populace. Individuals carrying the glutathione S-transferase genes GSTM1 (null genotype) and GSTT1 (non-null genotype) also exhibit a risk of stomach cancer as high as 2.4 times on prolonged consumption of tuibur as compared to non-users (Malakar et al., 2012). A close association between mtDNA D-loop mutation and polymorphism, tuibur use and stomach cancer has also been found; where a high frequency of mtDNA D-loop mutation was observed in tuibur users as compared to non-consumers, which might indicate higher risk of gastric cancer in the former (Lalmuanpuii et al., 2015).

Chemical characterization of tuibur demonstrated the presence of a diverse mixture of harmful compounds, heavy metals and others. A voltametric analysis of tuibur described the presence of heavy metals such as lead, nickel, arsenic, cadmium along with the presence of tobacco-specific nitrosamines (TSNAs) where N-nitrosonornicotine (NNN) was present in high concentration. Nicotine was detected using flame ionization detector (FID) and secondary tobacco alkaloids like anabasine, anatabine and myosmine were analysed using thermal ionization detector (TID) without much success (Sinha et al., 2006). A Fourier transform infrared spectroscopy (FT-IR) study reported the different functional groups which may be attributable to the presence of halides along with the presence of vibrational bands due to aromatic compounds as well as peaks linked to the presence of nicotine (Lalmuanpuii, 2016). Inductively-coupled plasma atomic emission spectroscopy (ICP-AES) analysis disclosed the presence of essential elements such as calcium, magnesium and iron. From an analysis by means of inductively-coupled plasma mass spectroscopy (ICP-MS) heavy metals like Pb, As and Cd were observed to exist in concentrations much higher than their USEPA permissible limits. Mass spectrometry analysis uncovered the presence of alkaloids and its derivatives along with phenolic compounds, quinones and TSNAs (Lalmuanpuii, 2016).

1.3. The Tobacco plant.

Among the 72 naturally occurring species of *Nicotiana*, only two species, namely, *Nicotiana tabacum* [Figure 1.5.(a)] and *Nicotiana rustica* [Figure 1.5.(b)], are highly valued and economically significant as they are extensively cultivated for manufacturing commercial tobacco. Besides, few other tobacco species are also grown as ornamental plants. in India, tobacco is mainly cultivated, on a commercial scale, in the states of Gujarat, Maharashtra and Uttar Pradesh (West and North India); Andhra Pradesh, Karnataka, Tamil Nadu (South India); West Bengal, Bihar and Orrisa (East India).

The tobacco plant has a thick and bushy erect stem (round and covered with viscid-glandular hairs) with simple yet significantly oval shaped leaves which are also hairy and oily sticky surface. The mature plant may reach about 120 - 185 cm in height and spawns clustered tube-shaped flowers (4 – 5 cm) which may be rosy (*N. tabacum*) or yellow (*N. rustica*) in colour. The optimal temperature for the cultivation of tobacco is between 20 – 30 ˚C but it grows quite well in varied climates and thrives in well drained, aerated, slightly acidic soils having pH between 5 – 6. The leaves of the tobacco plant are harvested in such a manner that only a few (2 – 3) fully matured leaves are picked/plucked by hand from each plant per harvest after which the leaves are typically tied in pairs and left to cure. Mechanical harvesting also takes place in countries like America and Canada. Different types of tobacco such as Virginia, Burley, Perique, Latakia (oriental), Cavendish etc., are mixed together to form blends. In India, FCV tobacco, bidi tobacco, cigar and cheroot, hookah tobacco, chewing and snuff, natu (*tabacum*), burley, lanka (*tabacum*) and HDBRG as well as pikka tobacco are grown (ICAR, 2023).

Taxonomic classification of tobacco plant

Domain	:	Eukarya
Kingdom	:	Plantae
Phylum	:	Magnoliophyta
Class	:	Magnoliopsida
Order	:	Solanales
Family	:	Solanaceae
Genus	:	*Nicotiana*
Species	:	*Nicotiana tabacum;* *Nicotiana rustica*
Common Name:		Tobacco
Habitats:		Native to America; cultivated in most tropical / sub-tropical regions.

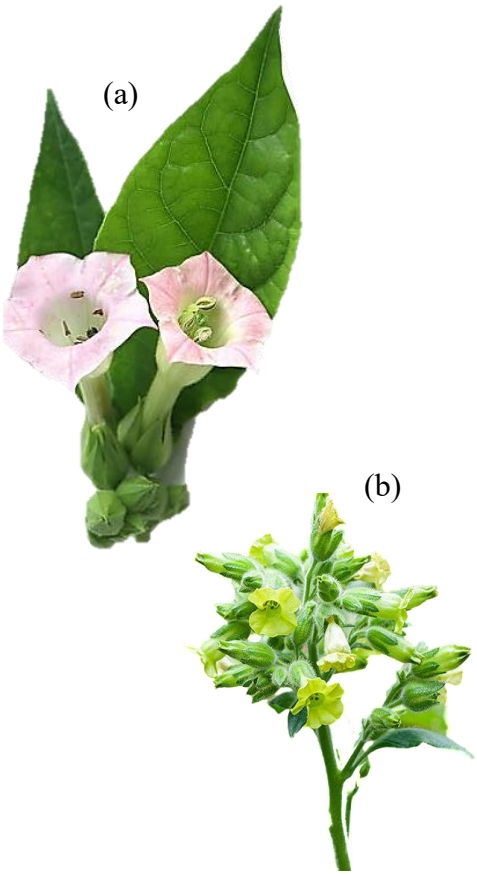

Figure 1.5. (a) *Nicotiana tabacum;* (b) *Nicotiana rustica.*

Tobacco leaves are cured, aged and fermented to improve aroma, flavor while decreasing the harsh and pungent odour of the leaves in order to develop a better taste. The most common types of curing methods for tobacco are air, fire, flue and sun curing. Air-curing is used for tobaccos such as burley and takes place by mechanical ventilation for 4 - 8 weeks inside a high roof building. Fire-curing employs the heat from open hardwood fired in barns to cure the tobacco which has been hung for 3 days to 10 weeks. Flue-curing is performed in small, tightly constructed barns with ventilators and flues stretched out under or around the floor. It requires 4 - 8 days for completion and is used for bright (Virginia) tobacco to produce tobacco for high grade cigarettes. In India, sun curing is the most employed technique used for tobacco curing. Tobacco is left to naturally dry out in the sun without a cover (World Health organisation, 2017). Curing turns the green chlorophyl in the tobacco leaves to

yellowish carotene and ultimately to mild golden brown or dark brown (depending upon the region), by drying (Figure 1.6.). The cured tobacco leaves are differentiated according to the extent and duration of curing into different grades, and stacked in large bulks or stored in closed containers in order to undergo further fermentation. This stage is also known as sweating the tobacco as water and ammonia are precipitated out of the leaves which reduces the nicotine, tar and acidity of the tobacco. Aging and fermentation aren't easily distinguishable in all cases save the activity of the former results in a more rapid and substantial release of heat and gases (Johnson, 1934).

Figure 1.6. Cured tobacco leaves.

Tobacco being a psychoactive, recreational, legal drug, has undergone extensive investigation to elucidate its chemical composition. The alkaloid composition of the *Nicotiana* genus consists of pyridine alkaloids such as nicotine, nornicotine, nicotyrine, anabasine, anatabine, cotinine and myosmine. In most species of *Nicotiana*, the predominant alkaloid was found to be nicotine, but some other tobacco species have nornicotine and anabasine as their primary alkaloids (Sisson & Severson, 1990). Tobacco leaf consists of hydrocarbons such as branched chain alkanes (iso and anteiso compounds), isoprenoids (farnesene, neophytadiene, etc.), terpenoids, sterols, aliphatic, aromatic and cyclic alcohols, esters, cyclic esters, aldehydes, ketones, quinones, phenols, phenolic esters, acids and bases including the aforementioned alkaloids. Plant metabolites including carbohydrates such as glucose, fructose, deoxyribose, etc.; amino acids, proteins and other related compounds like arginine, cystine, glutathione, histidine, tyrosine etc.; and inorganic constituents such as chloride, nitrate, nitrite, potassium, nickel, chromium, arsenic, cadmium, mercury, lithium, lead, zinc, copper, manganese, etc. present due to soil and environmental conditions as well as essential elements; are also present in the tobacco plant (Stedman,

1968). Several factors like soil pH and type, type of foliage residue, the genotype of the plant, application of herbicides, pesticides, fungicides, insecticides, fertilizers and others, can influence the elemental profile of the tobacco plant, hence, rendering a difference in elemental composition of tobacco leaves from region to region.

Curing influences the composition of tobacco leaves such that green tobacco leaves have higher starch and nicotine contents while yellowed and cured leaves have lower starch content with higher reducing sugar content as well as lower nicotine levels. The pH of the tobacco leaves whether green, yellowed or cured remain the same at approximately 5 to 6. Tobacco-specific nitrosamines (TSNA) are formed after harvesting of tobacco leaves and during the process of drying, curing, aging and for the most part during fermentation. Nitrite concentration of tobacco also plays a significant role in the formation of TSNAs. During curing of tobacco, due to microbial activity, nitrate is converted to nitrite, the nitrite thus formed elicits the formation of TSNAs by undergoing a nitrosation reaction with tobacco alkaloids.

Smoke from tobacco is a multifaceted and dynamic mixture of chemicals. Cigarette smoke is an aerosol made of droplets and has been classified as mainstream (inhaled directly through the column of the cigarette via the filter tip) and side-stream (smoke generated from cigarette by puffing which is inhaled by bystanders) smoke. Sidestream tobacco smoke is known to have higher concentrations of tobacco smoke constituents. (Engstrom et al., 2003) The gas or vapour phase of tobacco smoke consists of N_2, O_2, CO, CO_2, HCN, H_2S, CH_4, CH_3OH, HNO_3, CH_3CHO, $(CH_3)_2CO$, other hydrocarbons, acrolein, nitrosamines (gas phase) plus carbonyl compounds (Borgerding & Klus, 2005; Perfetti & Rodgman, 2011). The constituents of tobacco smoke particulate phase called total particulate matter (TPM) consist of TSNAs, poly aromatic hydrocarbons (PAHs), water, phenols, carboxylic acids, humectants, terpenoids, nicotine, paraffin waxes and aldehydes (Johnson et al., 1973). Tar is a material also known as particulate matter (TPM) that is containing nano-sized inorganic particles, PAHS, and carbonaceous materials. Formaldehyde as well as cyanide was indicated to be present in both phases of tobacco smoke (U.S. Department of Health and Human Services, 2010).

A necessary evil with regards to commerce, economics and agriculture, tobacco has many cons but exhibits some advantageous applications in agriculture other than for consumption. In some agricultural forums, tobacco decoctions are being recommended for its application as natural pesticides. Tobacco has been used as a natural pesticide/insecticide due to its nicotine content. The pyrolysis bio-oil generated from tobacco leaves produced by Booker et al., (2010) has shown inhibition of microorganisms such as *Pythium ultimum* (fungus)*, Clavibacter michiganensis* (Gram-positive bacteria) and *Streptomyces scabies* (bacteria) as well as pests like *Lepinotarsa decemlineata* (beetle). A study by Weber et al., (2019) showed the repellent activity of tobacco leaf extract towards *R. sanguineus* (tick larvae) even upon several dilutions of the extract; along with significant repelling activity against *Mucosa domestica* (fly larvae). These studies show that tobacco has great potential in the field of agriculture as pesticides and insecticides. Due to the slowly declining consumption of tobacco (W.H.O., 2024), there is a need for the introduction of alternative uses in regards to tobacco cultivators globally to ensure no loss of revenue, albeit additional exploration on the subject is required.

1.3.1. Some tobacco alkaloids.

The most abundant alkaloid found in *Nicotiana tabacum* and *Nicotiana rustica*, Nicotine or 3-(1-methyl-2-pyrrolidinyl) pyridine has been probed extensively. It is also found in several varieties of the nightshade family (Solanaceae) plants like aubergine, tea, potato and tomato. Nicotine is stored in the leaf vacuoles and is synthesized in the root cortical cells of the tobacco plant. Nicotine's biosynthesis occurs via the canonical jasmonate-signaling pathway and ~ 95% of total tobacco alkaloid content is made up of nicotine. Depending on the species of *Nicotiana*, further metabolism of nicotine can occur in the leaves giving rise to other alkaloids such as nornicotine. Nicotine is a strong insect repellent and used as a defence mechanism against herbivores by the plant. In injured plants or plants subjected to stress such as attacks from herbivores, correspondingly the alkaloid concentration is increased, indicative of the modulation of basal level of alkaloid due to different kinds of stimuli (Zenkner et al., 2019).

Nicotine's chemical structure consists of nitrogen containing two heterocycles: a pyridine and pyrrolidine ring with the empirical formula $C_{10}H_{14}N_2$ having a molecular weight of 162.23 (Figure 1.7.). Nicotine is an oily viscous liquid with a boiling point of ~246˚C and is colourless. The pyrrolidine moiety is synthesized biologically by the metabolism of polyamine putrescine while the pyridine moiety is a derivative of nicotinic acid. Nicotine is a polar compound capable of forming hydrogen bonds with polar protic solvents such as water, alcohols and acids. It is also highly soluble in solvents like petroleum ether, ether, chloroform, kerosene and oils (NCBI, 2023). Owing to an asymmetric carbon (chiral center) present in the pyrrolidine moiety, nicotine exists in 2 enantiomeric forms namely, R– and S– nicotine. The nicotine present in tobacco is principally the levorotatory isomer (S – isomer) which is also the only naturally occurring form of nicotine. Its R (+) form is derived upon pyrolysis and is rather weaker agonist relative to the S(-) form such that it does not bind as readily to nicotine receptors. Nicotine has two pKa values, viz., 3.0 and 8.02, therefore it is a weak base and oxidises to brown upon air and light exposure. The nitrogen on the pyrrolidine ring of nicotine is more basic as compared to the nitrogen on the pyridine ring (Gorrod and Warhen, 1993). At pH 7.4, nicotine exists in both as ionized as well as unionized forms due to the nitrogen on the pyridine ring remaining un-ionized. The more lipophilic unionized nicotine is easily absorbed through biological membranes in comparison to the hydrophilic ionized form (McKinney & Vansickel, 2016; Benowitz et al., 2009).

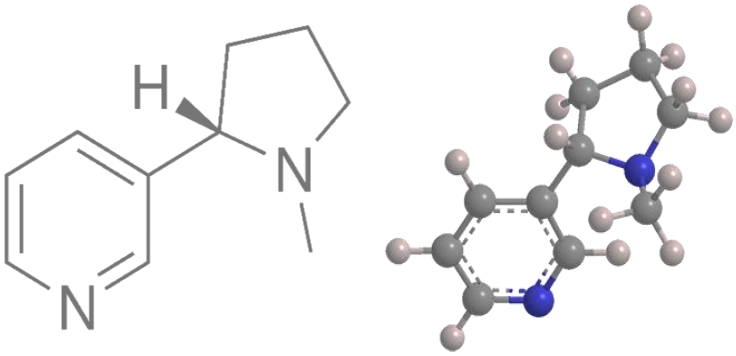

Figure 1.7. S (-) – Nicotine.

The endogenous neurotransmitter, acetylcholine, is quite similar in structure and polarity to nicotine. Consequently, nicotine mimics acetylcholine and therefore, binds easily to nicotinic acetylcholine receptors (nAChRs) in the Central Nervous System (CNS) impacting the action of acetylcholine within the body. Belonging to the Cys-loop family of ligated-ion channels (including serotonin, glycine and $GABA_A$

receptors), nAChRs form different subtypes under 16 homologous mammalian subunits (α and β). All these neuronal receptor subtypes are selectively permeable to small mono and divalent cations. Among the nAChRs subtypes, α4β2 subtype shows high affinity towards nicotine. The instigation of addiction to nicotine primarily involves the nAChRs of the midbrain dopamine area due to the presynaptic α7 nAChRs binding and activation on cholinergic afferents. This process encourages glutamate to be released onto the dopaminergic neurons of the midbrain. An activation in addition to desensitization of the nAChRs due to a longstanding exposure to nicotine in low-concentration may lead the receptors to be inactive. The α4β2 nAChRs present in the hippocampus on stimulation also aids in the release of γ-aminobutyric acid (GABA) and glutamate. Dysregulation of nAChRs due to chronic/prolonged desensitization resulting from inadequate recycling of receptors, eventually leads to upregulation of nAChRs which is presumed to play a key role in the progression and sustenance of nicotine addiction. Stimulation of nicotinic receptors in the brain via nicotine exposure generates the release of neuro-mediators such as acetylcholine, dopamine, nitric oxide, norepinephrine, epinephrine, vasopressin, etc. (Benowitz & Gourlay, 1997). Termination of tobacco use among long-term tobacco users normally manifests in minor but unnerving withdrawal symptoms such as shortfalls in cognitive abilities, irritability, restlessness, insomnia, anxiety, depression and increased appetite; which ultimately disappears with abstinence for a duration of a few weeks (Dani, 2001; Dani & Bertrand, 2007).

Due to the solubility of nicotine in water and lipids, it is easily absorbed by the respiratory tissues, mucosa, and the skin while much less so by the stomach due its acidic environment. Nicotine can be administered via ingestion, inhalation, nasal, oral and transdermal absorption by using tobacco and nicotine containing products. Oral tobacco products which are made alkaline to facilitate the relatively rapid absorption of nicotine through buccal mucosal epithelial cells. With a distribution half-life of ~ 9 minutes, nicotine circulates throughout the entire body with a steady-state distribution range between 2.2 – 3.3 L/kg. Biotransformation resulting in the formation of nicotine metabolites that mainly occurs in the liver while some in the kidneys and lungs. Cotinine is produced by the metabolism of nicotine via two steps: hydroxylation of nicotine by cytochrome P450 2A6 enzyme subsequently the intermediate would be

catalysed by aldehyde oxidase. Other metabolites such as nornicotine (0.4 – 0.8%) and nicotine glucuronide (3 – 5%) produced from nicotine are mediated via phase I and phase-II enzymes, respectively. Excretion of nicotine occurs via urination (15%) and renal excretion. Urine acidification reduces the amount of free unionized nicotine and helps in renal elimination (McKinney & Vansickel, 2016). Similarly, during the curing and senescence of tobacco leaves also nicotine degradation depends on its ability to undergo oxidation of the α carbon adjacent to the pyrrolidine nitrogen atom to form xenobiotics and metabolites (Bush et al., 1999).

One of the minor alkaloids of tobacco, cotinine or 1-methyl-5pyridine-3-yl-pyrrolidinone (Figure 1.8.) is a N-alkylpyrrolidine consisting of a N-methylpyrrolidione holding at the C-5 position (5S- enantiomer) a pyridin-3-yl substituent. It has a molecular formula $C_{10}H_{12}N_2O$ with a molecular weight of 176.21 g/mol and is a viscous oil with a boiling point ranging between 210 – 211˚C at 6 mmHg (NCBI, 2022). Cotinine differs in structure from nicotine by the presence of one carbonyl group which changes the pyrrolidine ring into a cyclic amide. Consisting of two conformers, cotinine's conformational difference mainly relies on the position of the pyridine substituent which adopts a twisted ring conformation at the equatorial position. Cotinine being capable of forming intramolecular hydrogen bonds C–H···O=C might as well be a factor that facilitates the rotation of the methyl group (Uriarte et al., 2017). It is also clear from its structure that it is susceptible to further oxidation at the carbon and nitrogen centres. N-demethylation can also take place to produce nornicotine from cotinine in some species excluding humans (Gorrod & Schepers, 1999). Cotinine is a predominant metabolite of nicotine by means of enzyme-mediated oxidation in humans and animals also used as a biomarker to detected exposure to nicotine since it can be expelled by most species while remaining unchanged. Nicotine is mostly metabolised in the liver to form cotinine (Figure 1.8.) though research findings suggest cotinine is also formed in the brain (Benowitz & Jacob, 1994; Jacob et al., 1997; Zhu et al., 2013). It is also known to be produced in small quantities during the tobacco curing process possibly by way

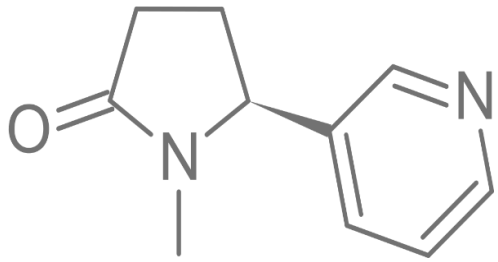

Figure 1.8. Cotinine.

of oxidation and bacterial activity on nicotine (Tan et al., 2021). 70 – 80% of the total nicotine consumed is converted to cotinine in the human body. It is photodegradable with a half-life of 15 hours and exposure to cotinine is commonly through ocular or dermal contact.

Studies have shown myriad effects of cotinine across diverse systems including cardiovascular, endocrine, immune, neurobehavioral system besides the nervous system and may congruently play a role in the tobacco dependency. Biotransformation of cotinine does not take place in the brain which leads to a higher degree of accumulation compared to nicotine. Cotinine is a stimulant which promotes the release of dopamine via the nAChRs in the nigrostriatal pathway but non-neuroactive in doses seen in smokers. In rats, at high doses, cotinine, in a dose-dependent manner lowers heartrate, blood pressure and aldosterone levels albeit such physiological changes are normally not observed in humans. Though cotinine is not categorized as a carcinogen by the International Agency for Research on Cancer (IARC), it has been found to inhibit anticancer drug doxorubicin induced cell death by supressing the caspase enzyme mediated apoptosis via Akt/PI3 kinase pathway and hence exacerbates the risk of cancer (Gray & Hall, 2014).

Nornicotine (3-pyrollidin-2-yl-pyridine), easily obtained by the demethylation of nicotine, has a similar structure yet different from nicotine only by the absence of methyl group at the pyrrolidine nitrogen. (Figure 1.9.) It is a hygroscopic colourless or pale-yellow liquid with a molecular formula of $C_9H_{12}N_2$, a molecular weight of 148.20 g/mol and has a boiling point of 260˚C. Much like nicotine, it is miscible in water and easily dissolves in solvents such as chloroform, alcohols, ether a well as petroleum ether, kerosene and oils. On heating it decomposes to toxic vapours of hydrochloric acid and nitrogen oxides though it is comparatively more stable than nicotine and does not change colour on exposure to light or air (NCBI, 2022).

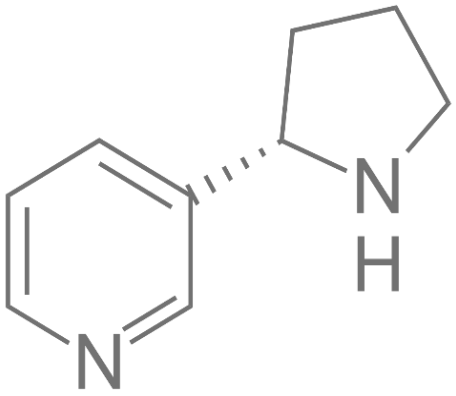

Figure 1.9. Nornicotine.

Nornicotine makes up about 2 to 5% of the total alkaloids found in the tobacco plant and its biosynthesis involves both the pyridine and pyrrolidine pathway; following the ring fusion of the two rings to form nicotine, demethylation takes place to produce nornicotine (Figure 1.10.). The conversion of nicotine to nornicotine happens in the root and leaf tissues by the role of the nicotine *N*-demethylase (NND) enzymes programmed by the CYP82E gene in tobacco plants. Specifically, CYP82E4, CYP82E5 and CYP82E10 genes, belonging to the cytochrome P450 monooxygenase family, have been observed to be involved in the demethylation process of nicotine to nornicotine (Guo et al., 2021). The presence of nornicotine is considered to be undesirable due to it being an antecedent of the tobacco-specific nitrosamine, N-nitrosonornicotine (NNN), which is classified as a Group 1 carcinogen. Knezevich et al., (2013) observed that incubating saliva with [pyridine-D_4] nornicotine alone could produce detectable levels of [pyridine-D_4] NNN and demonstrated that NNN could be formed just from nornicotine without addition of other substances using human saliva. Therefore, researchers have also developed ways to decrease nornicotine production in the tobacco plant by RNA interference-induced silencing of the CYP82E4 gene and its homologues to supress the conversion of nornicotine from nicotine (Gavilano et al., 2006; Siminszky et al., 2005). The formation of nornicotine via nicotine ingestion in humans have also been confirmed by the presence of nornicotine in human urine in very less quantity (1%) suggesting the further metabolism of nornicotine into other chemical compounds (Neurath et al., 1991).

As nornicotine is a major metabolite of nicotine, it is likely that it exhibits similar interactions with nAChRs though potentially with differing efficacy and affinity. Studies have shown that nornicotine exposure leads to the activation of α7 – receptors which may play a role in affecting cognition and concentration as well as mediating the activation of α6 – containing neuronal receptors reinforcing the effects of nicotine (Papke et al., 2007). It was found that dopamine release in animal models (rats) is nicotinic receptor-mediated. Also, the desensitization of neural nicotinic receptors occurs on exposure to S-(-)-nornicotine along with the occurrence of cross-desensitization indicating the contribution of common subtype of nicotinic receptors for both S-(-)-nicotine and S-(-)-nornicotine (Dwoskin et al., 2001).

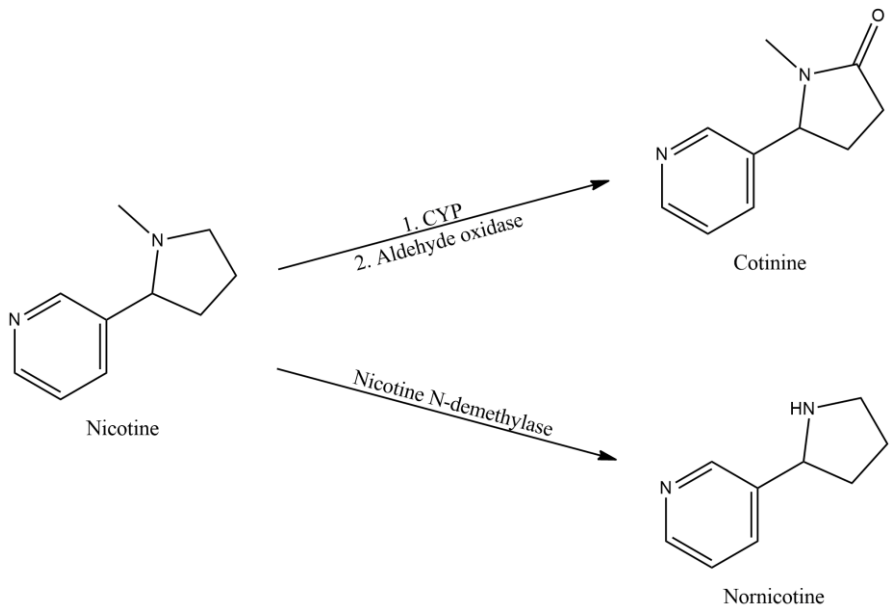

Figure 1.10. Metabolism of nicotine to cotinine and nornicotine.

1.3.2. Other chemical components of interest.

Nitric oxide ($NO^{\bullet}$), diatomic hydrophobic gaseous free radical, can diffuse across cellular membranes due to its high diffusion capacity . $NO^{\bullet}$ synthesis, in plants, occurs mainly via two routes – reductive (based on reduction of nitrite to $NO^{\bullet}$) and oxidative (oxidation of $^{+}NH_4$ species). Nitrate reductase reduces nitrate to nitrite and can cause further reduction of nitrite to produce $NO^{\bullet}$. Plants are capable of releasing $NO^{\bullet}$ from their leaves which is enhanced by the use of herbicides or nitrogen dioxide (NO_2) treatment. Under aerobic conditions, the levels of nitrate increases ensuing a 100-fold increase in $NO^{\bullet}$ emission. Plant mitochondria is also responsible for the generation of $NO^{\bullet}$ from nitrite similar to animal mitochondria including several other nitrite-dependent mechanisms involved in $NO^{\bullet}$ synthesis (Sun et al., 2003). A study showed in tobacco (*Nicotiana tabacum*) that $NO^{\bullet}$ emission from tobacco leaves were exclusively from the reduction of nitrite to $NO^{\bullet}$ (Planchet et al., 2005). Epidermal cell types such as trichomes, intercostal and costal epidermal cells, guard cells, subsidiary cells as well as palisade mesophyll cells have the potential to form $NO^{\bullet}$. Although chlorophyllous cells are associated with $NO^{\bullet}$ production, wherein tobacco short

trichomes may also be responsible for the generation of $NO^{\bullet}$ and derivatives (Gould et al., 2003).

$NO^{\bullet}$ has a biologically short half-life attributable to its rapid reaction with a wide range of molecules (Csonka et al., 2015; Bryan & Grisham, 2007). Reactive nitrogen species (RNS) are a group of molecules occurring as derivatives of $NO^{\bullet}$ radical and O_2^- anion formed by nitric oxide synthase (NOS) and various enzymes such as lipoxygenase, NADPH oxidase, cyclooxygenase etc. Nitrosative stress occurs when there is excess of RNS surpassing the system's capability to eliminate or neutralize them. Peroxynitrite ($ONOO^-$) is a resultant of the reaction between O_2^- and $NO^{\bullet}$ and initiates the formation of RNS. It can directly react with transition metal center containing proteins leading to modification of heme proteins like cytochrome c, haemoglobin and myoglobin as well as causing a change in protein structure on reaction with amino acids of the peptide chain (Thuy le et al., 2017). One of the main pathways of $NO^{\bullet}$ metabolism, in mammals, is its oxidation to nitrate and nitrite along with its oxidation in the presence of molecular oxygen to NO_2. NO_2 further reacts with $NO^{\bullet}$ molecule to produce N_2O_3 which may decompose to give nitrite. Nitrite may further be oxidised by oxyhaemoproteins to nitrate in addition to the direct reaction of $NO^{\bullet}$ with oxyhaemoproteins forming nitrate (Csonka et al., 2015; Bryan & Grisham, 2007).

Tobacco-specific nitrosamines (TSNA) are a class of highly carcinogenic nitrosamines derived via tobacco alkaloids such as nicotine, nornicotine, anabasine and anatabine. TSNAs primarily consist of N-nitrosonornicotine (NNN), 4-(methyl nitrosamino)-1-(3-pyridyl)-1-butanone (NNK), N-nitrosoanabasine (NAB), N-nitrosoanatabine (NAT) and 4-(methylnitrosamino)-1-(3-pyridyl)-1-butanol (NNAL) (Figure 1.11.). NNN and NNK are classified as Group 1 carcinogens while NAT and NAB are Group 3 carcinogens (IARC, 2016). Gas or solid phase nitrosation of tobacco alkaloids resulting from the presence of NO_x in tobacco during storage under warm temperature leads to the formation of TSNAs. Though the presence of nitrate in tobacco does not directly lead to TSNA formation, the presence of microbes which are able to convert nitrate to nitrite, which is highly reactive, enables the facile conversion of secondary tobacco alkaloids to nitrosamines (J. Wang et al., 2017).

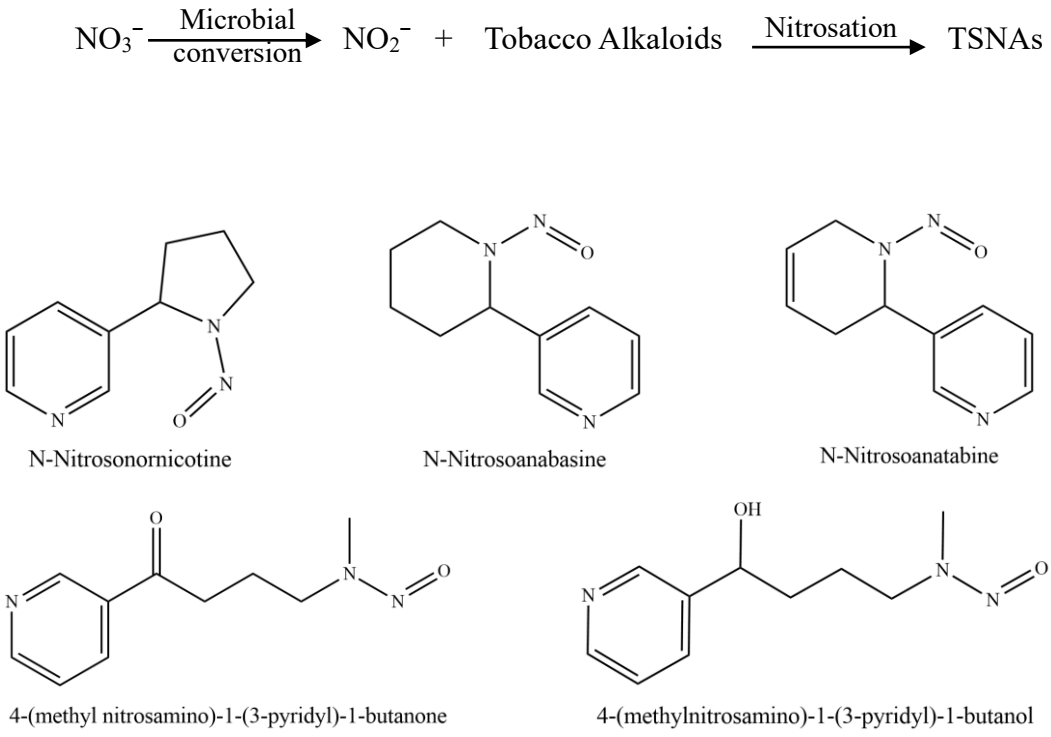

Figure 1.11. Tobacco specific nitrosamines (TSNAs).

Since tobacco uptakes considerably higher levels of nitrogen, potassium and phosphorous when compared to other plants, hence it demands lavish nitrogen rich fertilizer amendments. The lavishly applied nitrogen fertilizers greatly enhances the nitrate nitrogen (NO_3–N) levels in tobacco leaves, consequently accentuate the nitrite concentration levels. With the abundant nitrogen oxides in presence of alkaloids during the curing of tobacco leaves leads to the facile TSNAs formation (Lewis et al., 2012). Tricker et al., (1988) has also shown that under simulated gastric conditions, endogenous formation of NAT, NAB and NNN can in fact occur on exposure to oral tobacco products, where a constant nitrite content plays a crucial role. Poor oral hygiene which exacerbates the microbial reduction of nitrate to nitrite in the oral cavity combined with tobacco alkaloids from oral tobacco use contributes to the endogenous formation of TSNAs (Nair et al., 1996).

Quinones, having a structure that constitutes a benzene core with two carbonyl groups, is a group of compounds which naturally occur in bacteria, fungi as well as plants. In nature, they exist as benzoquinones, anthraquinones, naphthoquinones and

polycyclic quinones. They are crystalline yellowish solids which cause itching on dermal contact. Quinones have a characteristic unpleasant smell and is an oxidizing agent. Complete reduction of o- and p-quinones to their corresponding catechol and hydroquinone takes place. In the liver, the reduction of quinones may be catalysed by carbonyl reductases (Devi and Mehendale, 2005). When quinones are produced in biological systems, they undergo reactions with cellular nucleophiles or go through redox reactions to generate reactive oxygen species (ROS). Among the many pro-oxidant chemical compounds found in tobacco smoke, hydroquinone is the most abundant. Major metabolites of hydroquinone are hydroquinone sulphate and glucuronide conjugates (in high levels of exposure). The product of oxidation of hydroquinone to p-benzoquinone is a reactive metabolite which may produce mono/polyglutathione conjugates (IARC, 1987). Semiquinone radicals are formed as an intermediate during the conversion of hydroquinone to p-benzoquinone. More akin to other free radicals, the semiquinone radical species deprotonates the remaining hydroxyl group establishing an acid-base equilibrium (Figure 1.12.) (Asmus & Bonifačić, 2000).

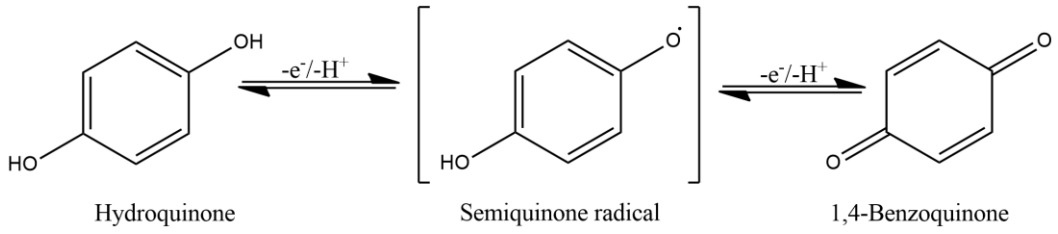

Figure 1.12. Hydroquinone to p-benzoquinone conversion with intermediate.

Tobacco-smoke tar phase contains significant concentrations of stable free radicals which were identified using electron paramagnetic resonance (EPR) as carbon-centered radicals (-C$^{\bullet}$) and semiquinone (QH$^{\bullet}$) radicals. EPR spin-trapping detection of quinone/semiquinone/hydroquinone (Q/QH•/QH_2) system in tar phase tobacco smoke was performed by Pyror (1992), where the stable free radicals were recognized as o- and p-benzosemiquinone radicals and the mechanism of conversion of O_2 to $O_2^{\bullet-}$ by QH$^{\bullet}$ radicals, which can cause dismutation to produce H_2O_2 followed

by a reaction with Fe^{2+} (which is abundant in tobacco-smoke tar phase) generating highly reactive and oxidizing hydroxyl radicals ($HO^{\bullet}$) through the Fenton reaction as seen bellow (Valavanidis et al., 2009):

$$Q + QH_2 \leftrightarrows 2QH^{\bullet}$$

$$QH^{\bullet} + O_2 \rightarrow Q + O_2^{\bullet -} + H^+$$

$$O_2^{\bullet -} + 2H^+ \rightarrow H_2O_2$$

$$QH_2 + O_2 \rightarrow H_2O_2 + Q$$

$$QH_2 + O_2 \rightarrow O_2^{\bullet -} + QH^{\bullet} + H^+$$

Fenton Reaction

$$Fe^{2+} + H_2O_2 \rightarrow Fe^{3+} + HO^{\bullet} + HO^-$$

Tobacco is a proficient metal accumulator in its leaves; particularly Cadmium (Cd) and zinc (Zn) (Kozak & Antosiewicz, 2023). Cd and zinc are taken up by the plant via the root system as divalent cations, by selective transporters contained at the plasma membrane. Metal species are mainly stored in the vacuoles, and metal transporter proteins play key role in the translocation of metals from root to the shoot and leaves (Kozak & Antosiewicz, 2023). Lugon-Moulin et al., (2006) conducted a quantitative study of Cd in 755 types of tobacco from across the globe comprising of burley, flue-cured and oriental tobacco; the concentration range of Cd in the tobacco samples was between 0 – 6.78 $\mu g g^{-1}$ dry mass. Zinc and nickel (Ni) concentration determination in flue-cured tobacco leaves range between 24 to 33 $\mu g g^{-1}$ dry mass of Zn and 2.20 to 2.92 $\mu g g^{-1}$ dry mass of Ni (Tso, 1972). The raw as well as processed Ethiopian tobacco leaves were also found to contain Cd, copper (Cu), chromium (Cr), Ni and Zn but lead (Pb) was non-detectible with Zn metal ions exhibiting higher concentration in the tobacco samples as compared to other heavy metals (Regassa & Chandravanshi, 2016). A multi-elemental study of tobacco leaves, roots and stem in by neutron activation analysis (NAA) as well as atomic absorption spectrometry (AAS) determined the presence and concentration of essential elements (calcium, magnesium, potassium, sodium, manganese, copper, iron, zinc) and 28 non-essential elements including heavy metals such as Cd, Pb, Cu, Ni, Cr and Zn along with rare earth metal ions in Northeast Indian tobacco samples (Lalrammawia et al., 2022).

1.4. Consequences of the tobacco industry.

From decades' worth of research, it is a well-known fact that tobacco consumption is an avoidable unhealthy habit. Tobacco cultivation also impacts the environment severely such as deforestation which in turn induces soil degradation and erosion concomitantly with biodiversity loss, water pollution and increased atmospheric CO_2 levels. The use of various agro-chemicals, for instance, growth regulators, fertilizers, pesticides, etc. for the crop to attain maturity is substantial and environmental run-off of these chemicals may contaminate water sources used for drinking, not to mention the depletion of nutrient from the soil as tobacco is nutrient (N, P, K) greedy compared to other crops. Moreover, non-recyclable waste containing nicotine and toxic waste (HCl, NH_3, methyl benzene and butanone) as by-products of the manufacturing process have irrevocable effects on the environment (Novotny et al., 2015). Over 124 countries in the world use an estimated 32 lakh hectares of tillable land for growing tobacco. This poses a questionable outcome as it impinges on land that can be otherwise used for the essential food crop cultivation as major tobacco producing countries are food-deficit and economically developing nations. India, with the largest population in the world riddled with poverty and food insecurity, is one of the third largest producers and the second largest consumer of tobacco in the world.

Green tobacco sickness (GTS) is caused due to tobacco poisoning in workhands engaged in tobacco cultivation and harvesting. Thus, the exposure of mature tobacco leaves ensues dermal nicotine absorption leading to intoxication. Symptoms characteristic of GTS include headache, nausea, vomiting, dizziness, muscle weakness and in extreme cases, seizures. It mainly occurs when garments of workers or tobacco leaves become wet by perspiration, dew or rain. Studies have concluded that incidence of GTS was 37% in individuals working with tobacco production with urine cotinine levels of 700 to 1000 ng/mL because of GTS (Cezar-Vaz & Cargnin, 2019; Park et al., 2018).

In human beings, different types of cancer of the respiratory tract and other vital organs, besides heart diseases including aortic aneurism, ischemic as well as respiratory heart disease, stroke, pneumonia and others, are epidemiologically linked with smoking tobacco (Wald & Hackshaw, 1996). Besides, the consumption of

smokeless tobacco also portends various non-communicable diseases. Moreover, SLTs use induces elevation of blood pressure with studies showing increase in the blood pressure with increased absorbed nicotine levels. (Fant et al., 1999) An increased heart rate of 16±2 beats per minute with approximately 50% epinephrine increase was also reported which makes SLT use as a hemodynamic as well as autonomic stimuli (Wolk et al., 2005). Furthermore, SLT use has many ill effects related to oral health. Gingival recession together with exposed teeth, periodontitis following calculus and plaque accumulation, leucoplakia, erythroleukoplakia, erythroplakia, oral submucous fibrosis and oral cancers including squamous cell carcinoma and verrucous carcinoma are common findings in patients with a history of SLT use (Muthukrishnan & Warnakulasuriya, 2018).

Diabetes, specifically type 2 diabetes, has been observed to have an increased risk of development with hazard ratio (HR) 1.15 (95%) in SLT current consumers versus former users with a HR of 0.86 (95%). Dose – dependent studies likewise revealed the relationship between increased SLT intake and increased risk of diabetes (Carlsson et al., 2017). In the middle-class Indian population, smoking/smokeless tobacco use is prevalent in diabetic patients (26.6%) compared to those without diabetes (14.4%) (Gupta et al., 2014). Reduction in birth weight of about 105 grams ($p = 0.02$) and 6.2 days ($p = 0.0001$) decrease in gestational age in infants with maternal SLT use has been observed (Gupta & Sreevidya, 2004).

Global cancer burden is greatly influenced by chronic tobacco use. The World Health Organization (WHO) estimates 80 lakhs preventable yet premature mortalities per year due to tobacco use. SLT use in particular has been observed to cause pancreatic, oesophageal as well as oro-pharyngeal cancers (International Agency for Research on Cancer, 2020). Furthermore, a systematic review of cohort studies showed that there was a high risk of oral cancer [Odds ratio (OR) 1.48 - 27.4], pharyngeal cancer (OR 1.6 - 2.1) plus oesophageal cancer (OR 2.06 - 12.8) occurrence in SLT consumers. A meta-analysis has likewise suggested a positive association between malignancy of the upper digestive tract and the consumption of SLTs with OR of 2.17 (95%, confidence interval 1.42 - 3.22) (Gupta et al., 2018; Sinha et al., 2018).

In 2020, 193 lakh new cancer cases besides 100 lakh deaths owing to cancer was estimated to have occurred worldwide. The Asian population has considerably contributed to 58.3% of global cancer deaths (Sung et al., 2021). In India, tobacco – related cancer accounts for nearly half, 49.3% (males) and 22.8% (females) of all cancer cases. On account of the Indian Council of Medical Research – National Centre for Disease Informatics and Research (ICMR-NCDIR) (2021) cancer profile of the North - Eastern region of India, it was observed that oesophageal cancer is the leading site associated to tobacco use in both males (13.6%) and females (7%). Similarly in Mizoram, where more than 77% of the populace are tobacco users, tobacco related cancer was observed to be 43.3% among males and 22.1% among females (Indian Council of Medical Research-National Centre for Disease Informatics and Research, 2022). In addition, the leading site for the proportion of cancer associated with tobacco use in Mizoram is the oesophagus (16.2%) in males and the lung (15.6%) in females (Indian Council of Medical Research-National Centre for Disease Informatics and Research, 2021).

1.5. Oxidative stress.

The consequence of an imbalance between the generation and accumulation of oxidants and the ability of intracellular antioxidant system to deactivate these oxidants is described as oxidative stress. These oxidants are generated as by-products of aerobic metabolism in the mitochondria during adenosine triphosphate (ATP) biosynthesis, but under pathological conditions, can be induced in elevated rates. Redox enzymes are the primary oxidant and antioxidant sources as well as sinks (Sies, 2020). Low-level physiological oxidative stress is a requirement for redox signalling while high-level supraphysiological oxidative stress is toxic therefore, maintaining presumptive redox homeostasis is imperative for minimizing oxidative stress. In tissues and cells, all forms of agents, i.e., physical, medical and/or microbial, can instigate oxidative stress. Oxidative stress occurs endogenously via cell metabolism as well as exogenously (exposome). Moreover, this phenomenon takes part in fundamental life processes including cell respiration in the mitochondria, synthesis of lipids, metal metabolism, lysosome function, phagocytosis of foreign bodies along with xenobiotic metabolism of organic compounds (Sies, 2019). An estimated 1 to 4 % of the oxygen is converted

to superoxide radical ($O_2^{-\bullet}$) species during the oxidative phosphorylation process. Oxidative stress is reported to be associated with the pathogenesis of numerous non-communicable diseases including different types of cancer (Finkel & Holbrook, 2000).

Reactive oxygen species (ROS) are molecules comprising of no less than one oxygen atom with one or more unpaired electrons which exist only transiently. They include chemical substances formed oxygen may be partially reduced. Most ROS are generated as by-products during mitochondrial electron transport. ROS include free radicals like superoxide radical ($O_2^{\bullet-}$), hydroxyl radical ($^{\bullet}OH$), hydroperoxyl radical ($HO_2^{\bullet}$), singlet oxygen ($^1O_2$) and nitrogen-based radicals or reactive nitrogen species (RNS) (Jakubczyk et al., 2020). These are principally signalling molecules in addition to inducing cell differentiation and apoptosis, contributing to the process of aging. ROS when produced in excess can cause damage to, plasma membrane, proteins and/or DNA besides they disrupt the signal transduction pathways and essential cellular metabolic processes. The unabated production of ROS combined with the moderate antioxidants content renders depleted antioxidant capacity, which limit the system's capability of neutralizing and eliminating ROS and thereby induce the oxidative stress. Enzymatic reactions are mainly responsible for the production of ROS. Endogenous formation of free radicals may occur due to immune cell activation, ischemia, inflammation, infection, cancer, excessive exercise, aging and mental stress; while exogenous formation of ROS may occur from the exposure to environmental pollutants, chemical solvents, heavy metals, specific drugs, cooking, alcohol, tobacco smoke and high energy radiations (Pizzino et al., 2017).

Antioxidants consisting of different types of antioxidant enzymes and low molecular mass antioxidants are the important defence mechanism against excess ROS. According to Halliwell & Gutteridge (1989), 'any substance that, when present at low concentrations compared with that of an oxidizable substrate, significantly delays or inhibits oxidation of that substrate', is termed as an antioxidant. They reduce oxidative stress-related damage by breaking the radical chain reactions induced by ROS. Primary enzymatic antioxidants directly act on ROS generated from incomplete reduction of singlet oxygen, and hydrogen peroxide. Superoxide dismutase (SOD) which is a metalloenzyme, scavenges the superoxide anion radical by catalysing the dismutation of $O_2^{\bullet-}$ radical to hydrogen peroxide and molecular oxygen while catalase

(CAT) and glutathione peroxidase (GPx) using glutathione S-transferases (GSH) eliminates hydrogen peroxide (Sharifi-Rad et al., 2020).

Lipid peroxidation is the oxidation of lipids where the products formed can be used as biomarkers for oxidative stress. Increase in lipid peroxidation products from smoking causes DNA and protein lesions which potentially poses a threat to biological processes. Malondialdehyde (MDA) is a product of the degradation of polyunsaturated fatty acids (PUFAs) and is used as a biomarker for lipid peroxidation in blood plasma, urine and saliva. Oxidation of proteins can be categorized into two forms: reversible and irreversible. Irreversible protein oxidation including carboxylation and nitration are consequences of tobacco smoke-induced ROS formation (Caliri et al., 2021). It can initiate formation of 8-oxo-2′-deoxyguanosine (8-OHdG), a malicious DNA lesion, which is possibly responsible for mutagenesis. Loss of epigenetic information, DNA oxidation, DNA structure modification, to name a few, are outcomes of oxidative stress (Pizzino et al., 2017). Oxidative stress, furthermore, instigates the breakdown of cell tissue along with DNA damage which can result in inflammation. Chronic inflammation entail lifestyle disorders like cancer and diabetes.

Apoptosis or cellular suicide, is a type of programmed cell death in biological processes, where damaged cells are selectively removed in an orderly manner from the tissue. This process is used for quality control during the development as it is an energy-dependent stochastic process leading to rapid but discrete removal of cells wherein excess cells are systematically dismantled and discarded. It naturally occurs during development and aging to maintain the cell population as well as a defensive mechanism involved in immune reactions. The cellular damage via apoptotic mechanisms occurs because of stimuli such as noxious agents or diseases (Robertson et al., 2009). Apoptosis involves the activation of caspases, a group of cysteine-rich proteases, which provide crucial links in cell regulatory networks responsible for orchestrating inflammation as well as cell death. Activation of executioner caspases (caspases -3, -6 and -7) via initiator caspases (caspases -8 and -9) coordinate their activity to stimulate other enzymes and destroy structural proteins. Two main apoptotic pathways, intrinsic or mitochondrial apoptosis and extrinsic or death receptor pathways encompass most apoptotic pathways (McIlwain et al., 2015). Shrinkage in size (dense cytoplasm, tightly packed cell organelles) and pyknosis (due to chromatin

condensation) of the cell are characteristic features of apoptosis. Apoptosis is vital in the maintenance of cellular homeostasis and its deregulation is involved in the pathology of various disorders in humans (Elmore, 2007). Apoptosis can clearly be distinguished from necrosis such that there is damaged or compromised cell membrane integrity followed by swelling and lysis of the cell undergoing necrosis. Necrosis occurs in a cluster of cells or tissue in a specific site, whereas apoptosis takes place only at the unit cell level, and is programmed genetically leading to fragmentation of DNA and formation of apoptotic bodies. Excess oxidative stress leads to either apoptosis or necrosis. Antioxidants have the ability to check apoptosis similar to caspase inhibitors. Bcl-2, an anti-apoptotic gene, with its antioxidant properties suppresses oxidative stress induced apoptosis. Mitochondria also plays a central role in apoptosis, where mitochondria permeability transition occurs under extreme stress (Kannan & Jain, 2000).

As mentioned earlier, tobacco use is a promoter of oxidative stress in the human body. Most of the metal species in tobacco have free radical generating capabilities. Pb has shown to exhibit pro-inflammatory effects due to oxidative stress. Likewise, arsenic (As) in tobacco causes pro-inflammatory effects by inducing ROS production in different cell type though its mechanism of action remains to be fully comprehended. By virtue of the exposure to As, the inhibition of cellular respiration perturbs oxidative phosphorylation leading to excess H_2O_2 production. Aluminium (Al), Ni, Cd and mercury (Hg) present in tobacco and tobacco smoke can also induce pro-inflammatory effects due to their ability to trigger oxidative stress by ROS generation (Milnerowicz et al., 2015). The main source of nicotine-induced free radicals are $O_2^{-\bullet}$ and H_2O_2, which also acts as oxidative stress markers. A decrease in antioxidant activity, uric acid levels, up-regulation of lipid peroxidation along with a strong correlation of nicotine and cotinine with nitroxidative stress markers was observed in a study of human saliva from SLT consumers (Begum et al., 2018). Salivary samples from both smokers and SLT users where a marked increase in salivary SOD and MDA followed by a decrease in GPx and CAT was observed in a case-control study by Balasubramaniam & Arumugham (2022). A cohort study on 934 tobacco consumers (smoking and SLT) showed an increase in MDA levels suggesting increased lipid peroxidation and decrease in antioxidant enzyme levels such as SOD,

CAT and glutathione reductase (GR) indicating significantly increased oxidative stress (Supriya et al., 2017). Comparative study of SLT consumers placentae vs. nonuser placentae showed that maternal SLT use during pregnancy may be associated with villus hypoxia and oxidative DNA damage since 8-OHdG as a biomarker was observed in SLT consumers when compared to nonusers. (Kumar et al., 2021) Tobacco related oxidative damage of sperm DNA may also be a causation of non-familial sporadic heritable retinoblastoma (NFSHRb) in children whose fathers had tobacco use history (Kumar et al., 2015). High micronuclei with DNA damage levels were reported ($p < 0.05$) in the buccal epithelial cells and peripheral blood of tobacco users (Chandirasekar et al., 2019).

Oxidative stress related diseases (OSRDs) are diseases linked to oxidative stress and excess free radical production which can be influenced by factors such as lifestyle, diet and environment. Due to the susceptibility of neural cells in the brain to oxidative stress compared to other tissues, in the late years of human life, when failure of the oxidative stress repair pathways are probable, oxidative stress related lipid peroxidation may give rise to oxidation of nucleic acid bases, protein damage followed by aggregation of neuronal dead cells. Examples include diabetic neuropathy, Alzheimer's disease, Parkinson's disease, multiple sclerosis as well as amyotrophic lateral sclerosis (Halliwell, 2006). Reduction of $NO^{\bullet}$ levels due to the formation of $ONOO^{-}$ from the reaction of $O_2^{-\bullet}$ and $NO^{\bullet}$ may be a major mechanism of vascular diseases. Atherogenesis with mechanisms including redox-sensitive transcription factor activation, induced lipid peroxidation, oxidation of proteins as well as nuclear and/or mitochondrial DNA damage is reported to be induced by vascular oxidative stress (Förstermann, 2010). Osteoporosis is another OSRD where it is believed that ROS is responsible for degrading and modifying fibronectin molecules in bone nodule (Saeidnia & Abdollahi, 2013). Cancer has been strongly correlated with oxidative stress related mutagenesis and sensitivity to mutagenic agents due to elevated levels of ROS. High ROS levels can provoke tumour proliferation through ligand-independent transactivation of the receptor tyrosine kinase (RTK) resulting in cancer metastasis (Saeidnia & Abdollahi, 2013).

1.6. Spectroscopic and analytical techniques.

Characterization of tobacco and associated additive chemicals has been an ongoing research interest. As the tobacco industry becomes more innovative in the creation of its products for consumption, spectroscopic methods are useful tools to discern the contents of these tobacco products. Molecular Spectroscopy methods, dependent on the wavelength of radiation, also encompasses the study of the interactions of particles such as protons, electrons and ions with other particles as a function of collision energy. Spectroscopy can utilize nearly the entire electromagnetic spectrum, from the lowest to highest frequencies i.e., radio waves, infrared radiation, UV-visible radiation, X-rays and γ-rays. Spectroscopic techniques are exceptionally sensitive, and are applied in both fields of science and technology (Chu et al., 2023).

Infrared (IR) spectrometry is based on the absorption of infrared radiation from ~10,000 to 100 cm^{-1} which reflect the vibrational energies of the molecules. The spectra is seen as vibrational bands exhibited by single vibrational energy change together with a number of rotational energy change. The band intensities are plotted as transmittance (ratio of transmitted radiation to incident radiation on the sample) and absorbance (the $\log_{10}$ of the reciprocal of transmittance). Molecular vibrations caused by IR are of two types: stretching which is a rhythmical motion along the bond axis and bending which brings about a change in bond angle. Only rhythmical change in dipole moment of molecules due to molecular vibrations are reflected in IR. The main focus of IR spectroscopy is the detection of functional group vibrations as the 'fingerprints' of molecules under probe (Silverstein et al., 2005). Fourier transform infrared (FT-IR) is the most popular and/or preferred method of infrared spectroscopy. FT-IR is precise, sensitive, enables sample recovery and is faster as compared to earlier techniques. It utilizes an interferometer which generates an interferogram, which is then transformed to the vibrational frequencies via the Fourier transform (a time-dependent mathematical function that deconvolutes wave forms into their corresponding frequencies) (Ernstsson & Wärnheim, 2007).

Attenuated Total Reflectance (ATR) is a sampling technique where IR radiation passes through a crystal, which enables total internal reflection at the sample-crystal interface and travels to the FT-IR detector. The evanescent wave (a portion of IR

radiation) travels into the sample during internal reflection and can be absorbed. Either liquid or solid samples can be placed onto the ATR crystal and analysed. Geranium and Zinc-Selenium are commonly used as crystal materials for ATR sampling while diamond is the best ATR crystal material. ATR-FTIR allows for rapid sampling, enhanced sample-sample reproducibility, reduced sample variation and improved spectrum acquisition as well as reproducibility (Kurrey et al., 2022).

Using solvent extraction method, FT-IR was used to qualitatively characterize nicotine in selected raw tobacco and local cigarette brands in Iraq (Al-Dahhan et al., 2022). A comprehensive chemical analysis of rapé (smokeless tobacco product of South America) using FT-IR also pointed out that the SLT is made from *Nicotiana rustica*. Identification of *Nicotiana* species as well as components of SLT other than tobacco such as areca nut, detection of nicotine and TSNAs using FT-IR was also performed on oral tobacco products (Stanfill et al., 2011; 2015). FT-IR analysis of tuibur tar has also presented a complex mixture of chemical constituents and has illustrated the heterogenous chemical environment of the SLT tar (Lalmuanpuii & Muthukumaran, 2016). In recent studies, employing chemometrics coupled with ATR-FTIR, total nicotine content has been quantified in Algerian SLTs via acid-base extraction of nicotine from the samples (Fekhar et al., 2023).

Raman spectroscopy is similar albeit complementary to IR given that it detects the interaction of light with matter but Raman spectrum arising from the scattering of photon that causes the change in polarization that manifests as vibrational frequencies of functional groups of molecules. This spectroscopic method employs Stokes and Anti-Stokes scattering to discern molecular structure of a sample. It is based on the principle of Raman scattering. When the LASER radiation of the near IR (NIR) or visible range interacts with a molecule, the LASER can undergo multiple scattering effects. Raman scattering is produced at higher energy levels when photons are scattered by excited molecules in which inelastic scattering of photons occur whereupon the kinetic energy of the incident particle is composed of Stokes and Anti-Stokes portions. Unlike Rayleigh scattering, Raman scattering is dependent on the polarizability of the molecule where the frequency of photons in the monochromatic light changes as it interacts with the vibrational states of a molecule. This makes

Raman Spectroscopy more sensitive to discern a molecule's framework as compared to IR which detects functional groups.

An advanced form of Raman Spectroscopy, Surface-Enhanced Raman spectroscopy (SERS), is a highly sensitive method in detection of molecules as a result of significant signal enhancement in comparison to normal Raman Spectroscopy. It utilizes nanotechnology by employing the surface chemistry of nanoparticles which exhibits higher surface area-to-size ratio of the material for better adsorption. The enhanced signal intensity being directly related to concentration of molecule, the increased surface area of the nanoparticle elicits a significant enhancement of the intensity of observed signal enabling better characterization and analytical capability.

Raman spectroscopy has been applied for the determination of alkaloid compounds from different plants including tobacco. Raman Optical Activity (ROA) spectroscopy was used to determine the presence of two trans nicotine conformers by obtaining ROA spectrum (Baranska et al., 2012). SERS with gold coated porous Si has been successfully used to characterize the presence of tobacco alkaloids in *Nicotiana tabacum* (A. Kumar et al., 2019). Raman spectroscopy has also been employed for the classification of three volunteer groups where tobacco consumers and oral cancer patients were differentiated from the healthy volunteer group using their saliva samples (Hole et al., 2022).

High-performance liquid chromatography (HPLC) is an analytical technique in chemical sciences used for the separation of compounds present in a chemical mixture. There are two phases in HPLC – mobile phase (composed of solvents/eluents comprising of a mixture of polar and nonpolar liquid components where the phase is in motion flowing through the column from sample injection to the detector) and stationary phase (immobile phase where the analyte undergoes physical separation). HPLC is able to detect different analytes via each analyte's retention time. The retention time is described as the time taken by the sample to move from the sample injection and the analyte‘s maximum peak signal in a chromatogram. When the affinity of analyte to the mobile phase is stronger, the faster retention time achieved, whereas greater the affinity of analyte to the stationary phase, slower retention time for that particular analyte is observed.

Two modes are generally applicable in HPLC depending on the mobile phase's composition. The HPLC system is referred to as a gradient eluent system when the composition of the mobile phase is changed (continuously or stepwise), however if the composition of the mobile phase remains the same during the entire separation period, it is referred to as an isocratic elution system. The column of HPLC is responsible for the desired separation of analytes in the sample as its efficiency is dependent on its inner diameter, length and particle size of the packing material. The detector produces a signal output in response to the separated analytes from the column.

HPLC is a common and effective separation technique for isolating compounds from tobacco and nicotine products. Nicotine was successfully separated and quantified from tobacco leaf extract by HPLC using ethanol as an eluent in the mobile phase (Fathi et al., 2018). The R and S enantiomers of nicotine have also been isolated from SLT, tobacco leaf extract, cigarette and e-liquids using normal phase HPLC; where the dominant (S)-(-)-nicotine was found in higher concentration than (R)-(+)-nicotine whose concentration was found to be much lower and similar all across the products. (H. Zhang et al., 2018) Aside from nicotine, HPLC has similarly been applied for the isolation of other components like tobacco sugars, solanesol and TSNAs (Hoffmann et al., 1979; Pang et al., 2006; Hu et al., 2015).

Mass spectrometry (MS), another powerful analytical tool in chemistry, works on the principle of ionization of a compound where the ions are differentiated based on their mass to charge (*m/z*) ratio. A number of ionization methods including gas-phase, electron impact, chemical, desorption, field desorption, fast atom bombardment, plasma desorption, laser desorption, evaporative, thermospray and electrospray methods are utilized for different samples. MS is commonly coupled with some sort of chromatography to introduce the sample into the spectrometer though direct insertion is possible in many instruments. An ion collector typically consisting of collimating slits, guides ions (a set at a time) onto the collector where ions are detected and amplified via the electron multiplier. The mass analyzer separates the ions according to mass-to-charge ratio (*m/z)* and it is typically recorded as a mass spectrum (Silverstein et al., 2005).

MS/MS or tandem mass spectrometry allows the fragmentation of the 'parent' ion of the initial fragmentation (from the conventional mass spectrum) to undergo further fragmentation leading to the formation of 'daughter' ions. These characteristic fragments or daughter ions, in complex mixtures, gives undeniable evidence for the presence of known compounds by providing further structural information. MS/MS is popularly used for ionizing crude samples owing to its selective detection of the required ions of study from the sample making it a powerful screening tool. This 'spectroscopic' technique of analysis eliminates the application of complex separation procedures. One way to accomplish MS/MS is to link in series, two or more mass analyzers to enable single ion selection followed by examination of the fragment ion (Silverstein et al., 2005).

HPLC tandem mass spectrometry (LC-MS/MS) is an impressive analytical tool that incorporates the impeccable separation ability of liquid chromatography with the highly precise and sensitive analysis of triple quadrupole MS. This technique is ideal for trace analysis and structure confirmation of the desired compound. N-nitrososarcosine (NSAR) was characterized using LC-MS/MS in both cigarette tobacco and smokeless tobacco products by electrospray ionization method proving to be a suitable analytical technique. (Wu et al., 2012) Tobacco sugar levels, alditols and humectants present in SLT products were determined using LC-MS/MS of which chewing tobacco contained the most sugar levels [9.3 – 27.5%(*w/w*)] (Wang et al., 2019). LC-MS/MS also proved useful for the determination of tobacco alkaloids and metabolites in urine samples with complete and efficient separation of nicotine and its metabolites (Marclay & Saugy, 2010).

UV-Vis spectrophotometry is a simple, reliable and cost-effective analytical technique that enables the determination of compounds at low concentration in samples of minimal quantity. This technique involves the absorption of near-UV and visible radiation by chemical species in solution. Electronic transitions occur in chemical species when they interact with the electromagnetic spectrum and absorb the energy. The amount of radiation absorbed by an analyte in solution under controlled conditions can be directly related to its concentration. Therefore, it can be useful in quantification of both organic and inorganic species (Worsfold, 2005). Absorption of the UV-Vis wavelength in the light spectrum is a frequent occurrence in organic

compounds and biomolecules. This spectroscopic technique is widely used in the determination of metabolites and proteins in biochemistry along with the kinetics of biochemical processes. It can be employed to determine micromolar concentrations of substances even though less sensitive than fluorimetry, it has a much wider range of applications (Rojas, 2005). Proteins absorb UV radiation owing to the presence of tyrosine, tryptophan and phenylalanine residues and conformational change determination can be performed using appropriate protocol and UV-Vis spectrophotometry (Biter et al., 2019). Enzyme activity and their kinetics can likewise be investigated by measuring the absorbance as well as rates of reactions using UV-Vis spectrophotometry methods.

1.7. Cell lines as model systems.

In vitro experiments are carried out using microorganism or cells outside their normal biological environment as model systems. These studies provide a starting point for biomedical researchers to garner insight into how the models respond to chemicals in an isolated environment. Cell culture is an *in vitro* model where the behaviour of plant or animal cells are studied under controlled environments. The exploratory experiments in cell culture began during the late 1800's and by the early 1900's, the first 'cell line' was developed (Rodríguez-Hernández et al., 2014). Since then, cell culture technology has seen significant advancements and now is considered a robust, reliable and relatively established technology. Cell culture is extensively used in academia as well as the industrial sector such as production of vaccine and drug discovery. They serve as excellent experimental models in basic and medical sciences by simplifying the experimental design and data analysis since cell lines are genetically defined and characterized. Studies on the effects of growth modulating substances, cytotoxicity of xenobiotics or other compounds, apoptosis, cell proliferation, activation and signalling can be executed using cell culture. In addition, genetic expression and cell cycle studies, pathology of cells, genetic manipulation and production of therapeutic drugs are all applications of cell culture (Arango et al., 2013).

Establishing cell culture systems can be accomplished from whole organisms, tissues, organs or biological fluids although it comes with biosafety risks. Newly

isolated cells or continuous cultures as well as supplementation of culture media with required organic and inorganic nutrients and antimicrobial agents counteracting contamination are key requirements to maintain proper a cell culture system. The main advantage of cell lines in experimental settings is the reproducibility and consistency of outcomes and results owing to their highly and precisely controlled physicochemical environment. Cell preparation techniques such as separation, fractionation followed by characterization are performed to obtain suitable samples for analysis and allow high yield and recovery. The first culture that grows successfully after isolation of cells from tissue is called the primary culture, then, the cells are sub-cultured/passaged until they reach senescence or in some cases, the cells are immortalized (Arango et al., 2013). Human cell lines are derived and propagated from primary cultures of human tissue or biological fluids and are immortalized cells. They are critical biological resources and are key players in toxicological studies, bioindustries and a variety of other applications. The American Type Culture Collection (ATCC) in their Cell Biology Collection has more than 1900 types of human cell lines in their roster which shows the importance of human cell culture in research.

Three types of cell lines are available, namely, primary (excised directly from tissue), immortalized (single cell type which can undergo serial propagation) and stem (self-renewable) cell lines. There are two modes for growing cell culture: cells in suspension (single cells or free-floating clumps) and attached/adherent cells (monolayer attached to the culture flask). The mode of growth reflects the type of tissue from which the cell line was derived. Adherent cells can be roughly classified into 4 main types depending upon their morphology, which are, epithelial [Figure 1.13.(a)], endothelial [Figure 1.13.(b)], neuronal [Figure 1.13.(c)] and fibroblast [Figure 1.13.(d)] cell types, while suspension cell lines are generally rounded in shape. The growth curve of cultured cells display a sigmoidal pattern to reach confluency. Firstly, they undergo the lag phase where cells adapt to their culture

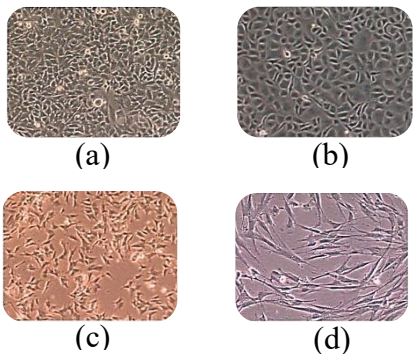

Figure 1.13. Types of adherent cells.
(a) Epithelial; (b) Endothelial;
(c) Neuronal; and (d) Fibroblast.

conditions and do not undergo division, secondly, they reach the logarithmic growth stage where active proliferation and cell density increases exponentially, this stage is where cells are most viable. The plateau or stationary phase is where proliferation decelerates and the cells become confluent and lastly, comes the decline phase where cell death is predominant and a reduction is seen in the number of viable cells (ECACC, 2018).

There are major advantages of using *in vitro* model systems as opposed to *in vivo*. *In vitro* systems use cells derived from tissues and have an infinite lifespan. This system provides the ability to study various biological processes under controlled conditions outside of the living organism. *In vitro* systems allow for specified experimental setups by the isolation of required components which in turn removes confounding factors otherwise present in complex organisms. It avoids the need for test subjects for research and drug testing eliminating ethical dilemmas concerning animal testing and human tissue/blood collection. This system also provides simple, cost-effective but efficient experimental models with reproducible outcomes besides enabling the management of multiple experiments simultaneously when compared to *in vivo* models.

Cell lines are invaluable *in vitro* model systems in molecular biology and biomedical research. They are widely used in cancer research as well as drug discovery. Historically, HeLa, RAJI, K562 and NB4 cell lines have been instrumental in the development of vaccines, treatment of cancer and the unravelling of infectious mechanisms (Mirabelli et al., 2019). Bioactivity of a variety of substances including plant extracts, fruit and tuber extracts, hormones as well as synthesized drugs have been successfully studied using cells lines by evaluating cytotoxicity (Pollio et al., 2016; Yao et al., 2019; Zaini et al., 2011; S. Zhao et al., 2002). Toxicity and/or bioactivity of tobacco in the form of smoked cigarette leachates, cigarette smoke and smokeless tobacco have been assessed using different kinds of cell lines as model systems (Johnson et al., 2009; Xu et al., 2019).

1.8. Bioactivity Assays.

The analytical techniques used for qualitatively or quantitatively measuring the presence, amount or activity of a target chemical substance, is termed as an assay. Cellular or cell-based assays are frequently used for compound screenings to determine if the substance has any effects on the proliferation of cells or cause cytotoxic effects eventually leading to cell death. For *in vitro* experiments, it is crucial to determine the viability of cells in use. There are a number of assays that can be utilized to estimate the number of viable cells such as tetrazolium reduction, protease activity and resazurin reduction assays which evaluate the enzyme activity or general metabolism as markers for the viability of cells. All these assays involve the conversion of a substrate to coloured or fluorescent products when incubating the cells with a reagent which can be detected using a spectrophotometer. Dead cells lose the ability to convert the substrate to product, this difference in product formation of live versus dead cells, forms the basis for many cell viability assays (Riss et al., 2004).

Tetrazolium reduction assays are frequently used assays in the determination of cell viability. Commonly used compounds include 3 - (4, 5 - dimethylthiazol - 2 - yl) - 2, 5 - diphenyltetrazolium bromide (MTT), 3 - (4, 5 - dimethylthiazol – 2 - yl) - 5 - (3 - carboxymethoxyphenyl) - 2 - (4 - sulfophenyl) - 2H - tetrazolium (MTS), 2,3-bis-(2-methoxy-4-nitro-5-sulphenyl)-(2H)-tetrazolium-5-carboxanilide (XTT) and water-soluble tetrazolium salt (WST-1) out of which MTT (positively charged) readily enters viable eukaryotic cells while the rest do not due to their negative charge. MTT was the first developed homogeneous assay for cell viability suitable for high throughput screening (HTS) to be performed in a 96-well plate format. It is a reliable and sensitive cellular metabolic activity indicator preferred over other methods. It is based on the ability of cellular nicotinamide adenine dinucleotide phosphate (NADPH) – dependent oxidoreductase enzymes to reduce the MTT dye to formazan crystals (Figure 1.14.) which is then dissolved using appropriate solvents. MTT assay has become the gold standard for the study of cell viability and proliferation from its inception and has inspired may modified versions of the assay including the previously mentioned MTS, XTT and WST assays (Gutiérrez et al., 2017; Iqbal & Keshavarz, 2017).

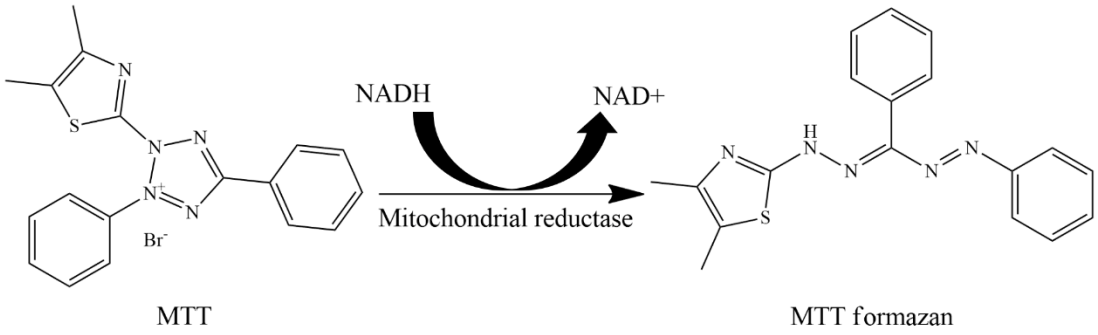

Figure 1.14. Reduction of MTT tetrazolium salt to MTT formazan crystal.

Dose-dependent cytotoxicity of smokeless tobacco extract on gingival epithelial cells (GEC) was assessed by Patil & Baeshen (2021), using the MTT assay. Tobacco dust exposure of bidi factory workers was studied to estimate tobacco dust induces genotoxicity by performing MTT assay in human blood lymphocytes treated with tobacco extract (Khanna et al., 2014). Tobacco smoke treated human adenocarcinoma lung epithelial cells (NCI-H292) was used as a model to determine the usability of MTT assay as a cytotoxicity assay where they found that the effect of complex chemical compounds such as tobacco smoke on cell viability could be assessed by using MTT assay (Caruso et al., 2021). Smokeless tobacco extracts prepared from different SLT products in Tabuk region, Saudi Arabia, were used to test for cytotoxicity and cell viability on human gingival fibroblast (hGF), human diploid lung tissue (MCR5), human liver cancer (HepG2) and human colorectal adenocarcinoma (HT29) cell lines by employing MTT assay as a high throughput screening method (Mesaik et al., 2022).

Protein estimation assays are analytical experiments designed to determine the concentration of specific or an array of proteins in a solution. Numerous colorimetric assay techniques as well as spectrophotometric and fluorescent-based assays have been developed over the years which has increased the accuracy and sensitivity of the process for protein content estimation. Before performing any kind of proteomics or comparative experiments, the estimation of total protein concentration in sample solutions is a key and routine step in molecular biology. These different kinds of assays are preferred over each other depending upon the downstream experiments to be

carried out. All of these protein assays have their advantages and disadvantages relative to ease of use, sensitivity and accuracy. Some of the colorimetric assays used for protein estimation are: (1) Biuret reaction, based on the formation of cupric ion and protein complex which gives a violet-purple colour at its end point; (2) The Lowry method, based on the amplification of the biuret method followed by a reaction with Folin phenol reagent; (3) Bradford assay (or CB dye-binding assay), works on the principle of Coomassie brilliant blue G-250 (CB) dye binding to proteins in acidic pH, resulting in a blue dye-protein complex with an increase in A_{max} at 595 nm from 465 nm in solution; and (4) Bicinchoninic acid (BCA) assay, an adaptation of the Lowry method, where cuprous ions, generated from cupric ions by reacting with protein in an alkaline environment, are detected (Becker et al., 1996; Shen, 2023).

Enzyme linked immunosorbent assays or ELISA(s) are assays utilized for the detection of minute quantities of antigens, antibodies, glycoproteins, proteins, peptides, nucleic acids, hormones, viruses and other substances in biological systems. ELISA, both a quantitative and qualitative colorimetric method, has evolved from other kinds of immunoassays and is at present a popularly used biological technique in clinical as well as basic science. ELISA utilizes antibody specificity and affinity to a diverse assortment of antigens for identification and quantitation of the analyte or molecule. To measure the presence of a particular analyte/molecule, an antigen or antibody is affixed to a solid surface which successively binds to a complementary antibody or antigen (Anagu & Andoh, 2022).

There are four main types of ELISA based on process of immobilization of the analyte, namely, direct, indirect, sandwich and competitive ELISA (Figure 1.15.). Direct ELISA is realized when the antibody is coupled or adsorbed directly onto the enzyme; whereas, in the case of indirect ELISA, the analyte is bounded by using a primary antibody after which a secondary enzyme-antibody conjugate is further added. Sandwich ELISA commonly requires the utilization of a pair of distinct monoclonal antibodies or alternatively, a mixture of polyclonal antibodies for capture and detection of the analyte. Competitive ELISA employs the addition of known quantity of the analyte to the analyte-containing sample along with a specific antibody (Drijvers et al., 2017).

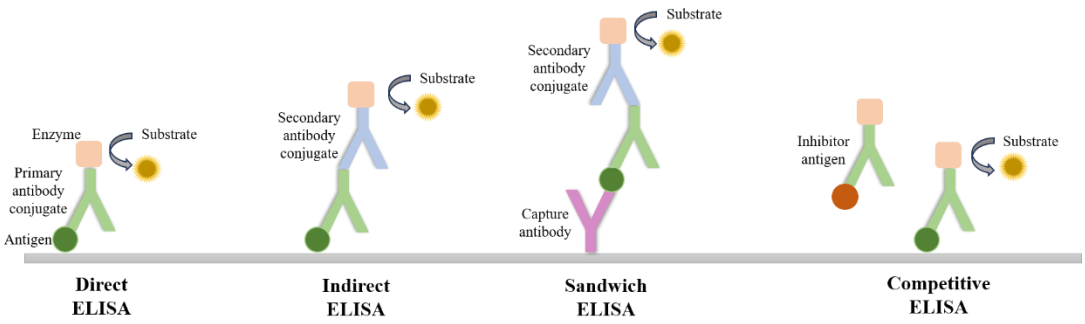

Figure 1.15. Schematic representation of types of ELISA.

Antioxidant enzymes are often used as oxidative stress biomarkers which include enzymes such as SOD, GPx and CAT. In order to detect and quantify these biomarkers, some form of ELISA is commonly used. Measurement of activity of these enzymes using ELISA can shed light on the mechanisms of oxidative stress in a biological system caused by a toxic substance. Antioxidant capacity is a fundamental tool used to measure the collective activity of antioxidants present in the biological system offering an integrated parameter as compared to a sum of single quantifiable antioxidants, thus, giving a more biologically relevant account. Total antioxidant capacity (TAC) assay assesses the redox status of the interaction of ROS with antioxidant enzymes and molecules helping to evaluate the environmental, nutritional and physiological factors in the system being studied. Common methods to measure total antioxidant capacity are the trolox equivalence antioxidant capacity (TEAC), ferric ion reducing antioxidant power (FRAP) and oxygen radical antioxidant capacity (ORAC) assays (Ghiselli et al., 2000; Fraga et al., 2014). TAC assay has been used for assessing the cellular total antioxidant capacity of cell lines (CHL/IU, TK6, L5178Y) treated with cigarette smoke (Yamamoto et al., 2022). Total antioxidant capacity assay was likewise used to determine the cellular antioxidant defence system of electronic cigarette aerosols treated human epithelial normal bronchial cells (Nuli1) (Ganapathy et al., 2017).

Nitric oxide ($NO^{\bullet}$) measurement is one of the frontline methods in research to assess pathological and physiological processes. Total $NO^{\bullet}$ determination is difficult as $NO^{\bullet}$ has a short half-life, i.e., a few seconds, therefore, total $NO^{\bullet}$ production is

estimated using nitrate as well as nitrite. Many advances in the development of various analytical techniques to determine nitrate and nitrite in biological samples has been observed. Some of these techniques include direct and indirect methods like colorimetric assay called Greiss Assay, fluorescent analysis, chemiluminescence, flow or sequential injection analysis and electrochemical detection in addition to chromatographic separation techniques. The determination of nitrate and nitrite can be accomplished using different biological fluids such as saliva, urine, blood serum and plasma, cerebrospinal fluid (CSF) and tissue culture medium (Guevara et al., 1998; Jabit et al., 2009).

Greiss assay, also known as diazotization assay, has been used extensively in biological sample analysis. This assay is based on the treatment of nitrite in acidic media with a diazotizing agent (e.g., sulphanilamide) forming an intermediate diazonium salt, which reacts with a coupling reagent (N-naphthyl-ethylenediamine) forming a stable azo compound whose absorbance can be spectrometrically measured at ~540 nm. The reagents mostly widely used for this assay in quantitative analyses are sulphanilamide and N-naphthyl-ethylenediamine (NED or NEDA) (Csonka et al., 2015; Tsikas, 2007; Sun et al., 2003). The azo dye produced at the end of Greiss reaction is purple in colour and is water soluble with the formula $C_{16}H_{13}N_3SO_3$. Acidified Greiss reaction held much importance in the estimation of $NO^{\bullet}$, formed from macrophages and released via endothelium, in haemoglobin. Diazotization from sulfanilic acid with naphthylamine and derivatives yields azo dyes with an absorbance in visible range i.e., 540 nm while 2, 3 - diaminonaphthotriazole results in a highly fluorescent and stable 2, 3 – naphthotriazole (NAT). Diazotization reaction is nitrite specific and depends on the presence of acid (Tsikas, 2007). Greiss assay has been successfully used for the determination of $NO^{\bullet}$ generation in body fluids such as serum, urine and CSF by Guevara et al. (1998). A modified Greiss assay was also employed to asses NO_x in blood plasma with precision and accuracy as well as to quantify the rate of recovery of nitrate and nitrite (Giustarini et al., 2008). The endogenous production of $NO^{\bullet}$ was also assessed in Murine endothelial cells using the Greiss reaction (Cartwright et al., 2000).

Fluorescence microscopy functions on the basis of a phenomenon called fluorescence. Fluorescence is a type of photoluminescence, where, the absorption of

photons (from ultraviolet or visible light) in the singlet ground state results in excitation of the molecule to singlet excited state with re-emission of radiation which ceases very shortly after the excitation source is extinguished (Figure 1.16.). The emitted radiation/photon is lower in energy as compared to the absorbed photon (due to vibrational relaxation emitting energy in the form of heat) which results in longer wavelength of the emitted light as compared to that of the absorbed light. This shift in emitted radiation energy towards the longer wavelength is called Stokes shift. A molecule with the ability to undergo fluorescence is called a fluorophore. The principle of fluorescence microscopy lies in the utilization of fluorescent dyes or stains called fluorophores for tagging cellular structures/molecules of concern. It is an useful tool to discern the functioning and spatial information concerning endogenously auto-fluorescent and exogenously tagged/labelled structures or molecules. There are two main sources of light in fluorescence microscopes: mercury vapour and xenon arc lamps; they excite the fluorophore/fluorochrome which then emits fluorescent light. Fluorescence microscopes separate emitted light from the excitation light which is achieved via optical filters and efficient imaging depends on the selection of light with respect to the indicators in use. This device is applied as an investigative instrument for organic as well as inorganic materials and live or fixed cells or tissues (E. C. Jensen, 2012).

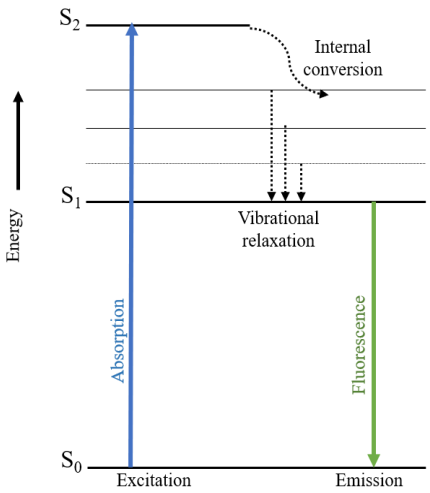

Figure 1.16. Jablonski diagram.

There are different types of fluorescence microscopes used today. Epifluorescence microscopy operates by focusing the emitted light as well as fluorescence on the detector using the same objective as that of the excitation. Confocal microscopy includes one or more detectors, multiple wavelength selective laser systems, a beam scanning ensemble and computer for output, image display, processing as well as storage. Multiphoton fluorescence excitation microscopy use high energy lasers which results in non-linear optical effects like multiphoton fluorescence due to the large energy density at the focal point. Total internal reflection

fluorescence (TIRF) microscopy, fluorescence correlation spectroscopy (FCS), fluorescence recovery after photobleaching (FRAP), fluorescence lifetime imaging (FLIM) and fluorescence resonance energy transfer (FRET) are other techniques used in fluorescence microscopy (E. C. Jensen, 2012; Sanderson et al., 2014).

Fluorescent dyes are substances which absorbs as well as emits light strongly in the visible region of the electronic spectrum and have intense fluorescence properties. Fluorescent staining is an advanced visualization technique that provides high resolution imaging with specificity and applications in flow cytometry, immunofluorescence as well as fluorescent in situ hybridization (FISH). There are different fluorophores employed for tracking, isolating and identifying a specific molecule or substance within the cell. Rhodamine and fluorescein are good examples for amine-reactive probes used for cell tracing, immunochemistry, FISH, fluorescent analogue cytochemistry and radiolabelling by forming bioconjugates. Proteins and nucleic acids are commonly labelled by using thiol-reactive probe for detecting ligand-binding mechanisms, conformational change and multi-subunit complex formation (Huber et al., 2018).

Dyes such as acridine orange easily navigates the cell membranes and accumulates in the lysosomes since it is a weak base and facilitated by means of an ATP dependent proton pump in the membrane. This helps in detection of and differentiation of cell death because of the acridine orange being intact in the initial stages of apoptosis in the lysosome and removed from the organelle when necrosis occurs (Vermes & Haanen, 1994). Ethidium bromide, a fluorescent dye, which intercalates between DNA base pairs as well as RNA, is another valuable dye for DNA visualization and yields consistent results. Dual staining by acridine orange and ethidium bromide (AO/EB) on osteosarcoma cells to differentiate apoptotic cells proved to be a reliable method by Liu and collegues (2015). AO/EB fluorescent microscopy verified to be a reliable technique in detecting apoptosis in human leukocyte cells giving reproducible results (Baskić et al., 2006). Dual AO/EB staining therefore, is an economical, consistent and reproducible method to be used for fluorescent microscopy staining.

Flow cytometry (FC) is a laser-based technique for the qualitative as well as quantitative measurement of intrinsic (size, shape, granularity, density and pigment presence) and extrinsic (DNA composition, content and/or synthesis; receptors – internal and external, like antibodies; structural modifications of cellular membrane, apoptosis and necrosis plus physiological factors) characteristic properties of individual cells in a heterogenous cell population. FC runs on the principle of physical property dependent scattering of light based on the size of a particle passing through a laser beam which is recorded using an opto-electronic coupling system. Fluidic systems (solution suspended cells) are introduced into the sheath flow stream within the flow chamber where up to thousands of events can be measured per second. Modern FCs are multi-color system, i.e., they sort cells with the application of three to five laser systems by measuring over 15 parameters. As the laser beam encounters the cell, forward scattering of light (FSC) reveals size, while side scattering (SSC) discloses internal complexity and granularity of the cell. Besides, FC measures the intensity of fluorescence emitted from individual cells when labelled with fluorescent stains or molecules. Absorption and emission spectra of these fluorescence compounds are specific at particular wavelengths of excitation as well as emission. Detectors produce an electronic pulse upon collecting light signals processed via the electronic system. The parameters of the electronic pulse is dependent on the cell size and shape in addition to fluorescence intensity (Alfonso & Al-Rubeai, 2011; Chantzoura & Kaji, 2017).

One important application of FC is the separation of sub-populations of cells predicated on viability, reactivity, phenotype, DNA content and physiological aspects. Fluorescence-activated cell sorter or Flow-activated cell sorting (FACS) is a specialized form of FC dependent on the deflection of charged droplets. The vibration of the flow chamber deflects the charged droplets where they undergo electrostatic charge via deflection plates and are deflected to the right or left collection tube dependent on their charge. In simple terms, cell isolation is indicated via FSC, SSC and fluorescence intensity of a channel (Alfonso & Al-Rubeai, 2011; Chantzoura & Kaji, 2017). Conventional FC analysis consists of gating a cell population and applying analytical parameters on the gated cells. cell cycle analysis is performed via ploidy modelling to determine the cell cycle phases and high dimensional data analysis

uses analytical tools such as Spanning-tree progression analysis of density-normalized events (SPADE), t-Distributed Stochastic Neighbour Embedding (tSNE), Principal component analysis (PCA) and FLOW clustering without K (FLOCK) (McKinnon, 2019).

Some common applications of flow cytometry includes protein expression studies using fluorescent proteins such as GFP, CFP, YFP and mCherry; cell proliferation studies using dyes such as fluorescein and cell physiology analyses. Cell physiological processes such as intracellular pH determination. Cellular membrane potential, antioxidant concentration, calcium concentration as well as ROS generation can all be determined using FC. The intracellular production of H_2O_2 can be monitored and quantified using FC. The most widely used ROS activity fluorogenic probes are dihydrorhodamine 123 (DHR123) and 2',7'- dichlorofluorescin - diacetate (DCFH-DA) (Alfonso & Al-Rubeai, 2011). The measurement of induced ROS production using DCFH-DA and flow cytometry in nanomaterial treated human leukocytes and whole blood was found to be reliable and accurate (Kermanizadeh et al., 2018).

CHAPTER 2

MATERIALS AND METHODS

CHAPTER 2

MATERIALS AND METHODS

The age-old practise of tuibur is a traditionally significant custom among the people of Mizoram. Research studies on characterization, environmental as well as biological effects, whether related to the pros or cons of tuibur, is extremely limited. It is crucial to put to light the constituents along with the health effects of this distinct tobacco-smoke infused concoction as analogous products related to tuibur are a rarity. This chapter describes the detailed protocol of characterization of different grades of tuibur using analytical spectroscopic techniques, in addition to providing comprehensive protocols used to assess the biological effects, in the form of biological assays combined with spectroscopy and microscopy.

2.1. Tuibur manufacturing.

Tuibur is uniquely prepared from burning tobacco even though it is categorized as a smokeless tobacco product. Locally made by small scale cottage industries in Mizoram, it employs an exceptionally innovative method of manufacturing though it has been traditionally practised for ages. Tuibur production starts with obtaining a mixture of different parts of the tobacco plant i.e., tobacco stalk, veins and petioles. Harvested *Nicotiana tabacum*, grown by Mizo farmers, undergo tramping and sun drying followed by dissection of the dried brown leaf to isolate the petioles, stalk, central vein and lamina. Though used for home production of tuibur as well as zozial (lamina of the leaf), locally grown tobacco is deemed undesirable for mass production of tuibur; consequently, jute bags of mixed tobacco petioles, stalk and veins are imported from the neighbouring country of Myanmar. Myanmar grows two main varieties of tobacco – *Nicotiana rustica* (hsey ywet kyee) and *Nicotiana tabacum* (Viginia), mainly in the regions of Mandalay and Magway (Sein, 2020). These two varieties are combined in a 1:3 ratio (*Nicotiana rustica* : *Nicotiana tabacum*) and is deemed as the standard for tuibur production. Myanmar tobacco curing follows a procedure where tobacco leaves sprayed in brine solution (slaked lime solution) to prevent fungal growth, are layered in piles inside a pit with a depth of ~ 3 to 4 ft and

covered with soil for fermentation. The fermented brown coloured leaves are taken out after ~1 or 2 months, the leaves get separated into lamina (retailed for the manufacturing of cigarettes), veins and petioles. In addition, the main stalk of the plant is likewise cut down and sundried, and are cut along with the veins and petioles into even sizes and packed (Lalmuanpuii, 2016).

The tuibur manufacturing setup consists of iron containers stacked upon one another. The upper chamber called 'Tuibur Lu' is literally translated to 'tuibur head'. It has on its underside a hole at the center to insert 'Tuibur Lai' (joint/connector) which is placed vertically below it to connect the upper chamber to the lower chamber 'Tuibur Mawng', situated at the bottom of the contraption. The tuibur lai is sealed on the outside using clay to keep the apparatus fixed which can be eventually destroyed to decant tuibur and discard by-products like tar from the lower chamber. Pipes are connected to the lower chamber to allow hydro-powered suction of air inside the lower chamber via a body of running water such as a small stream or river near the manufacturing site. This is achieved by placing pipes in rapidly flowing/running water diverted from rivulets or streams through large pipes. This is to ensure that aspiration takes place inside the lower as well as upper chamber of the setup to allow smoke to pass (Figure 2.1.).

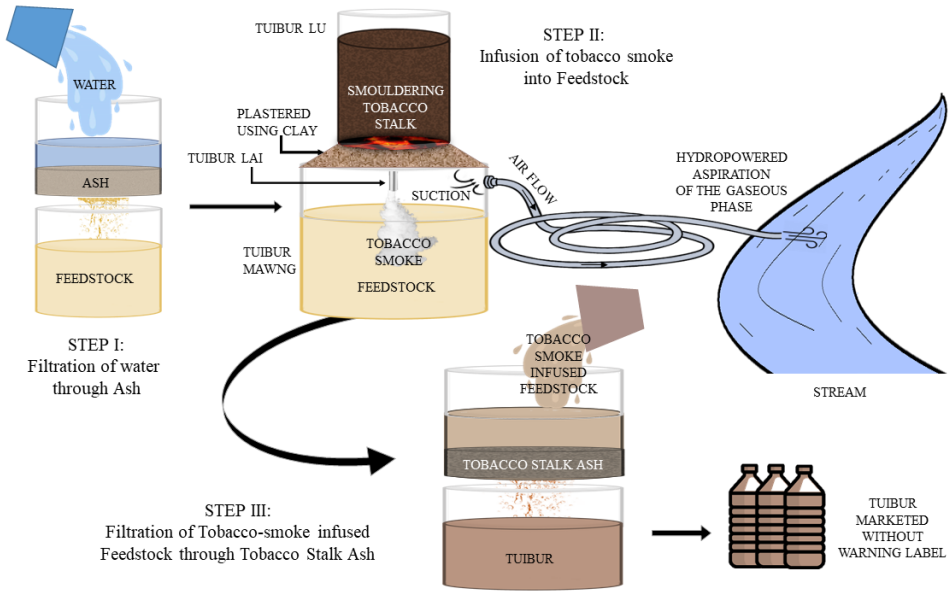

Figure 2.1. Tuibur Manufacturing setup.

The general protocol followed for tuibur manufacturing is as follows:

Step 1: Feedstock is prepared by filtering water through ash to render it alkaline. The water used for feedstock preparation is acquired from the stream or rivulet near the factory, local wells, government supplied tap water or water bought in tanks from water sellers, though it is more likely the former. The ash used for turning the water alkaline is either bought in bags from rural areas inside Mizoram or the tobacco ash burnt up during tuibur processing is used. This practise differs from factory to factory. The ash filtered water (feedstock) thus produced is called "Chingal" (Figure 2.2.).

Figure 2.2. Ching al preparation.

Step 2: Production of tuibur ensues by tightly packing the tuibur lu with the tobacco stalk, veins and petioles. Tuibur mawng is filled with the previously prepared chingal, just enough to submerge a part of the tuibur lai (joint). The tobacco placed in the upper chamber is then scorched, the smouldering tobacco produces tobacco smoke, which is sucked through tuibur lai into the liquid ching al contained inside the lower chamber [Figure 2.3.(a-d)]. The polar components or particulate phase of tobacco smoke such as nicotine, TSNAs, phenols, humectants, terpenoids, carboxylic acids, etc., gets dissolved with ease into the alkaline water. The smoke passes over the alkaline water and bubbles inside tuibur mawng, followed by the release of excess smoke via the pipes connected to the stream. The hydro-powered aspiration process employed via the pipe system allows for this to occur easily.

Step 3: In this step, crude tuibur is poured out of the tuibur mawng. This concoction is now ready for commercial distribution. Furthermore, some factories add an extra step where they filter the concoction through the tobacco ash that has been used for producing tobacco smoke. Others also add lime to their tuibur mixture in order to increase the alkalinity and heighten its potency.

Figure 2.3. (a) Smouldering tobacco stalk inside tuibur lu; (b) Tuibur manufacturing apparatus; (c) Water source; (d) Tuibur factory; (e) Bottled Tuibur.

There are different grades of tuibur available for purchase. The different grades of tuibur are produced based on the amount of tobacco per litre of water used as well as the duration of smouldering the tobacco (approximately 12 hours). The longer the duration of smouldering, the higher the grade, likewise, the greater the amount of tobacco used, the higher the grade of tuibur. The duration of smouldering automatically becomes longer while producing the higher grades of tuibur due to the greater amounts of tobacco used. Local names of tuibur grades include terms like Al, Al lo, Double, Bol Bol, etc. which literally describes whether the tuibur is alkaline (Al) or not (Al lo). Tuibur is bottled/re-bottled (used plastic bottles from commercial beverages) in plastic disposable containers which are reused over and over [Figure 2.3.(e)].

2.2. Sample Collection.

For this study, a total of 10 Tuibur samples of different grades (Figure 2.4.) were collected in and around Aizawl, Mizoram; covering the major manufacturers and suppliers of the city. Tuibur samples are graded locally by sellers, such that the alkalinity or grade of the product is reflected. For uniformity in this study, the samples were graded according to the concentration (g/L) of tuibur, i.e., the amount of tobacco used per litre of water. This study's tuibur grading system is as follows – low (100-300 g/L), medium (300 – 500 g/L) and high (500 and above g/L). The list of collected tuibur samples is as seen in Table 2.1. The pH measurements of each tuibur sample was taken using a pH meter (Electronics India Deluxe pH meter, Model 101) at room temperature, in triplicate.

Figure 2.4. Collected Tuibur samples.

Table 2.1. List of tuibur samples collected.

Sl. No	Sample ID	Place of Collection	Grade	g/L of Tobacco
1	T1	Armed Veng	Medium	333
2	T2	Armed Veng	Low	167
3	T3	Falkland 1	Medium	357
4	T4	Falkland 1	Medium	429
5	T5	Falkland 1	High	571
6	T6	Falkland 1	High	857
7	T7	Falkland 2	Medium	438
8	T8	Falkland 2	Low	250
9	T9	College Veng	High	686
10	T10	Armed Veng	High	500

2.3. Chemical analysis using ATR-FTIR.

Attenuated Total Reflectance Fourier-Transform Infrared Spectroscopy is a technique that allows the detection of functional groups through vibrational transitions via absorption of infrared radiation in a chemical compound. Attenuated total reflectance allows direct examination of the samples by means of a high refractive index crystal, requiring minute amounts of sample leading to minimal sample loss. ATR-FTIR measurements was coupled with chemometrics (a statistical analysis tool) to semi-quantify specific chemicals present within 21 collected samples.

2.3.1. Standard Samples.

Benzoquinone (≥98%), Hydroquinone (≥99%) and Nicotine (1.0 mg/mL in methanol) were purchased from Sigma-Aldrich. Methanol (99.5%), analytical reagent, was purchased from SDFCL Sd Fine Chem Limited. The high solubility of quinones and nicotine in methanol was used to obtain accurately mixed solutions. 1.0 mg/mL of Benzoquinone and Hydroquinone in Methanol (w/v) were prepared as stock solutions. The stock solutions were thoroughly mixed using a vortex. Serial dilution was performed (v/v) for each of the standard chemicals (Benzoquinone, Hydroquinone and Nicotine) using Methanol as a common solvent from the stock solution in concentrations ranging from (v/v) 1 to 0.0019 mL in 1.5 mg/mL microcentrifuge tubes (Tarsons). The standard samples were mixed thoroughly by pulsation using a pipette (Tarsons Accupipette).

2.3.2. Sample Preparation.

Tuibur samples (10) of different grades were collected from factories (consisting of major local Aizawl market suppliers) located in Aizawl, Mizoram. (Table 2.1 & 2.2) The samples were refrigerated in order to retain their properties prior to measurement. No digestion or extraction of the samples was performed.

2.3.3. ATR - FTIR Spectral measurement.

ATR - FTIR spectroscopy measurements were performed using IRAffinity-1S Fourier Transform Infrared Spectrophotometer, SHIMADZU, Japan. The standard chemicals and test sample spectra were collected between 4000 – 400 cm^{-1}, with a nominal resolution of 16 cm^{-1} and a scan rate of 40 scans per spectrum. A background scan (blank) was performed before introducing each sample. To avoid contamination and to ensure the elimination of residuals from the previous samples, the sample holder and tip of the ATR sample holder was wiped down thoroughly with chloroform before measuring each new standard and test sample. Each liquid sample was vortexed to ensure homogenisation before loading onto the sample holder. The absorbance values for the spectral data of each standard and test samples were exported using Lab Solutions software.

2.3.4. Multivariate Analysis using Chemometrics.

For prediction of concentration of nicotine, hydroquinone and benzoquinone in unknown (tuibur samples), multivariate analysis was utilised. Multivariate analysis produces a more reliable and accurate quantification as compared to univariate method by allowing the identification of incongruities in the selected region of the spectral data by means of using a large number of variables. Partial Least Square (PLS) Regression analysis was performed using Unscrambler X (version 10.4.1) by Camo Analytics. PLS enables the discovery of latent (hidden) variables in the X-matrices by modelling the X and Y matrices.

The PLS-R decomposition takes the form as follows:

$$X = TP^T + E \qquad (1)$$

$$y = Uq^T + f \qquad (2)$$

where, T & P = the scores and loadings of spectral data matrix X, E the residual matrix of X;

U = the scores matrix of concentration matrix;

y, q & f = the loading and residual vector of y.

2.3.5. Standard Solution Calibration and Validation models.

10 standard samples each of benzoquinone and hydroquinone were taken as calibration and validation sets. 7 samples form a calibration set while 3 samples were used as a validation set. As for the Nicotine calibration model, 11 samples were taken as calibration and validation sets. 7 samples form a calibration set while 4 samples were used as a validation set. Significant spectral regions of the standard samples were selected for predicting the concentrations in tuibur samples. Tuibur sample concentration prediction was executed using the calibration model of prepared standard solutions of known concentration.

2.4. Nicotine characterization using SERS.

Raman spectroscopy is a technique that utilizes the existence of Stokes and Anti-stokes scattering in the examination of the vibrational and rotational modes of a molecule. Surface-Enhanced Raman Spectroscopy utilizes nanomaterials to increase surface area to enable signal enhancement which produces a highly sensitive chemical structure probing technique.

2.4.1. Synthesis of spherical-shaped gold nanoparticle.

Spherical-shaped gold nanoparticles were synthesized by a single step heating method. In 99 mL of deionized Milli-Q (Resistivity: 15 MΩ.cm) was taken in a three-neck round-bottom flask with one neck fitted with water condenser while the other two were fitted with stopper used for chemical addition. The water in the three-neck round-bottom flask was heated to boil under a constant magnetic stirring (150 RPM) after which 1.25 mL of 10^{-2} M $HAuCl_4.3H_2O$ solution was added dropwise into the water and made to boil. In this vigorously boiling water, 750 mL of 1% trisodium citrate solution was further added drop-by-drop at a constant rate under constant stirring condition As the solution started boiling again, the colour of the solution changed from black to blue, then violet, and finally to blood red. The solution was kept under the same boiling and stirring condition for another 30 minutes to complete the reaction. Upon completion of the reaction, heating was discontinued and subsequently, the solution was allowed to cool down to the room temperature with constant stirring. the cooled nanoparticle solution was then centrifuged at 5000 RPM in a *Thermo Scientific Heraeus Biofuge Stratos* centrifuge. The centrifuged nanoparticle was then collected, diluted and its absorbance was measured to understand its plasmonic properties and TEM was performed to ascertain their size, shape, and crystallinity.

2.4.2. Sample preparation and spectral data collection.

SERS was performed using a homemade Raman setup. A continuous wavelength diode-pumped solid-state laser from Laserglow Technologies, Canada (LRS0671- PFM-00300-03), operating at 671 nm as an excitation light source was used (at a fixed excitation energy of 3 mW, using neutral density filters throughout the experiment). An In Photonics made 670 nm fiber optics Raman probe with a spectral range of 200-3900 cm^{-1} (Stokes) for sample excitation and data collection was used for efficient focusing and filtering. The Raman probe consists of two single fibers (105

μm excitation fiber and 200 μm collection fiber) with filtering and steering micro-optics (numerical aperture 0.22). The excitation fiber was connected to a Thorlabs-made fiber port to align the laser, whereas the collection fiber was connected to a spectrometer. A miniaturized QE65000 scientific-grade spectrometer from Ocean Optics was used as the Raman detector with a spectral response range of 220-3600 cm^{-1}. The Raman spectrometer was equipped with a TE-cooled 2048-pixel charge-coupled device and was interfaced with a computer through a USB port. The obtained Raman spectrum was collected using the Ocean Optics data acquisition SpectraSuite software.

20 μL of the above synthesized gold nanoparticles (AuNP) colloidal suspensions was dispersed into 5 μL each of tuibur (10 samples) and nicotine standard solutions, respectively. These mixtures were then diluted to 200 μL. This diluted AuNP composite was then taken in a sample holder for surface-enhanced Raman spectral (SERS) measurements. SERS measurements assess the intensity of nicotine C-N vibrational frequency peak at 1030 cm^{-1} for standard as well as tuibur samples, respectively. Obtained raw data were subsequently processed using Origin Pro (2018) for plotting the vibrational spectral features.

2.4.3. Statistical Analysis.

Pearson's correlation analysis was performed using SPSS v16.0 statistical software. Correlation between the pH and peak intensity in conjunction with the nicotine vibrational frequency band intensity versus concentration (g/L of tobacco) of tuibur samples was performed. The result of statistical evaluation was regarded as significant when the $P \leq 0.05$.

2.5. Alkaloid concentration estimation using LC-MS/MS.

Liquid chromatography tandem mass spectrometry (LC-MS/MS) was utilised to offer a highly selective and sensitive technique for concentration determination of nicotine and cotinine in the collected tuibur samples (Table 2.1).

2.5.1. Sample preparation and LC-MS/MS analysis.

Stable isotope-labelled internal standards (ISTDs) were prepared prior to sample analysis. The tuibur samples were diluted using 1M ammonium acetate buffer (pH 6.5) and filtered using a syringe filter (13mm, 0.22µm). After further dilution using deionized water, the samples were mixed with the ISTDs. The prepared tuibur samples (10 µL/sample) were injected into the LC-MS/MS instrument. LC – MS/MS was performed following the experimental method described by Shih et al. (2019). The eluted samples were ionised to generate charged particles using electrospray ionisation. The charged particles then pass through a series of three quadrupoles where the parent ion is selectively rendered to pass through the ionizer (first quadrupole) to generate fragment daughter ions. The generated fragments then travel to the third quadrupole (mass filter) which only transmits ions with a specified *m/z* value. These fragmented ions are the quantified via an electron multiplier. This is also known as multiple reaction monitoring (MRM) mode as fragmentation a induced by colliding inert nitrogen gas with the parent ion and the prominent daughter ion is considered for quantitation. Since both the parent and subsequently the daughter ion is quantitatively analysed, the analysis of nicotine and cotinine are considered more reliable and more accurate. Henderson-Hasselbalch equation was used to calculate the amount of unionised nicotine in each sample as follows:

$$pH = pK_a + \text{Log}_{10}([A^-]/[HA])$$

2.5.2. Statistical analysis.

Linear regression along with Pearson's correlation were performed using Origin Pro (V 8) and SPSS v16.0 to assess the relationship between g/L of tobacco used vs. concentration of tobacco specific alkaloid. The result of statistical evaluation was regarded as significant when the $P \leq 0.05$.

2.6. Assessment of oxidative stress effects of Tuibur.

Behavioural studies of biological systems exposed to tuibur are scarce in number. The following set of experiments aims to highlight toxicity in terms of oxidative stress as well as DNA damage in cells exposed to tuibur and its corresponding chemical constituents.

2.6.1. Micronucleus assay on buccal epithelial cells.

2.6.1 (a). Sample collection, preparation and dual staining.

As a preliminary investigation, Micronucleus assay was performed on a randomised group of volunteers. The population chosen for sample collection was aged between 20 – 60 years of age, having no tobacco habits along with volunteers with tuibur habits and sahdah habits. A total of 300 epithelial cells swabs from the oral mucosa of tuibur consumers (n =100), sahdah users (n=100) and no tobacco habit control group (n=100) were collected from willing volunteers from certain regions of Mizoram. The buccal epithelial cells were collected by swabbing the buccal mucosa (inner lining of both cheeks) by means of an interdental brush. The volunteers were advised to rinse their mouth prior to swabbing. The collected epithelial cells were stored in 1X PBS for further analysis. Cells were fixed onto glass slides using 70% ethanol. Fluorescent staining was performed using acridine orange dye. Stained cells were scored using a EVOS fluorescent microscope (Invitrogen by Thermo Fisher Scientific). The number of micronuclei per cell were scored per 1000 cells per sample in duplicate.

2.6.1 (b). Statistical analysis.

Pearson's correlation was performed using SPSS v16.0 to assess the relationship between age vs. MN count, Dose vs. MN count and duration of use vs. MN count. ANOVA test was performed followed by the Tukey's HSD test to determine the significant difference between the three sample groups - controls, tuibur users and sahdah users. The statistical evaluation output was regarded as significant when $P \leq 0.05$. Statistical analyses were performed using SPSS v16.0.

2.6.2. Choosing cell line as a model system.

Tobacco use has been linked to several forms of cancer. Cancer of the gastro-intestinal tract including stomach, intestinal and oesophagus have been associated with the use of tobacco products. The association of increased gastric cancer incidence and aggressiveness as well as mortality due to tobacco use has been widely documented. (Trédaniel et al., 1997) Phukan et al. (2005) has also linked stomach cancer and tobacco use among the population of Mizoram. Moreover, Malakar et al. (2012) had also stated that tobacco use along with tuibur use were important risk factors for the development of gastric cancer in Mizoram. Therefore, Human Gastric Adenocarcinoma (AGS) cell line, was chosen for the experimental model system of this research. AGS cell line originates from the isolated gastric adenocarcinoma tissue of a caucasian female, aged 54, in 1979. It is a hyperdiploid human cell line exhibiting epithelial morphology and is an adherent (monolayer) cell type. (American Type Culture Collection, 2003) AGS cell lines have been used for a number of cytotoxicity studies for different types of substances ranging from drugs to plant extracts to nanoparticles. All the following cell culture experiments were conducted inside a laminar-flow cabinet or tissue culture hood which was sterilised using uv light and wiped down with alcohol each time prior to the start of the experiments.

The AGS cell line used in the following experiments was purchased from the National Centre for Cell Science (NCCS), Pune, India. The purchased cells were kept in a T-25 (Tarsons) cell culture flask with RPMI 1640 (Gibco) culture media and supplemented with 20% Fetal Bovine Serum (FBS) and 5% Penicillin – Streptomycin Pen Strep (Gibco) at 37˚ C with 5% CO_2 in an incubator and left to grow. The RPMI 1640 cell culture medium is a mammalian cell culture medium composed of glutathione, vitamin B_{12} and others, biotin and para-aminobenzoic acid (PABA), in addition to the main constituents such as glucose, salts and amino acids. Fetal bovine serum, a widely used serum-supplement in cell culture, is used due to its elevated content of embryonic growth promoting factors to satiate specific metabolic requirements of the cell in culture. Pen Strep is added as an antibiotic supplement to the culture media to restrict bacterial contamination. Upon attaining 70 - 80% confluency (population doubling time is approximately 20 hours), the cells were detached from the flask using Trypsin (Gibco), a proteolytic enzyme; and sub –

cultured/passaged into T-25 (with 5 mL culture media) and T-75 (with 10mL culture media) cell culture flasks for further use.

2.6.3. Cell seeding.

Cell seeding at the correct density is an integral part of cell culture basics. The confluent flask of AGS cell line was detached using Trypsin (covering 0.5 mL per 10 cm^2) from the wall of the flask. The cells were processed according to the normal passaging protocol for adherent cells as per the GIBCO, cell culture basics handbook. The pelleted cells were suspended in a minimal volume of media. Trypan Blue exclusion was performed by mixing AGS cell line in media (10 µL) with 0.4% Trypan blue in 1X PBS (10 µL) in a 1:1 ratio, to score the viable cells. Trypan blue is an anionic hydrophilic azo-dye which labels only dead tissue/cells to a blue colour. The dye was incubated with the cells for 3 minutes to allow the dye to penetrate the cell membrane of dead cells. After incubation, the cell and dye mixture was loaded onto a haemocytometer for counting. The viable cells were counted from all 4 quadrants of the haemocytometer, and the cell concentration was calculated as follows:

Cell concentration (per mL) = Average number of cells per square x Dilution factor x Depth of Haemocytometer

where, the dilution factor = 2 (for 1:1 cell to dye ratio)

the depth of hemacytometer = 10^4 (for 0.1 mm depth,

i.e., each large sq. is $1/10{,}000^{th}$ of a mL)

The cell suspension after counting, was diluted to the seeding density as recommended by GIBCO, cell culture basics handbook, for each type of culture well-plates used.

2.6.4. MTT Assay for Cell Viability.

MTT or 3 - (4, 5 - dimethylthiazol - 2 - yl) - 2, 5 - diphenyltetrazolium bromide assay is a colorimetric assay used for measuring the metabolic activity or viability of cells. The assay is based on the principal that viable cells with metabolic activity promotes the reduction of MTT tetrazolium salt to a purple-coloured insoluble formazan crystal with an absorbance maximum (A_{max}) close to 570 nm. MTT is

reduced by the enzymes in the mitochondria and lysosomal/endosomal compartments after entering cells via endocytosis and is transferred to cell surfaces to form needle-like MTT formazans. MTT assay measure viability in terms of reductive activity as dehydrogenase present in mitochondria of living cells convert tetrazolium to insoluble formazan though there is involvement of reducing agents as well as enzymes in organelles like endoplasmic reticulum in this process. (Kuete et al., 2017)

Dead cells lose the ability to convert MTT to purple formazan hence making the change in colour a convenient viability marker. The insoluble MTT formazan crystals accumulate inside the cell and also deposits on the cell's surface as well as culture media. These crystals require solubilization prior to absorbance measurement. This is commonly achieved by solvents such as acidified isopropanol (IPA), dimethylsulfoxide (DMSO), dimethylformamide (DMF), sodium dodecyl sulphate or sodium lauryl sulphate (SDS) along with combinations of organic solvent and detergent to stabilize the colour formation, avoid evaporation and to reduce phenol red and other culture media interference.

2.6.4 (a). Cell viability.

To access cell viability, AGS cell lines in RPMI 1640 (Gibco) with 20% Fetal Bovine Serum, FBS (Gibco) and 5% Penicillin - Streptomycin Pen Strep (Gibco) culture media were seeded in triplicate at a cell density of 0.05 x 10^6 cells/well in 96-well flat-bottomed culture plates (Tarsons). The cells were exposed to varying concentrations of serially diluted Tuibur (0 – 160 µg/µL), S - (-) - Nicotine (0 – 0.0032 µg/µL), Hydroquinone (0 – 0.16 µg/µL), Potassium Nitrate (0 – 0.16 µg/µL) and Sodium Nitrite (0 – 0.16 µg/µL) (Sigma Aldrich) along with control wells where the cells were left without treatment, for 24, 48 and 72 hours. After the treatment incubation, the media and chemicals were aspirated and the cells were washed once with 1X PBS. 110 µL of 1:10 MTT (3-(4,5-dimethylthiazol-2-yl)-2,5-diphenyltetrazolium bromide) in culture media made from 5mg/mL MTT (HiMedia) stock solution was added to each well and incubated at 37˚C for 3 – 4 hours. 100 µL of dimethyl sulfoxide (DMSO) was added to dissolve the tetrazolium salt. The well plates were incubated in the dark for 2 – 3 hours at room temperature. The absorbance was measured at 570 nm using a microplate reader (Varioskan LUX Multimode

Microplate Reader, Thermo Fisher Scientific). The MTT assay protocol was performed as mentioned by Riss et al. (2004) Cell viability was calculated using the absorbance or optical density (O.D.) values as follows:

$$\% \text{ Cell viability} = \frac{(\text{Sample O.D.} - \text{Blank O.D.})}{(\text{Control O.D.} - \text{Blank O.D.})} \times 100$$

2.6.4 (b). Statistical analysis.

Pearson's correlation was performed using SPSS 16.0 to assess the relationship between concentration of chemical and cell viability. 50% Inhibition concentration (IC_{50}) was calculated by performing non-linear regression dose-response inhibition (logarithmic regression) using GraphPad Prism 6. The result of statistical evaluation was regarded as significant when the $P \leq 0.05$.

2.6.5. ELISA for oxidative stress assessment.

2.6.5 (a). Cell Lysate Preparation.

AGS cells were cultured using RPMI 1640 (Gibco) with 20% FBS (Gibco) and 5% Penicillin - Streptomycin Pen Strep (Gibco). 0.3 x 10^6 cell/well were cultured in a 6 well culture plate (Tarsons). After 24 hours, the cells were treated with the IC_{50} of Tuibur, Nicotine, Hydroquinone and Potassium Nitrate for 72 hours. After the treatment period, the media was aspirated and the cells were washed once with ice-cold 1X Phosphate Buffer Saline (PBS). 200 µL of Protease Inhibitor and 1X RIPA lysis buffer (HiMedia) mixed in a 1:100 ratio was added to lyse the cells. The adherent cells were detached using a cell scraper. The lysate was collected in a 1.5 mL microcentrifuge tube and agitated by vortexing for 30 minutes at 4 ˚C. The cell lysate was centrifuged at 12000 rpm for 20 minutes. The supernatant was collected in fresh microcentrifuge tubes and total protein was estimated using the Bradford Method. 2mg/mL bovine serum albumin (BSA) in RIPA buffer was used as the standard solution for Bradford total protein estimation.

2.6.5 (b). Total Antioxidant Capacity (TAC) Assay.

TAC assay was performed using the Total Antioxidant Capacity Assay Kit (MAK187) purchased from Sigma Aldrich. The kit was equipped with Cu^{2+} reagent,

assay diluent, protein mask and trolox standard (1 µmole). To obtain a standard curve, the Trolox standard provided in the kit was diluted into serial concentrations as instructed by the kit. The standard solutions prepared are as listed below:

Table 2.2. Trolox standard solution preparation.

Standard Sample	Volume of Trolox standard 1nmole/µL (µL)	Volume of water (µL)	Final volume of standard solution (µL)	Final concentration of standard solutions (nmole/well)
Standard 1	20	80	100	20
Standard 2	16	84	100	16
Standard 3	12	88	100	12
Standard 4	8	92	100	8
Standard 5	4	96	100	4
Blank	0	100	100	0

In a 96-well plate, 100 µL of each standard solution and 30 µL of sample in each well brought up to a total volume of 100 µL with the addition of water were mixed with 100 µL Cu^{2+} working solution using a pipette. The reaction was incubated for 90 minutes at room temperature and protected from light. Absorbance was measured at 570 nm (A_{570}) using a microplate reader (Varioskan LUX Multimode Microplate Reader, Thermo Fisher Scientific). The Trolox standard curve was obtained using Origin Pro (V 8) to calculate the trolox equivalent of unknown sample per well. The concentration of trolox equivalents in nmole/µL of each sample was calculated as follows:

$$C = S_a/S_v$$

where, C = Concentration of antioxidant in sample (nmole/ µL)

S_a = Trolox equivalent of unknown sample per well from standard curve.

S_v = Sample volume (µL) added into the wells.

2.6.6. DCFDA (ROS generation) Assay.

AGS cell line was seeded at 0.05 x 10^6 cells/well in a 96 well flat-bottomed plate in duplicate. RPMI 1640 (Gibco) with 20% FBS (Gibco) and 5% Penicillin - Streptomycin Pen Strep (Gibco) was used as the culturing media. After 24 hours, the cells were treated with the IC_{50} concentrations of KNO_3, Hydroquinone, Nicotine and Tuibur. The treated cells along with untreated control cells were incubated for 72 hours at 37˚C with 5% CO_2. After Incubation, the media was aspirated and cells were washed once with serum-free media. Cells were stained with 10 µM DCFDA (Sigma Aldrich) in serum free media and incubated at 37˚C. After a waiting time of 30 minutes, the cells were washed with 1X PBS and detached using trypsin. The action of trypsin was neutralized by adding 1X FBS and the cells were collected in 1.5 mL microcentrifuge tubes. The cells were centrifuged at 1500 rpm for 5 minutes and washed once with 1X PBS while vortexing. The cells were centrifuged once again and resuspended in 100 µL of 1x PBS while vortexing and statistical data was recorded (10,000 events/sample) between 485 – 535 nm using BD Accuri^{TM} C6 Plus Flow Cytometry (FACS).

2.6.7. Griess Assay for Nitrite determination.

AGS cells were seeded at 0.3 x 10^6 cells/well in a 6 well plate (Tarsons) in duplicate. Treatments with IC_{50} of Tuibur, Nicotine, Hydroquinone and Potassium Nitrate were given to the cells along with untreated control well of cells. Incubation period of 72 hours was imposed on the cells and cell lysates were prepared from the control and treated cells as stated above in 2.6.4 (a). Griess Assay was performed using the Griess reagent Kit for Nitrite Determination (G-7921) purchased from Invitrogen. This kit is specific for nitrite quantitation in biological samples. Greiss reagent kit provided two components – N-(1-naphthyl)ethylenediamine dihydrochloride (0.01%) and Sulfanilic acid (1% in 5% phosphoric acid which are to be mixed to prepare the Griess reagent. The kit also comes with a nitrite standard solution (1.0 mM sodium nitrite in deionized water) ready for use. All the components of the assay kit were stored in a 2˚C refrigerator prior to use. The nitrite standard solution was serially diluted using deionized water into concentrations ranging between 0 - 100 µM of sodium nitrite. Standard curve was plotted using Origin Pro (V 8) to calculate the

nitrite concentrations. The standard solutions and their concentrations are listed below in Table 2.3.

Table 2.3. Nitrite standard solution preparation.

Sample	Volume of nitrite standard solution 1000 µM/1.0 mM (µL)	Volume of diluent/ deionized water (µL)	Final volume of standard solution (µL)	Final concentration of standard solutions (µM)
Standard 1	15	135	150	100
Standard 2	12	138	150	80
Standard 3	9.0	141	150	60
Standard 4	6.0	144	150	40
Standard 5	3.0	147	150	20
Standard 6	1.5	148.5	150	10
Diluent	0	150	150	0

150 µL each of the standard solutions thus prepared and the cell lysates (control and treatments) prepared beforehand were mixed with 20 µL each of Griess reagent and 130 µL of deionized water with a reference sample of 20 µL Griess reagent and 280 µL of deionized water. The mixtures were incubated for 30 minutes and the nitrite-containing samples' absorbance was measured at a wavelength of 548 nm using a microplate reader (Varioskan LUX Multimode Microplate Reader, Thermo Fisher Scientific). The extent of nitrite released (in µM) by the samples was determined using linear regression in comparison to the Nitrite Standard solution.

2.6.8. Acridine Orange/Ethidium Bromide (AO/EB) Staining for Apoptosis.

AGS cells were seeded at 0.3 x 10^6 cells/well in a 6 well plate (Tarsons) in duplicate. Treatments with IC_{50} of Tuibur, Nicotine, Hydroquinone and Potassium Nitrate were given to the cells. After 72 hours, the treatments and media were aspirated and the cells were fixed using 70% ethanol. 100 µL of 1:1 mixture of Acridine Orange (5 mg/mL) and Ethidium Bromide (3 mg/mL) in each well was used to stain the cells. The fluorescent images were observed under an inverted Fluorescence Microscope (Olympus - IX71). Cells were scored using Image J and differentiated into normal, early-stage apoptotic and late-stage apoptotic cells for each sample. 1000 cells were scored per each well for each treatment in triplicate. The formula for calculation of apoptotic index (AI) was used as described by Pinzaru et al., (2021):

AI (%) = (Number of apoptotic cells/Total number of cells) x 100

CHAPTER 3

CHEMICAL CHARACTERIZATION AND OXIDATIVE STRESS RELATED BIOLOGICAL ACTIVITY OF TUIBUR

CHAPTER 3

CHEMICAL CHARACTERIZATION AND OXIDATIVE STRESS RELATED BIOLOGICAL ACTIVITY OF TUIBUR

3A. Chemical characterization of Tuibur.

Tobacco specific alkaloids as well as other chemical species present in tuibur were qualitatively and quantitative characterised using attenuated total reflection Fourier transform infrared spectroscopy (ATR-FTIR) combined with chemometric tools such as partial least square regression analysis, surface enhanced Raman Spectroscopy (SERS) and high-performance liquid chromatography tandem Mass spectrometry (HPLC- MS/MS) methods. Tuibur samples collected were categorised into different grades based on the concentration i.e., amount of tobacco matter combusted (in g) per litre of alkaline extract employed during the production of each grade of tuibur.

3A.1. pH.

The pH of tuibur samples (T1 – T10) analysed were in the pH e range of 8.85 to 9.33. The mean average pH of tuibur samples collected are presented in Table 3.1.

Table 3.1. pH of grades of tuibur samples collected at different production sites in Mizoram, India.

Sample ID	Production Site	Grade	g/L of Tobacco	pH
T1	Armed Veng	Medium	333	9.02
T2	Armed Veng	Low	167	8.85
T3	Falkland 1	Medium	357	9.19
T4	Falkland 1	Medium	429	9.21
T5	Falkland 1	High	571	9.24
T6	Falkland 1	High	857	9.26
T7	Falkland 2	Medium	438	9.08
T8	Falkland 2	Low	250	9.12
T9	College Veng	High	686	9.29
T10	Armed Veng	High	500	9.33

3A.2. Characterization of different grades of Tuibur samples using FT-IR.

Assessment of vibrational frequency features of nicotine, hydroquinone and benzoquinone as well as different grades of tuibur samples was performed using ATR-FTIR spectroscopy method. Characteristic vibrational bands corresponding to different functional groups are depicted in figure 3.1. The nicotine standard (1 mg/mL in methanol) solution exhibited vibrational bands corresponding to methanol and nicotine. A broad vibrational band observed at 3317 cm^{-1} was ascribed to hydroxyl group possibly arising from the solvent methanol. Bands at 2939 cm^{-1} and 2831 cm^{-1} can be attributed to characteristic C-H sp^3 stretching and C-H sp^2 stretching vibrations, respectively. The vibrational bands at 1450 cm^{-1} attributed to C=C ring stretching and the concomitant C-H bending vibrations at1411 cm^{-1} were observed. The sharp vibrational band at 1018 cm^{-1} was observed which is indicative of the presence of C-O stretching mode most likely arising from a primary alcohol. The weak vibrational band around 1110 cm^{-1} ascribed to C-N stretching vibration, more likely due to secondary aliphatic amine, was observed. The weak peak at 771 cm^{-1} linked to the mono-substituted C-H bending vibration of aromatic ring protons that was masked by the broad N-H out of plane vibrations at 623 cm^{-1} is shown in the figure 3.1.

The hydroquinone (standard) showed a broad peak at 3172 cm^{-1} corresponding to -O–H stretching of the hydroxyl group. The vibration bands indicative of aromatic C=C stretching vibrations at 1629 cm^{-1}, 1516 cm^{-1} and 1465 cm^{-1} were observed. Bands observed at 1257 cm^{-1}, 1097 cm^{-1} and 1009 cm^{-1} corresponds to C-O stretching vibrations of the phenolic groups. Vibrational bands corresponding to para- and ortho-substituted aromatics C-H bending vibrations were also observed at 832 cm^{-1} and 754 cm^{-1}, respectively. The observed vibrational bands are indicative of the functional groups present in hydroquinone. In the case of benzoquinone, a sharp peak at 3057 cm^{-1} attributed to aromatic C-H stretching (SP^2) was demonstrated. A vibrational band at 1724 cm^{-1} was observed which corresponds to C=O stretching along with C-C stretching vibration observed at 1308 cm^{-1} as an indication of the presence of a carbonyl group. The sharp band at 754 cm^{-1} suggests aromatic C-H bending due to ortho- or para- substitution in the compound.

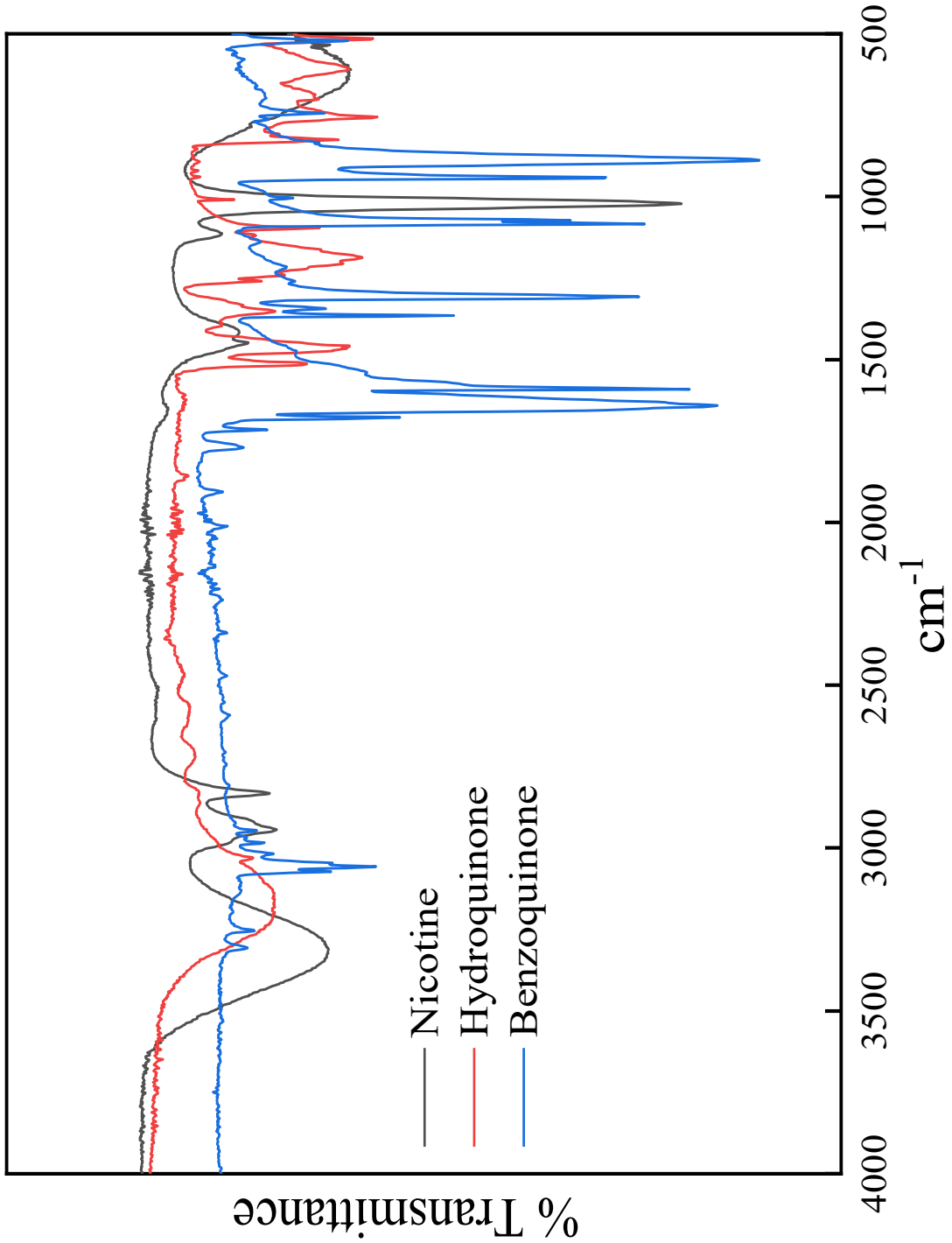

Figure 3.1. ATR-FTIR spectra of Nicotine, Hydroquinone and Benzoquinone standard (neat) samples.

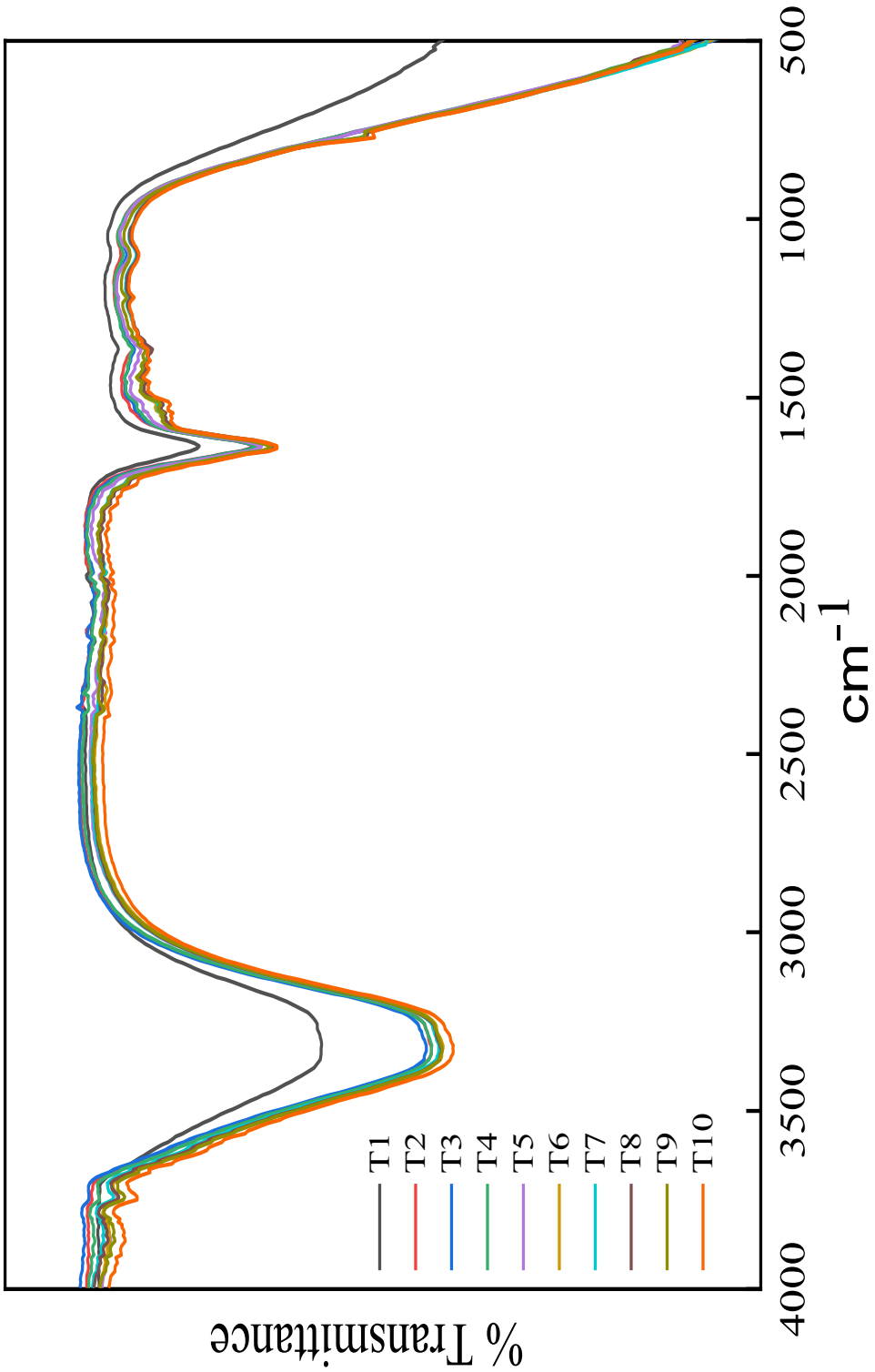

Figure 3.2. ATR-FTIR spectra of 10 tuibur samples of different grades.

Different grades of tuibur samples showed similar spectral features (Figure 3.2.) where a broad peak at 3302 cm^{-1} corresponding to -O–H functional group most likely due to the water molecules of tuibur solutions was observed. A band at 1635 cm^{-1} corresponds to C=C stretching which may be an indication of the presence of an aromatic ring containing compound (also observed in the hydroquinone standard spectrum) or may be attributed to C=O stretching of amides being present. In the fingerprint region of the FT-IR spectra, a weak absorption band at 1363 cm^{-1} indicates aromatic C-N stretching, pointing towards the presence of compounds such as pyridine. This band can also correspond to more likely presence of aliphatic NO_2 compounds in the tuibur. C-C-O and C-O vibrational bands attributable to alcohols, phenols and/or carboxylic acids were observed as weak bands at 1219 cm^{-1} and 1099 cm^{-1}, similar to that of the hydroquinone. Within the far-infrared region, a weak band at 769 cm^{-1} corresponding to substituted aromatic compounds is also seen, more akin to those of nicotine, hydroquinone and benzoquinone. The vibrational spectral data of nicotine, hydroquinone, and benzoquinone as chemical, standards for the present study, and different grades of tuibur samples are displayed in table 3.2.

Table 3.2. ATR-FTIR spectral data of nicotine, hydroquinone, benzoquinone and tuibur.

Spectral region (cm^{-1})	Wavenumber, cm^{-1}				Functional group assignments
	Nicotine	Hydroquinone	Benzoquinone	Tuibur	
4000 - 2500	3317	3172	-	3302	O-H
	-	3032	3057	-	C-H stretch
	2939	-	-	-	C-H sp^3
	2831	-	-	-	C-H sp^2
2500 - 1400	-	-	1724	-	C=O stretch
	-	1629	1639	1635	C=C stretch
	-	1516	-	-	C=C stretch
	-	1465	-	-	C=C stretch
	1411	-	-	-	C-H bend
1400 - 600	-	-	-	1363	C-N stretch
	-	-	1308	-	C-C stretch
	-	1257	-	1219	C-C-O
	1110	1097	1081	1099	C-O
	1018	1009	-	-	C-O
	-	832	-	-	C-H bend
	771	754	754	760	C-H bend

3A.2.1. Identification of significant region of the ATR-FTIR spectra for analysis.

Table 3.3. displays the PLS analysis of specific spectral regions of three neat chemical compound spectral features under consideration. When the full spectra ranged between 4000-400 cm^{-1} were used for the PLS model, and the corresponding R^2 values of 0.90, 0.84 and 0.73 were obtained for nicotine, hydroquinone and benzoquinone, respectively. Benzoquinone showed a rather low goodness of fit for the PLS model in most of the spectral sub-regions under consideration with the exception of the considered spectral range as mentioned below. Similarly, a R^2 value <0.85 was observed for hydroquinone. However, all spectral regions under consideration for nicotine, R^2 value was ≥0.88. Since R^2-values of each spectral sub-regions showed only low to moderate goodness of fit, significant regions in the IR spectra of nicotine, hydroquinone and benzoquinone as well as the samples under study (tuibur) were identified and isolated to assess the best fit for the PLS calibration models. The significant regions were selected to include specific vibrational bands corresponding to each chemical species without solvent interference as well as to cancel out spectral noise with the aim of attaining the maximum R^2 value in the calibration models. When the spectral regions of 760-650 cm^{-1} for nicotine, 860-440 cm^{-1} for hydroquinone and 1700-1600 cm^{-1} for benzoquinone were selected for the PLS calibration models, maximum R^2-values of 0.99, 0.93 and 0.98 were obtained. Table 3.3 presents the analysis of specific sub-regions of spectra for the development of the prediction model.

Table 3.3. R^2 – values for PLS models using different spectral regions of chemical standard spectra.

Spectral Region (cm^{-1})	R^2 - value		
	Nicotine	Hydroquinone	Benzoquinone
4000 – 400	0.9040	0.8354	0.7261
3000 - 2500	0.8838	0.1603	0.4322
2500 - 2000	0.9255	0.8426	0.1142
2000 - 1500	0.9166	0.5455	0.1395
1500 - 1000	0.9444	0.5280	0.1737
1000 – 500	0.9372	0.1911	0.1451
1700 - 1600	-	-	0.9824
860 – 440	-	0.9312	-
760 – 650	0.9999	-	-

3A.2.2. Calibration models for quantitative analysis of nicotine, hydroquinone and benzoquinone.

The PLS model performance indicators are shown in table 3.4. The R^2 – values for nicotine, hydroquinone and benzoquinone spectral analysis approximates ≥ 0.93 for the calibration and ≥ 0.74 for the validation data sets. The SEC estimates were ≤ 0.05, likewise, SEP estimates were also ≤ 0.30. Hence, the PLS calibration model for the standard chemicals using the selected significant spectral regions were chosen for the prediction of the unknown concentrations of nicotine, hydroquinone and benzoquinone in the different grades of tuibur samples. Figure 3.3. shows the PLS calibration models plots of the three standard spectra.

Table 3.4. Chemometric analysis of chemicals using significant spectral regions.

Chemicals	Spectral region (cm^{-1})	Calibration model		Validation model	
		R^2 – value	SEC	R^2 – value	SEP
Nicotine	760 - 650	0.9999	0.0029	0.8821	0.1507
Hydroquinone	860 - 440	0.9312	0.0473	0.7434	0.2899
Benzoquinone	1700 - 1600	0.9824	0.0466	0.8989	0.1259

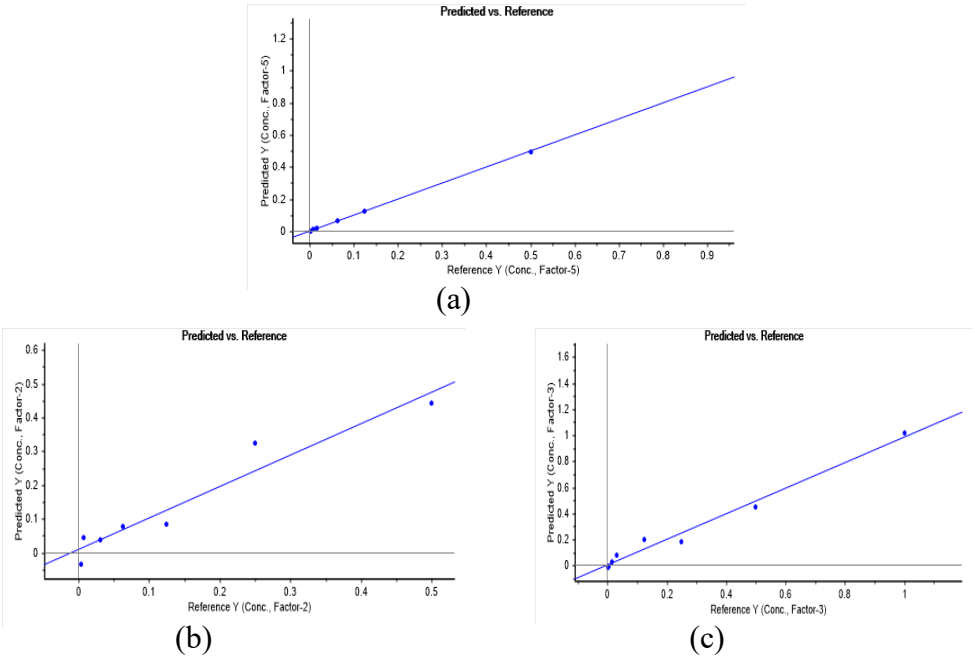

Figure 3.3. PLS calibration model plots of (a) Nicotine, (b) Hydroquinone and (c) Benzoquinone.

3A.2.3. Chemical analysis of tuibur samples using PLS model.

Serial dilutions of nicotine, hydroquinone and benzoquinone in methanol were prepared and subsequently analysed via a combination of ATR-FTIR spectroscopy and chemometrics methods for the development of calibration models from PLS regression analysis. The observed results for the predicted concentrations of nicotine, hydroquinone and benzoquinone ranged between 4.49±0.77 to 7.69±1.40 mg/mL, 1.78±4.34 to 2.19±4.27 mg/mL and 7.96±11.61 to 13.81±17.29 mg/mL, respectively. The predicted concentration values were summarized in table 3.5. From the estimated results, the relative grading of different tuibur samples based on the predicted concentrations of nicotine, hydroquinone and benzoquinone could not be achieved because of negligible difference between the predicted concentration values for each grade of tuibur with respect to each chosen chemical species of interest.

Table 3.5. Outcome of the predicted concentration in tuibur samples using standard chemical calibration models.

Name/ID	Grade	Predicted Nicotine Concentration (mg/mL)	Predicted Hydroquinone Concentration (mg/mL)	Predicted Benzoquinone Concentration (mg/mL)
T1	Medium	4.49±0.77	2.00±4.05	7.96 ±11.61
T2	Low	7.17±1.43	2.07±4.40	11.33±16.97
T3	Medium	7.69±1.40	1.78±4.34	11.50±16.81
T4	Medium	6.95±1.41	1.85±4.26	11.63±16.69
T5	High	7.15±1.41	1.98±4.28	12.16±17.04
T6	High	7.54 ±1.48	2.10±4.33	13.10±17.65
T7	Medium	7.03±1.45	2.18±4.32	13.23±17.78
T8	Low	7.50±1.45	2.07±4.16	13.49±17.73
T9	High	7.02±1.33	2.19±4.27	13.08±17.08
T10	High	7.21±1.41	2.04±4.17	13.81±17.29

3A.3. Nicotine characterization using SERS.

To further assess the concentration levels of nicotine in different grades of tuibur, surface enhanced Raman spectral (SERS) analysis was performed for both nicotine solution and different grades of tuibur samples (T1 - T10). The rationale for our attempt to assess tuibur by applying a robust and sensitive Raman spectroscopic method, viz., SERS is that water being a strong dipolar compound present in tuibur samples as a solvent which could have interfered strongly during the FTIR measurements by absorbing as many IR photons. However, Raman spectroscopy method is based on the inelastic scattering of laser photons in the visible region, and water is relatively a poor scatterer of visible radiation photons. Besides, nicotine in its unionized state is a non-polar molecule that could exhibit better polarizability attributes by virtue of inelastic scattering in the visible region. By virtue of favourable surface plasmon resonance conditions in presence of noble metal nanoparticles in solution that substantially enhances signal intensity, it is feasible to detect very low concentrations of chemical compounds in solution.

In addition, Figure 3.4. represents the SERS spectrum of a neat nicotine solution. Evidently distinct from the corresponding IR spectrum, the observed SERS spectrum of nicotine solution displays a neat spectrum with characteristic peaks in the fingerprint region (2000 - 900 cm^{-1}). A weak band at 913 cm^{-1} was observed which is most likely due to the pyrrolidine moiety of nicotine (Alharbi et al., 2014). An intensely sharp band was observed at 1030 cm^{-1} which may be attributable to the symmetric pyridine ring ‘breathing’ mode (Farquharson et al., 2019). The more accentuated and characteristic vibrational band at 1030 cm^{-1} was thus selected as internal standard for the estimation of nicotine content in tuibur samples since the band is relatively free from interference.

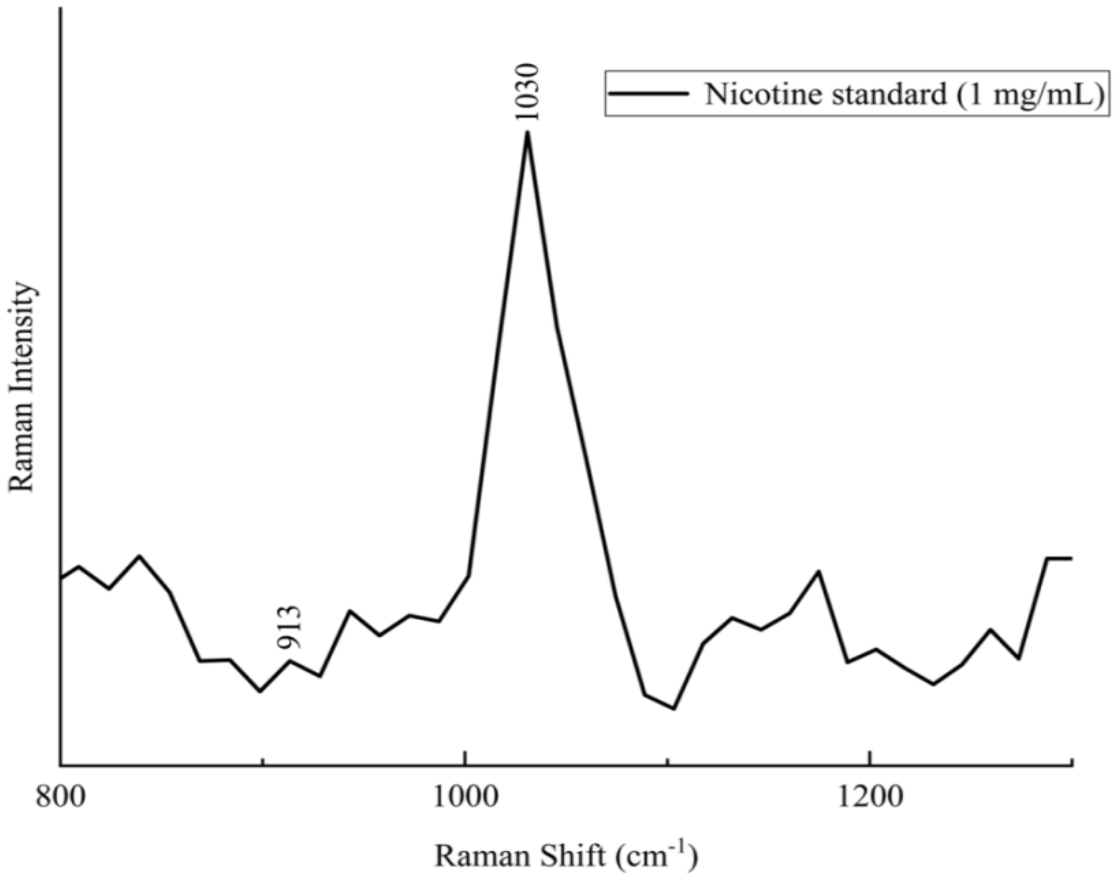

Figure 3.4. SERS spectrum of nicotine standard solution.

The observed SERS spectra of different tuibur samples (T1-T10) are displayed in Figure 3.5. For every tuibur variant (T1 - T10), an accentuated peak at 1030 cm^{-1} can be observed corresponding to the symmetrical pyridine ring breathing mode of vibration. The band originates from C-N vibrations of pyridine moiety at 1030 cm^{-1} which commensurate with the nicotine spectral features which in turn proves not only the presence of nicotine in tuibur samples but also acts as the internal standard to quantify nicotine in various tuibur samples. The intensity of the 1030 cm^{-1} peak observed in the SERS of each tuibur sample as well as the nicotine standard solution was subjected to the background correction, i.e., the observed baseline was subtracted from the observed maximum intensity of the peak at 1030 cm^{-1} for each sample.

From the assessed peak intensity, it was observed that tuibur samples made by infusing (bubbling) tobacco smoke for longer duration in feedstock, viz., high concentrations of volatile, water soluble and polar components of tobacco smoke in the alkaline feedstock correspondingly exhibited accentuated peak intensity albeit the occurrence of a few exceptions where some lower concentration tuibur samples (lower grade tuibur) also exhibited relatively higher peak intensity.

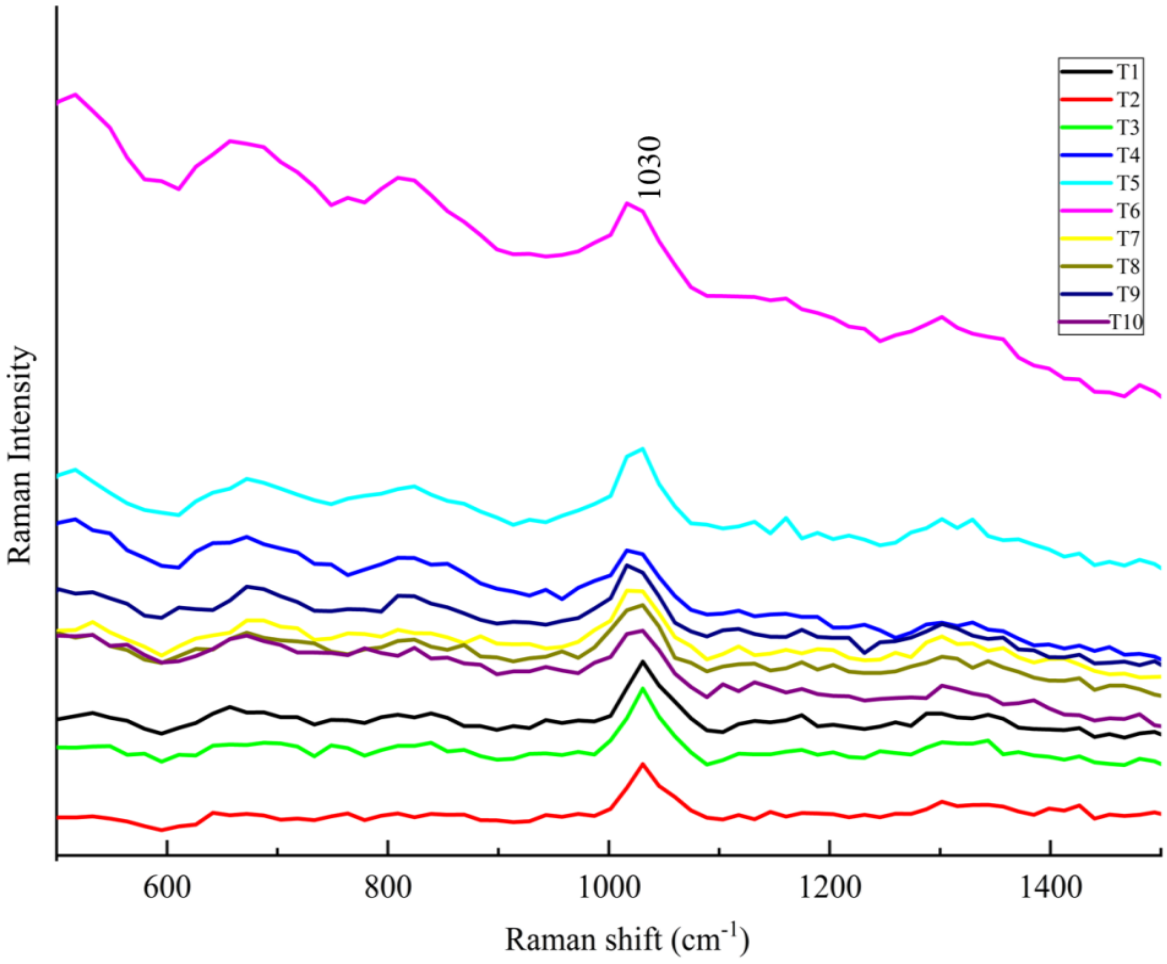

Figure 3.5. SERS spectra of tuibur samples with AuNP colloidal solution.

However, due to the prevailing alkaline pH conditions in different grades of tuibur solutions, in our present study, the vibrational bands of C-N stretching frequencies corresponding to the mono-protonated and di-protonated nicotine species were not observed (Baranska et al. 2012). It is important to note that the comparison of SERS peak intensity (1030 cm^{-1}) between nicotine neat solution (1mg/mL) and different grades of tuibur samples (T1-T10), revealed that moderate to modest concentrations of nicotine are present in various tuibur samples as shown in Figure 3.6.

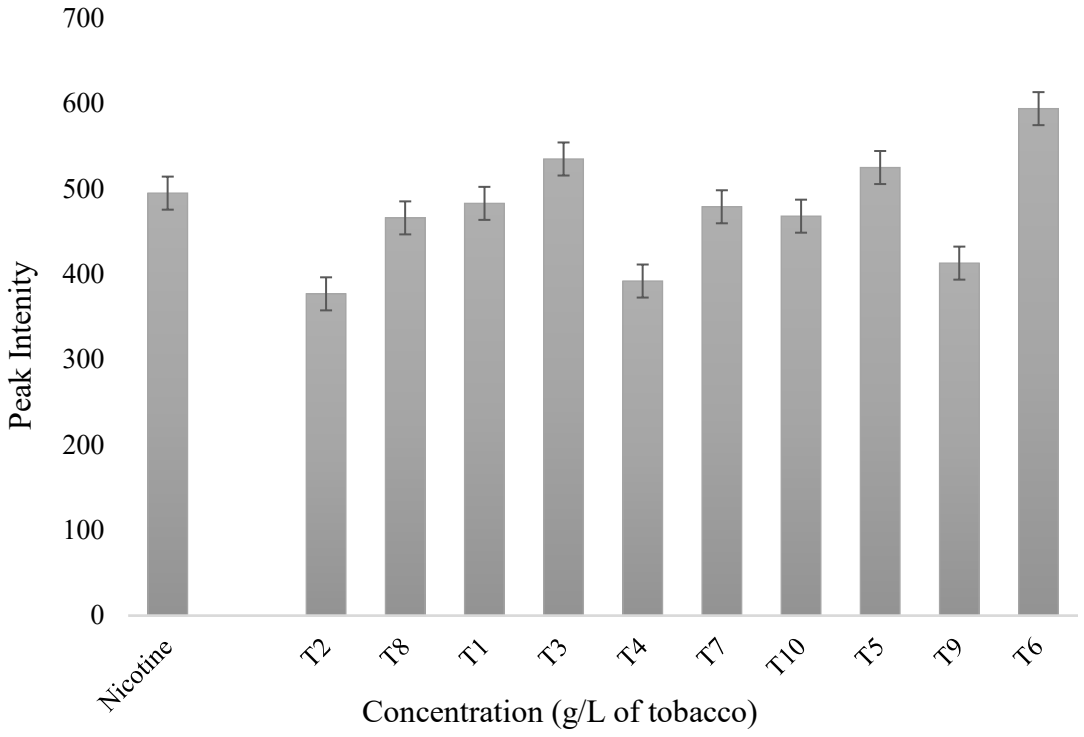

Figure 3.6. Peak Intensity at 1030 cm^{-1} of nicotine standard and tuibur solutions.

The lowest and highest SERS peak intensity for nicotine among the collected samples was observed to be lowest for T2 and highest for T6 where, 167 g/L and 857 g/L of tobacco stalk was combusted for tuibur production, respectively. From this observation, it is evident that, qualitatively, the peak intensity of the different grades of tuibur correlated with the amount of tobacco used for tuibur production.

Moreover, Pearson's correlation was performed between pH and the peak intensity of tuibur samples (T1-T10) which resulted in a non-significant weak positive correlation as shown in Table 3.6. Pearson's correlation between SERS peak intensity of tuibur samples and the concentration of tuibur (g/L of Tobacco used) was also performed which likewise revealed a positive correlation albeit it was not statistically significant as shown in Table 3.7.

Table 3.6. Pearson's correlation of pH vs. Peak Intensity of tuibur samples.

Correlations		
	pH	Peak Intensity
pH	1	.382
Peak Intensity	.382	1

Table 3.7. Pearson's Correlation of Peak Intensity vs. Concentration of tuibur samples.

Correlations		
	Peak Intensity	Concentration
Peak Intensity	1	0.517
Concentration	0.517	1

3A.4. LC- MS/MS quantification of tobacco specific alkaloids in tuibur.

By the virtue of its inherent sensitivity and selectivity, the quantitation of tobacco specific alkaloids, namely, nicotine and cotinine in different grades of tuibur can be effectively performed by applying LC-MS/MS methods. The tuibur samples were categorized into three grades – low, medium and high depending on the amount of tobacco used per litre of water during the manufacture of tuibur. The concentration of nicotine in the 10 tuibur samples ranged between 506 – 1877 µg/mL while cotinine concentrations ranged between 6.5 – 44.4 µg/mL (Table 3.8.).

Table 3.8. Concentration of tobacco specific alkaloids – nicotine and cotinine, in tuibur solutions (T1 – T10).

Sl. No.	ID	Amount of Tobacco (g/L)	Tobacco Specific Alkaloids (µg/mL)	
			Nicotine	Cotinine
1	T2	167	569	6.5
2	T8	250	845	14.8
3	T1	333	666	7.5
4	T3	357	747	13.6
5	T4	429	962	16.4
6	T7	438	1083	20.0
7	T10	500	506	9.5
8	T5	571	1114	22.8
9	T9	686	1114	14.5
10	T6	857	1877	44.4

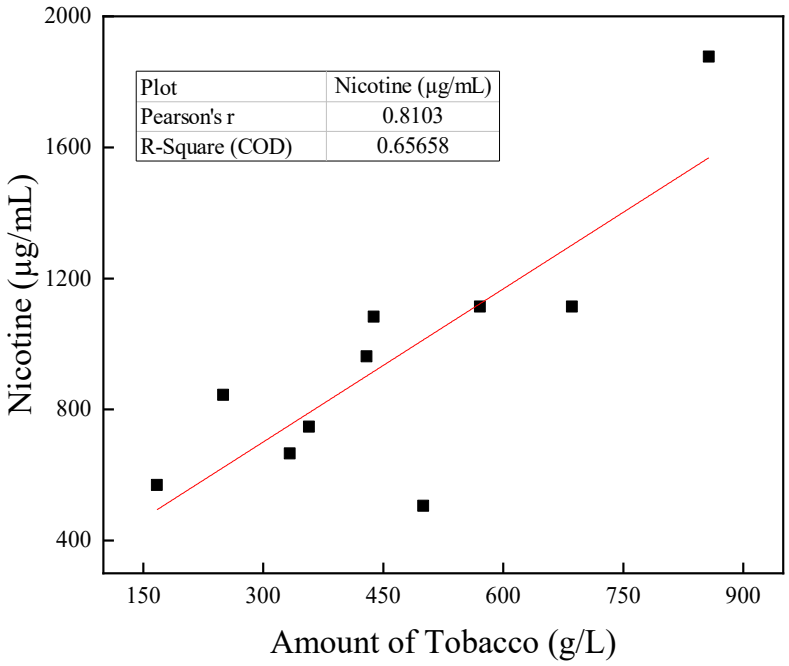

Figure 3.7. (a). Linear regression plot for Amount of tobacco.

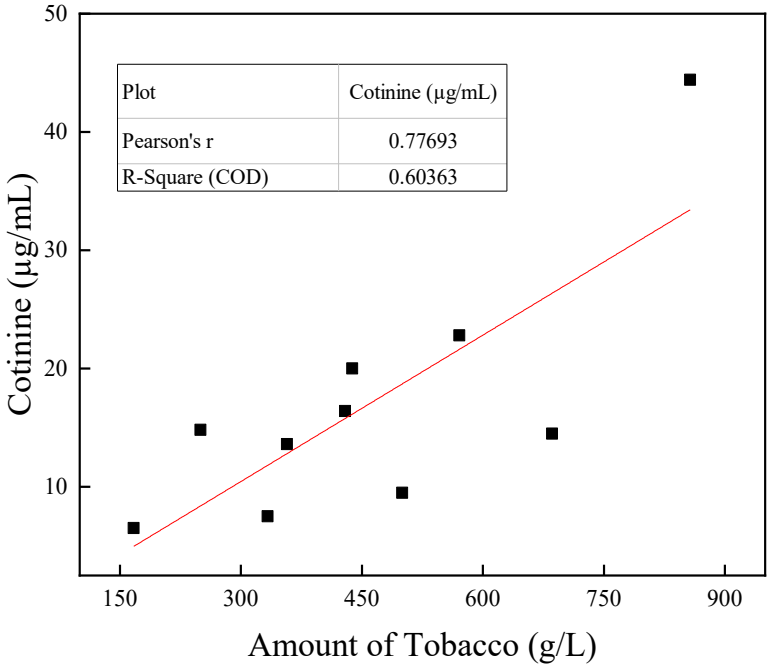

Figure 3.7. (b). Linear regression plot for Amount of tobacco vs. Cotinine.

The relationship between the amount of tobacco used for tuibur production and the concentration of nicotine was studied using linear regression and Pearson's correlation where, the goodness of fit of the data set in the linear regression model was moderate ($R^2 = 0.657$) [Figure 3.7 (a)] along with a strong positive correlation which is statistically significant ($r = .810$, $p < 0.01$) (Table 3.9.). Similarly, for the amount of tobacco used vs. cotinine concentration, the data set showed a moderate fit for the linear regression model ($R^2 = 0.604$) [Figure 3.7 (b)] and the Pearson's correlation coefficient showed a strong and statistically significant correlation ($r = .777$, $p < 0.01$) (Table 3.9.).

Table 3.9. Pearson's correlation between amount of tobacco used and concentration of alkaloids (LC-MS/MS).

Correlations			
		Nicotine	Cotinine
Amount of Tobacco	Pearson Correlation	.810**	.777**
	Sig. (2-tailed)	.004	.008
	N	10	10
**. Correlation is significant at the 0.01 level (2-tailed).			

The amount of unprotonated or unionized nicotine was calculated using the Henderson-Hasselback equation from the measured pH and concentration of total nicotine in different grades of tuibur. The pH of tuibur ranged between 9.5 – 9.8, indicative of high alkalinity of tuibur. The calculated unprotonated tuibur concentrations in each tuibur sample was found to be ≥ 97% of the total nicotine concentrations as quantified by LC-MS/MS methods (Table 3.10.).

Table 3.10. Calculated unprotonated nicotine concentration of tuibur samples.

Sl. No.	ID	Amount of tobacco used (mg/mL)	pH	Total Nicotine (µg/mL)	% Unprotonated Nicotine	Unprotonated Nicotine (µg/mL)
1	T2	167	9.6	569	97.32	554.16
2	T8	250	9.6	845	97.60	824.75
3	T1	333	9.8	666	98.29	654.26
4	T3	357	9.7	747	97.95	731.24
5	T4	429	9.7	962	97.81	941.19
6	T7	438	9.7	1083	97.76	1058.61
7	T10	500	9.5	506	96.65	489.05
8	T5	571	9.8	1114	98.17	1093.55
9	T9	686	9.8	1114	98.39	1095.84
10	T6	857	9.8	1877	98.25	1843.967

3A.5. Discussion.

Tuibur is normally prepared as an alkaline solution as feedstock solution is rendered highly alkaline by allowing relatively acidic rapid stream water to percolate through tobacco ash or plant ash. Subsequent infusion of tobacco smoke through feedstock apparently moderates the high pH of feedstock solution by at least 0.6 – 1.1 units of pH. The observed pH of tuibur solutions therefore, was also found to be alkaline in this study. More akin to other popular smokeless tobacco products, tuibur is an orally consumed SLT and retained in the mouth for several minutes as this practice would allow the moderate nicotine content in tuibur, to preponderantly exist as unionized and non-polar nicotine, that can be more readily absorbed by buccal epithelial tissue. Concomitantly, the orally absorbed non-polar nicotine would be metabolized to cotinine, trans-3'-hydroxy cotinine, and nornicotine. The rate of absorption of nicotine by the oral epithelial cells is relatively rapid while using these types of high alkaline SLTs, however the consequent increase in nicotine levels at the brain is rather slower compared to smoking tobacco products (Benowitz et al., 1988).

Although the alkalinity of tuibur is most likely due to the feedstock as well as filtration of crude tuibur through ash, some manufacturers tend to add slaked lime to make feedstock to be more alkaline. Tuibur is subsequently graded by the alkalinity of the product as well as the duration of tobacco smoke extraction. “Al” is the name of the higher (more alkaline) grade and “Al-lo” is the less alkaline or lower grade tuibur. However, the grade of tuibur used by the consumers is dependent on personal preference. It has been widely reported in literature (Tomar & Henningfield, 1997; Richter et al., 2008; Stepanov et al., 2015) that the rate of nicotine transport across the plasma membrane is related to the concentration of nicotine in its free-base form.

Once nicotine (pk_{a2} = 8.02) is deprotonated to its free-base form (completely unprotonated or un-ionized form) at higher pH, it can easily diffuse through buccal mucosa and more readily adsorbed orally to a greater extent than the corresponding ionized forms (Richter et al., 2008). Natural tobacco is acidic in nature and hence nicotine remains in its ionic form (monoprotonated form), which is unsuitable for the transmembrane transport and subsequent adsorption (Figure 3.8.). Even though saliva contains bicarbonate (HCO_3^-) ion which can act as a salivary buffering agent albeit it can only transform modest quantity of nicotine into its unionized form at a modest alkaline oral pH milieu, however this process may take place over a longer period of time and hence not at all a preferred way of tobacco consumption. Thus, the primary effect of alkaline pH in a SLT formulation is to elevate the rate of nicotine absorption as well as potentiate and reinforce the drug's psychoactive attributes (Yildiz, 2004).

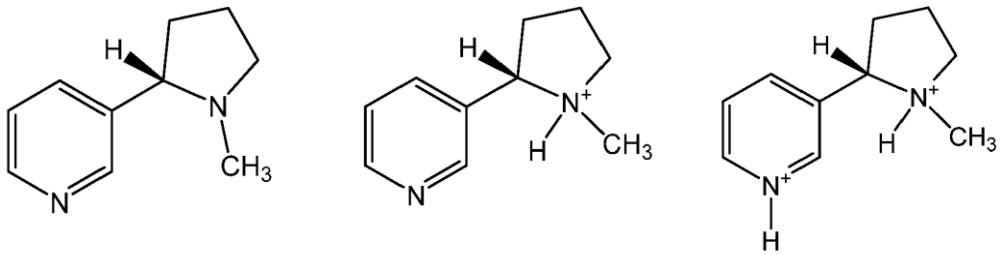

(a) Unprotonated nicotine **(b) Mono-protonated nicotine** **(c) Di-protonated nicotine**

Figure 3.8. Structure of (a) unprotonated nicotine, (b) mono-protonated nicotine, and (c) di-protonated nicotine.

Tuibur is manufactured in such a manner that the predominant ingredient is water. Consequently, almost all the polar and ionic chemical constituents of tuibur, either arising from tobacco ash (involatile inorganic and organic constituents) or from tobacco smoke (volatile and semi-volatile inorganic and organic components), would be present only in diluted concentration levels. Though this is the case, it does not mean that the chemical composition of tuibur is any less harmful and/or toxic as it is a complex mixture of several components, some of which, are directly linked to some of the debilitating lifestyle disorders including gastritis and cancer. ATR-FTIR, being a non-destructive method of chemical analysis, sample loss was minimised while maintaining its sensitivity to detect chemical species present in tuibur. As seen in figure 3.2., in the FT-IR spectra of tuibur samples, O–H broad band is predominant in all the samples. This broad band overlaps with the C–H stretching vibrations as well as N–H stretching vibrations usually found around 3500 – 2200 cm^{-1}. Moreover, C–H bonds are nonpolar and exhibit weaker peaks in the IR spectrum. These vibrational bands are found in the IR spectra of tobacco plant extracts may be attributed, in part, to polysaccharides, amines, nitrosamines and proteins. (Zhang et al., 2022) Tuibur is considered as the alkaline aqueous extract of tobacco smoke and therefore exhibits characteristic vibrational bands such as C-O and C=C stretching vibrations as well as vibrations due to amides as observed in tobacco smoke such as aromatic amines, acids, esters, quinones, etc., (Terpugov et al., 2019; Zhang et al., 2022). The observed vibrational frequencies are more akin to nicotine, hydroquinone and benzoquinone vibronic signatures corresponding to C–N str., C=C str., C–H bend., C–O str. etc., in the tuibur samples of this study, cannot be absolutely determined most likely due to overwhelmingly the most accentuated and the coinciding O–H stretching, bending and the H-bonded H---O–H vibrational bands (Figure 3.2.) (Lalmuanpuii & Muthukumaran, 2016). It is important to note that tuibur is a heterogeneous mixture of different types of water soluble polar and ionic chemical constituents, where vibrational bands of different chemical compounds may be overlapping in the mid-IR and Far-IR regions of FT-IR spectrum. However, it is evident from our preliminary study of the IR spectrum of ‘dry’ tuibur (which is relatively dry and devoid of water as compared to tuibur), a kind of precipitation or deposition of reddish-brown layer along the sides of tuibur container, that these chemicals are in fact, present in tuibur.

The occurrence of these chemicals were also described by Lalmuanpuii, (2016b) along with the presence of a series of minor tobacco-specific chemical constituents including cotinine, nornicotine, anabasine, anatabine; TSNAs - NNN, NNK, NNAL; quinones, alcohols as well as an assorted list of organometallic as well as inorganic compounds including heavy elemental species.

Nonetheless, IR spectrum cannot be exclusively applied as an quantitative analytical method as it can only provide qualitative information about functional groups' vibrational frequencies and hybridization/polarity of chemical bonds. However, FT-IR spectral vibrational frequency assignments of nicotine, hydroquinone and benzoquinone, in combination with chemometrics, could become a powerful analytical tool for the prediction of selected chemical constituent(s) in a mixture of compounds (Fekhar et al., 2023). Multivariate analysis performed by using PLS regression method for a heterogenous mixture such as tuibur while carrying out the requisite standard calibrations to predict the concentrations of some chemical constituents, an easy as well as accessible method for a possible semi-quantitation analysis may be achieved. This method could predict the selected chemical species' contents – nicotine, hydroquinone and benzoquinone present in the different grades of collected tuibur, besides to a certain extent, it may also be possible to assess whether the amount of tobacco used in production has any effect on the levels of these chemicals in the tuibur samples collected.

This semi-quantification method of applying ATR-FTIR in conjunction with chemometrics, however, has its own limitations. The most dominant and the broad vibrational band(s) due to water in tuibur (~3000 – 3400 cm^{-1} and 1600 cm^{-1}) as well as overlapping vibrational bands of different chemical constituents present in tuibur can cause the unwarranted masking of vibrational bands which may prevent the requisite classification and the potential quantitation of different chemical components in tuibur. Moreover, by virtue of the limited solubility of nicotine in polar solvents during the preparation of the standard solutions at different concentration levels, viz., a methanolic stock solution of nicotine where the highest prepared standard concentration could not exceed 1 mg/mL, i.e., the concentration of the purchased stock solution. Benzoquinone and hydroquinone are volatile compounds and extremely reactive chemical species. They readily undergo oxidation on contact with light and

air making it extremely challenging to accurately prepare standard solutions. The standards prepared via serial dilution (v/v) could not be obtained beyond certain concentrations. Hence, only a limited number of standards were prepared for establishing a calibration curve. The increasing amount of solvent further complicated the semi-quantitative analysis, with the dilution of nicotine solution. This could potentially affect the signal-to-noise aspects of IR spectrum of the standard itself, where unwarranted masking of the vibrational bands of nicotine/hydroquinone could take place. This may render the constructed semi-quantitative method less reliable and may yield results with varying degrees of accuracy. In PLS regression, R^2 values as much close to 1 in the calibration model is highly desirable to achieve considerable accuracy of predicting the concentrations of the unknown sample. However, in the present study, for the PLS calibration models for the spectral data of chosen standards, R^2 values of only >0.90 could be obtained only within narrow spectral regions of approximately 100 cm^{-1} ranges especially for hydroquinone and benzoquinone. This significantly impacted the ability of this method in incorporating all specific spectral peaks of the species under study which in turn may have a negative effect on the reliability of prediction. Moreover, while obtaining the IR spectrum of volatile substances, loss of sample due to oxidation of benzoquinone and hydroquinone may take place, which negatively influences the accuracy of the observed results in FTIR with chemometrics technique. Hence, from the results observed in this study, the grading or ranking of tuibur samples could not be accomplished based on nicotine levels as predicted by this method. Therefore, the application of other spectroscopic techniques is warranted for the estimation of nicotine levels in different grades of tuibur solutions.

Subsequently, a more sensitive surface-enhanced Raman Spectroscopy (SERS) method was performed to identify and estimate nicotine levels in different grades of tuibur samples. SERS method is also a non-destructive analytical technique while ensuring negligible quantities of sample loss. SERS analysis, is considered a more sensitive approach as compared to FT-IR in a mixture of compounds with varying polarity such as tuibur, since O–H peak due to water is observed as a narrow and weak peak around ~3450 cm^{-1} (Pershin, 2005) leading to negligible interference or overlapping of O-H peak with the characteristic vibronic frequencies required to

identify and possibly quantify nicotine contents. SERS assay was formulated by preparing a composite by adding trisodium citrate (TSC)-capped AuNPs either into neat nicotine solution or tuibur solution. Nicotine molecules present in tuibur can interact through chemisorption. Chemical constituents of tobacco can be adsorbed or bound to the surface of gold nanoparticles through electrostatic interactions and/or chemisorption else physisorption forces depending on the charge, non-bonding lone pair of electrons in nitrogen atoms. The substituent group(s) on the nitrogen atoms of heterocyclic compounds in nitrogen impose steric hindrance and impede the chemisorption and therefore, for such compounds most probably the physisorption may occur (Yajima et al., 2012). Nitrogen-containing functional groups in nicotine, such as the pyridine ring and pyrrolidine ring could elicit chemisorption or physisorption interactions with the gold atoms at the surface of Au NPs. The SERS spectrum of nicotine standard solution obtained as well as the spectra of different grades of tuibur are markedly different from the corresponding IR spectra and exhibit a neat spectrum with distinctive and characteristic spectral features in the range of 1300 - 800 cm^{-1}. Comparison of the SERS spectral features of tuibur samples and nicotine solution clearly demonstrate the presence of nicotine in the different grades of tuibur samples. Therefore, this study establishes a simple, rapid and robust evaluation method for the identification and evaluation of nicotine levels in different grades of tuibur.

The ability to detect tobacco alkaloids in tobacco samples using SERS is well documented in literature (Barber et al., 1994; A. Kumar et al., 2019). In SERS, a roughened surface of noble metal nanomaterial, chiefly Au or Ag, is prepared where the target analyte/molecule, in our case, nicotine, is adsorbed on surface in close proximity to the rough surface. The optical activity of metal-based nanomaterials and SERS activity are closely related and allows for the enhancement of the local electromagnetic field, which can be largely attributable to the induction of surface plasmon resonance. The molecular polarizability and the concomitant inelastic scattering, the hallmark of Raman phenomenon is therefore, substantially enhanced, which imparts high sensitivity, specificity and selectivity for the detection as well as identification of the molecules containing lone pair of electrons or polarizable functional groups. The strength of the SERS signal is dependent on the location of

number of hotspots and analyte molecule in the plasmonic structure (Pérez-Jiménez et al., 2020). In this study, the observed gradual increase in the peak intensity at 1030 cm^{-1} in tuibur samples is in good agreement with the increase in the amount of tobacco stalk combusted for generating tobacco smoke (vide supra) during the tuibur production process demonstrating the ability to classify or grade the tuibur sample as a function of the characteristic nicotine vibrational band intensity at 1030 cm^{-1} in tuibur SERS spectra. Nonetheless, the nanoparticle used for the enhancement of signal strength in each sample – nicotine standard and tuibur, were not recovered after use. Therefore, it is unascertainable as to whether or not each aliquot from the same batch of nanoparticles used for this study, have the same roughness, number of hotspots or dimensions. The experimental design of this study, excludes the acquisition of data required to calculate the number of molecules in known standard solution involved in the adsorption forces. This is because the standard preparations via serial dilution of the nicotine stock solution, much like the standard preparation for IR, has drawbacks and limitations, therefore it was not attempted for this analysis. Also, all nicotine molecules in the volume of the sample being probed will not have an equal contribution to the overall Raman signal. Consequently, the grading and evaluation of nicotine levels in different grades of tuibur samples could be achieved as no more than a semi-quantitative estimation.

Finally, for a more reliable and precise quantitation of nicotine and cotinine in the collected different grades of tuibur samples, LC-MS/MS method was employed. By exploiting variations in the chemical constituents' polarity, the analyte of interest was separated out from the tuibur solution with syringe filtration and liquid chromatography by employing suitable eluent system, which enables a better separation, simultaneous detection and the concomitant determination of selected groups of chemical components present in a heterogenous mixture like tuibur. When liquid chromatograph is hyphenated with tandem mass spectrometry (MS^2), in multiple reaction mode (MRM) the identification and the analysis of both the parent ion as well as selected daughter ions can take place, thus the analytical method becomes a highly sensitive, more precise and selective method for the quantitative determination of tobacco specific alkaloids. From the heterogenous mixture of tuibur, nicotine and cotinine are co-eluted using high-performance liquid chromatography

(HPLC) method. With the precise calibration of liquid chromatography, polar eluent system(s) to separate out nicotine and cotinine from tuibur, well resolved peaks can be achieved. Mass spectra of nicotine was reported where a base fragment peak at *m/z* 84 and a small molecule peak at *m/z* 162, while cotinine exhibited peaks at *m/z* 98 and *m/z* 176 (Iwai et al., 2013). Similar ion peaks were selected from the first quadrupole using mass spectrometry and were further fragmented to yield product ions for quantification in the MRM mode. As observed in table 3.10., the tobacco specific alkaloids present in different grades of tuibur are present in modest (µg/mL) concentrations. There is little or no relevant data available on the quantitation of nicotine or cotinine in tuibur and therefore this is the first quantitative study that has revealed the concentrations of these tobacco specific alkaloids in tuibur. In our study, a linear relationship although moderate, is observed along with a positive correlation between the amount of tobacco combusted and the alkaloid concentrations determined in different grades of tuibur indicating that an increase in the amount of tobacco stalk combusted during the production concomitantly increases the concentration of nicotine and cotinine in tuibur. Therefore, an appropriate grading in tuibur samples based on the concentration levels of nicotine could be achieved confirming the hypothesis that with the increasing amounts of tobacco stalk used for the production, an increase in the nicotine contents of ascending range for a wide range of tuibur samples can be achieved.

From table 3.10., there are some exceptions from the results of this study, where the concentration levels of nicotine increased with increase in amount of tobacco, though this is true for most of the samples. In the case of samples T8 (250 g/L of tobacco) and T10 (500 g/L of tobacco), the nicotine contents were not in accordance with the presumed concentrations based on the observed trend. This may be due to the variations in the nicotine content in the tobacco stalk used or the production conditions (rapid stream water flow rate / wind speed at the site of production on the day of production) were different during the preparation of these tuibur samples and it would be immature to speculate on these variants as these conditions were not followed critically. Sein (2020) has stated that both *N. tabacum* and *N. rustica* commonly known in Myanmar as hsey ywet kyee are grown. As the tobacco stalk for the tuibur manufacture is procured from Myanmar (Lalmuanpuii, 2016b) by layman merchants,

the tobacco purchased may contain a mixture of both *Nicotiana rustica and N. tabacum* stalks of which *Nicotiana rustica* is known to contain higher nicotine content than *N. tabacum* (Sierro et al., 2018). The nicotine content in both smoked and smokeless forms of tobacco products vary considerably according to the varieties of tobacco. In addition, the alkaloids content in tobacco plant is dependent on a wide range of factors such as agriculture practices, soil moisture content, genetic potential, blending proportion of varieties, etc. (Djordjevic & Doran, 2009). Nicotine in plants is metabolised to cotinine as well as to nornicotine. Nitrosation products of tobacco specific alkaloids like nicotine and nornicotine are termed as tobacco specific nitrosamines (TSNAs). They include species such as NNN, NNK, NAT, NNAL, NAB, etc., where, NNN and NNK are potent carcinogens and play major roles in the induction of many malignancies (Hoffmann et al., 1991). The lethal dose of nicotine for adults is 60 mg or less (30-60 mg) (Mishra et al., 2015). Though this may be the case, it appears that tuibur contains sufficient unprotonated nicotine contents to initiate and sustain the psycho-addictive dependency on tobacco. It is important to note that chronic tuibur intake may be insidious for tuibur consumers as tuibur may also contain TSNAs (*vide supra*) since *de novo* synthesis of TSNAs occur during the combustion of tobacco matter (Muthukumaran et al., 2023).

3B. Biological Activity of Tuibur.

The putative negative effects of tuibur was examined on the viabilities of AGS cells in a series of biological assay studies where the dosage and incubation times were varied. These biological assays provide a measure of plausible cytotoxicity, genotoxicity and putative DNA damage because of tuibur exposure to cells in vitro, since isolated and immortal cells are considered as a rudimentary and simple model system. MTT assay, ELISA and fluorescent staining assays were performed for assessing the putative negative effects of tuibur in vitro. Since, tuibur is essentially an alkaline aqueous extract of polar and possibly semi-polar chemical constituents, both inorganic and organic chemical species with a wide range of polarities, the possible cytotoxic and oxidative effects of few of the potential and putatively preponderant components of tuibur, such as nicotine, hydroquinone, and nitrate anion, were also examined, independently, in a series of in vitro studies, similar to tuibur for gaining a better insight into the possible adverse health effects of tuibur using in vitro experiments.

3B.1. Tuibur oxidative stress biomarker assessment.

Micronucleus (MN) assay was carried out by using the DNA-specific fluorescent stain (acridine orange) for fluorescence microscopy as a biomarker of oxidative stress and genotoxicity in tuibur and sahdah users. Normal buccal epithelial cell and buccal cell detected with MN are shown in figure 3.9. The demographic profile of individuals such as age, gender, years of SLT use and SLT dosage are summarized in table 3.11. The frequency of micronuclei formation in the three study groups are shown in figure 3.10. The mean micronuclei scores for control (healthy volunteer), tuibur user and sahdah user groups are 2.3 ± 0.99, 20.59 ± 12.09 and 14.36 ± 6.72, respectively (Table 3.12.). The difference between MN frequency of tuibur users, sahdah users and controls were compared as shown in table 3.12. Pearson's correlation analysis for tuibur users showed weak negative correlation between age and MN count along with weak positive correlation between dose vs. MN count as well as duration of use and MN count however it was statistically insignificant. Similarly, weak negative correlation was observed in sahdah users between age vs. MN count, dose vs. MN count and duration of use vs. MN count albeit statistically not significant.

Table 3.11. Characteristics of the three groups under study.

Characteristics	Tuibur users (n = 100)	Sahdah users (n = 100)	Control (n = 100)
	Mean ± SD (range)		
Age (years)	37.76 ± 9.45	36.52 ± 8.23	39.94 ± 10.81
Dosage (frequency of use per day)	9.62 ± 5.49	10.94 ± 5.23	0.00 ± 0.00
Duration of use (years)	18.18 ± 8.84	15.84 ± 9.89	0.00 ± 0.00

Table 3.12. Mean micronuclei count in the three study groups.

Groups	N	Mean MN count	Standard Deviation
Control	100	2.3	0.99
Tuibur users	100	20.59	12.09
Sahdah users	100	14.36	6.72

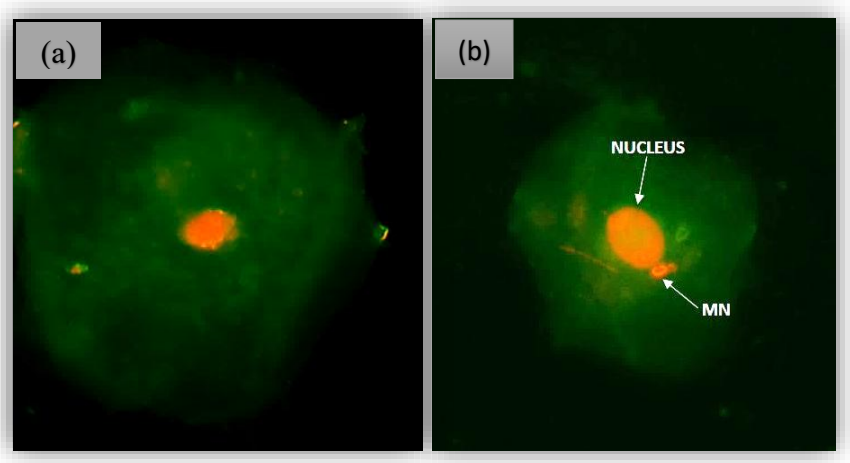

Figure 3.9. (a) Normal buccal epithelial cell; (b) Buccal epithelial cell with micronucleus.

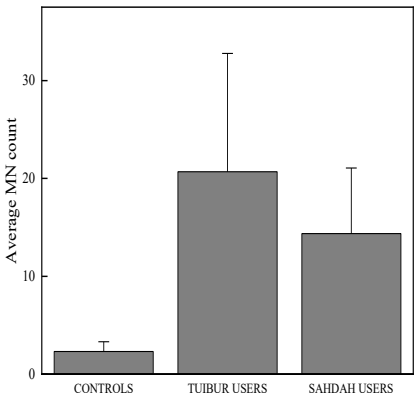

Figure 3.10. Comparison of MN frequency in control and smokeless tobacco user populations.

The analysis of variance (ANOVA) also indicated a significant difference in micronuclei (MN) counts among the three groups: Tuibur users, Sahdah users, and the control group ($p < 0.001$). The Tukey's Honestly Significant Difference (HSD) test was then conducted to compare the mean MN counts between the groups.

The Tukey's HSD test revealed significant differences in MN counts between tuibur users and sahdah users ($q = 7.91$, $p < 0.001$), tuibur users and controls ($q = 22.96$, $p < 0.001$), as well as sahdah users and controls ($q = 15.04$, $p < 0.001$). The highest difference was observed between tuibur users and controls, indicating substantial negative health effect of tuibur by virtue of high frequency of MN formation compared to healthy volunteers who do not indulge in any type of tobacco use (Table 3.13.).

Table 3.13. Multiple comparisons of mean MN in the three study groups.

Groups	N	Mean MN ± S.D.	Mean Difference
Control	100	2.3 ± 0.99	18.37
Tuibur users	100	20.59 ± 12.09	
P value		< 0.001	
q-tukey		22.96	
Control	100	2.3 ± 0.99	12.04
Sahdah Users	100	14.36 ± 6.72	
P value		< 0.001	
q-tukey		15.04	
Tuibur users	100	20.59 ± 12.09	6.33
Sahdah Users	100	14.36 ± 6.72	
P value		< 0.001	
q-tukey		7.91	

3B.2. *In vitro* cytotoxicity screening via MTT assay.

3B.2.1. Tuibur cytotoxicity.

The serial dilutions of tuibur were introduced for AGS cell colony in the treatment regime in order to assess the cytotoxicity effect(s) of tuibur (MTT bioassay) and it is followed by analysing the proliferation of AGS cells in presence of tuibur. The concentration range of tuibur used for the treatment is between 0 – 160 µg/µL. No significant change in cell viability was observed up to 10 µg/µL in the 24 h tuibur treated AGS cells. However, a rapid decline to 56% (SE = 5.84) cell viability of tuibur treated AGS cells was observed from treatment of 20 µg/µL of tuibur. An anti-proliferation of AGS cells to ~ 27% (SE = 5.29) for the highest dose tuibur treatment i.e., 160 µg/µL was detected. A modest variance in the trend was observed for 48 h tuibur treated AGS cell line, where, at 5 µg/µL of tuibur treatment, a decline to 69% (SE = 2.95) cell viability was observed. A continuous decline in the cell viability ensued upon higher dosages to 22% (SE = 2.28) cellular proliferation for the highest dose treatment. However, when AGS cells treated tuibur for 72 h, a decline of cell viability was witnessed, with 38% (SE = 2.16) cell viability at the low dose of 1.25 µg/µL of tuibur, subsequent dose-dependent reduction in cell viability of 89% (SE = 5.77) for 2.5 µg/µL of tuibur treatment was observed. A similar declining trend was followed as found in the two former incubation periods, however, only ~ 15% (SE = 0.96) viable cells remaining at the highest dose treatment regime (Figure 3.11.). The

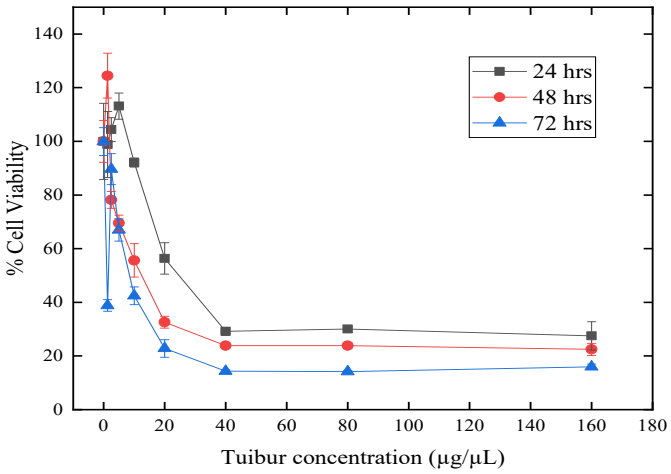

Figure 3.11. Cytotoxicity of tuibur on AGS cells. Cells were exposed to tuibur in concentration ranging from 0 to160 µg/µL for 24, 48 and 72 h. Cell viability was determined using MTT assay. The data presented are shown as mean ± S.E, n = 3.

Pearson's correlation indicated a negative correlation between the tuibur concentration levels and AGS cell viability for three time-dependent tuibur treatment groups in which only 24 h ($p< 0.05$) study was statistically significant.

To measure the cytotoxicity of tuibur in AGS cells, 50% inhibitory concentration (IC_{50}) was calculated for the time – and concentration – dependent tuibur treatment using non-linear regression, dose-response-cell viability. The normalized absorbance vs log [inhibitor] curve depicting the kinetics of cell viability is shown in Figure 3.12. The IC_{50} values were obtained for 24, 48 and 72 h tuibur exposed AGS cell line, 15.30 µg/µL (R^2 = 0.9130), 6.606 µg/µL (R^2 = 0.9402) and 6.808 µg/µL (R^2 = 0.9682), respectively, as shown in Figure 3.13. The IC_{50} value after the 24 h incubation was approximately 2-fold higher than the estimated IC_{50} values for the 48 and 72 h incubation time experiments. Since, the data set for incubation time of 72 h was the best fitted using the regression model as compared to the other two incubation times, hence this model was chosen with its IC_{50} value for the subsequent in vitro studies.

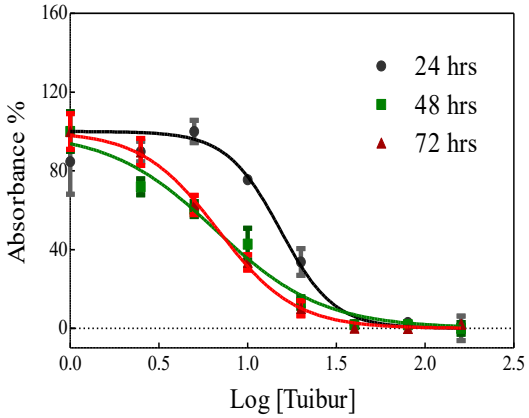

Figure 3.12. Kinetics plot of tuibur treated AGS cells. Data presented as log[tuibur] vs. % absorbance for evaluating IC_{50}.

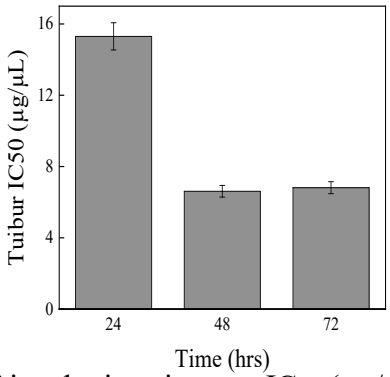

Figure 3.13. Effect of incubation time on IC_{50} (µg/µL) values of tuibur exposed AGS cells after 24, 48, and 72 h, respectively, in cell counting assay.

3B.2.2. Nicotine cytotoxicity.

MTT assay was performed to assess the possible cytotoxicity potential of nicotine on AGS cells by measuring the cell viability in a cell counting assay. The incubated cells were treated with gradually increasing doses of nicotine besides cells were also incubated with nicotine in a time dependent manner. Figure 3.14. illustrates the dose and time-dependent nicotine treated AGS cells. For an exposure period of 24 h, the nicotine treated cells did not show any noticeable change in the cell growth, rather, the cell viability remained practically constant with ~ 100 % cells were still viable after the incubation time for the incrementally increasing doses of nicotine. However, an increase in cell growth and the percentage cell viability was observed after 48 h nicotine treatment when compared with the untreated cells. Indeed, an accentuated growth spurt as high as 125% (SE = 3.38) for AGS cells upon 0.0008 µg/µL of nicotine exposure was obtained. More importantly, cellular proliferation to ~ 102% (SE = 3.20) was observed at 0.0002 µg/µL nicotine treatment, followed by a small but a steady anti-proliferation leading to ~60% (SE = 6.44) cell viability at 0.0032 µg/µL nicotine treatment (which is the highest dose) after 72 h treatment period was observed.

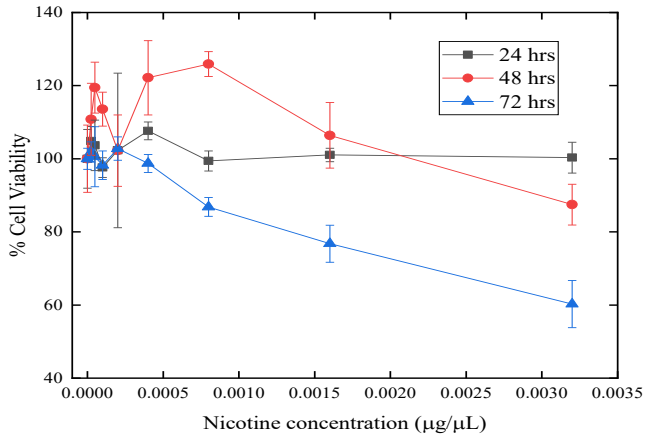

Figure 3.14. Cytotoxicity of nicotine on AGS cells. AGS cells viability after 24, 48 and 72 h treatment with the dosage of nicotine ranged from 0 to 0.0032 µg/µL. The data were presented as mean ± S.E, n = 3.

The correlation coefficient of the 24 and 48 hrs MTT nicotine treatment studies showed non-significant negative correlation between cell viability and nicotine dose while the 72h cell viability study revealed a strong negative correlation ($p<0.01$).

In order to measure the cytotoxicity of nicotine on AGS cell line, IC_{50} value was calculated for the time– and dose–dependent nicotine treatment studies using non-linear regression, dose-response-inhibition. The log [inhibitor] vs cellular response was summarized as a plot in figure 3.15. The calculated IC_{50} values for nicotine exposed AGS cells were 0.000161 µg/µL (R^2 = 0.2322) for 24 h and 0.001104 µg/µL (R^2 = 0.7886) for 72 h as shown in figure 3.16. The 48 h nicotine treatment data did not follow a trend (neither proliferation nor inhibition of proliferation) and could not be fitted by applying the regression model. Hence, the calculation of IC_{50} could not be accomplished. The remaining time-dependent study, i.e., 72 h study data was fitted by applying the non-linear regression model and the calculated IC_{50} value for nicotine was for further experiments.

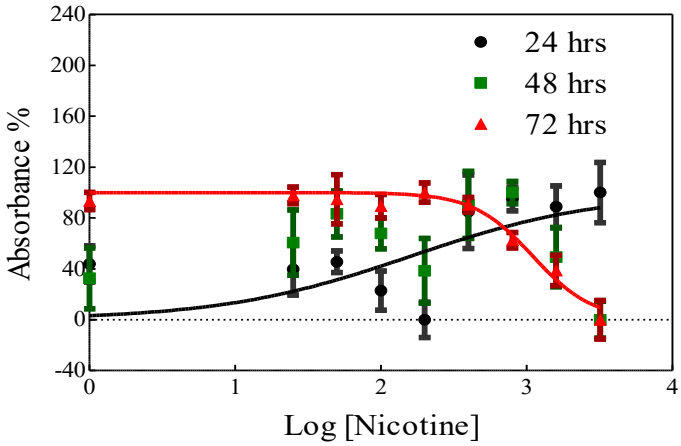

Figure 3.15. Kinetics of nicotine cytotoxicity on AGS cells. Cells were observed by relative absorbance and IC_{50} value for nicotine was calculated. The data are presented as mean ± S.E, n = 3.

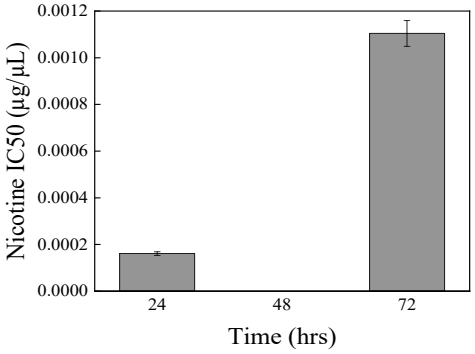

Figure 3.16. Time evolution of IC_{50} (µg/µL) values of nicotine in AGS cells with increasing incubation times (24, 48 and 72 h). Bars represent mean ± SEM for 3 replicates.

3B.2.3. Hydroquinone cytotoxicity.

The inhibition of AGS cell proliferation due to hydroquinone exposure was evaluated by means of MTT assay (Figure 3.17.). AGS cells treated with 0.002 µg/µL hydroquinone for 24 h exhibited a 56% inhibition of proliferation demonstrating a considerable cytotoxicity by the lower dose of hydroquinone and higher dosage of hydroquinone exhibited more efficient cytotoxicity effects. Indeed, AGS cells showed significant sensitivity towards hydroquinone and markedly enhanced cytotoxic potency of hydroquinone was witnessed for 0.16 µg/µL hydroquinone exposure and concomitantly only 19% (SE = 1.86) AGS cell viability was observed. However, the antiproliferative trend of hydroquinone was noticeably reversed in AGS cells at higher exposure times. The 48 h treatment experiment showed a much steadier ~ 29% (SE = 0.80) cell viability for 0.02 µg/µL hydroquinone exposure followed by a further rise in cell viability to 41% proliferation (SE = 4.39) for 0.16 µg/µL of hydroquinone exposure. With prolonged exposure, apparently, AGS cells may have more likely supressed the antiproliferative effects of hydroquinone. Interestingly, after 72 h exposure, due to 0.005 µg/µL hydroquinone treatment, ~ 40% (SE = 3.67) viable AGS cells was observed. With higher dose exposure (0.01 µg/µL hydroquinone) after 72 h, only a modest 14% (SE = 2.99,) cell viability was observed. More importantly, with 0.08 µg/µL hydroquinone dose, consequently 0.85% (SE = 1.52,) of AGS cells only

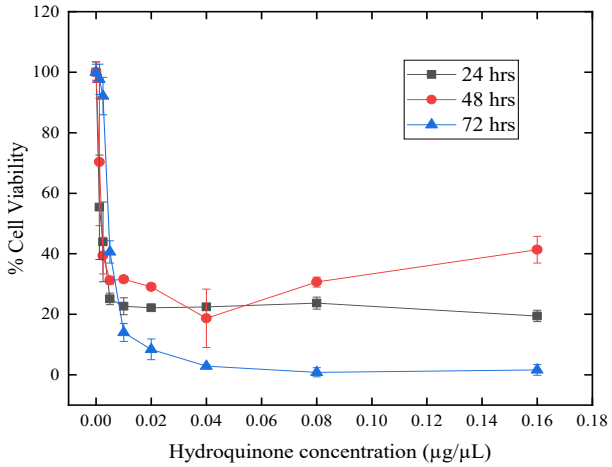

Figure 3.17. Cytotoxicity of hydroquinone on AGS cell line. The cells were exposed to hydroquinone doses ranged between 0 to 0.16 µg/µL for 24, 48 and 72 h, respectively. Cell viability was measured using MTT assay. The data presented are mean ± S.E, n = 3.

remained viable. Nevertheless, for the MTT assay, all hydroquinone treatment groups showed an insignificant negative correlation between cell counts and cell viability.

Cytotoxic activity of hydroquinone on AGS cell line was measured for calculating the IC_{50} value for hydroquinone dose-response-inhibition study using a non-linear regression model. The log [inhibitor] vs normalised response curves are shown in Figure 3.18. The calculated IC_{50} values for hydroquinone exposed AGS cells were 0.001115 µg/µL (R^2 = 0.8403), 0.001373 µg/µL (R^2 = 0.6843) and 0.00463 µg/µL (R^2 = 0.9793) for 24, 48 and 72 h exposure, respectively (Figure 3.19.). As the 72 h study data was demonstrably best fit for the non-linear regression model, and therefore, the corresponding IC_{50} value of hydroquinone was chosen for further experiments.

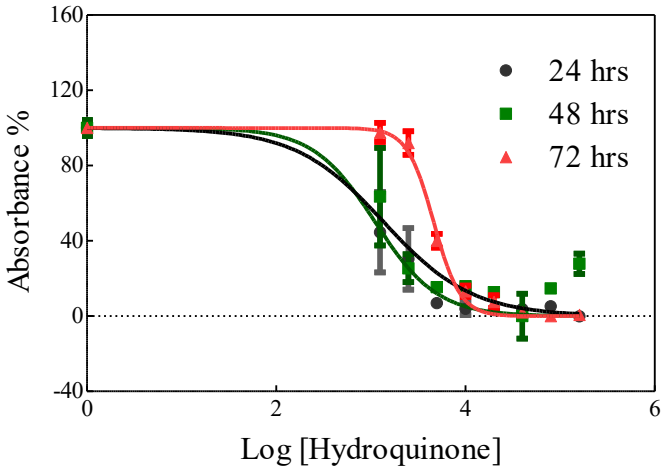

Figure 3.18. Concentration-response curve for hydroquinone exposure to AGS cells after 24, 48 and 72 h incubation, respectively. The data are presented as mean ± S.E, n = 3.

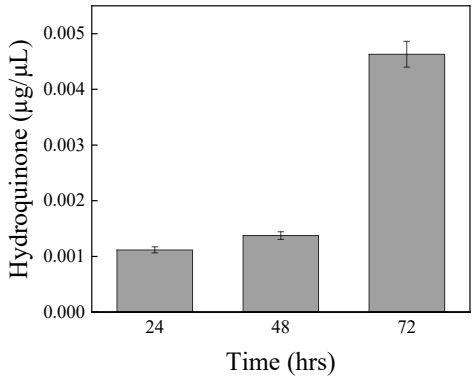

Figure 3.19. The histogram depicting the time evolution of IC_{50} values of hydroquinone in AGS cells. MTT Assay was applied to measure the proliferation inhibition rate of hydroquinone. Bars represent mean±SEM for 3 replicates.

3B.2.4. Potassium Nitrate (KNO_3) cytotoxicity.

The cell viability of AGS cells were evaluated when exposed to KNO_3 by measuring the extent of cell growth by employing the MTT assay. Figure 3.20. displays dose-response curve of KNO_3 in AGS cells for various incubation times. The nitrate induced cytotoxicity in AGS cells were apparently modest depending upon the incubation period and dose regimen. The KNO_3 treated AGS cells after 24 h incubation time showed a negligible antiproliferative activity from the lowest concentration (84% at 0.0012 µg/µL, SE = 5.85) to the highest (85% at 0.16 µg/µL , SE = 4.67) concentration levels. Cells treated with KNO_3 for 48 h did not exhibit any noticeably significant cell growth inhibition activity, on the contrary, upon treatment with 0.0012 µg/µL KNO_3 (SE =3.08), 102 % cell viability was observed, followed by increased cell growth at higher KNO_3 concentrations, whereas a modest antiproliferative activity for the highest KNO_3 concentration (87.54% at 0.16 µg/µL, SE = 2.78) was detected. After 72 h incubation time, the cell growth remained practically unchanged till a sudden drop in percentage cell viability of 0.47% (SE = 0.33) was seen at 0.08 µg/µL of KNO_3 treatment, to 0.43% (SE = 0.34) cell viability at the highest exposed concentration (0.016 µg/µL). The Pearson's correlation coefficient for the 24 h MTT KNO_3 treatment study showed a statistically insignificant weak negative correlation between cell viability and growth inhibitor concentration while strong negative correlation was observed for both 48 ($p<0.05$) and 72 ($p<0.01$) h MTT assay due to KNO_3 treatments.

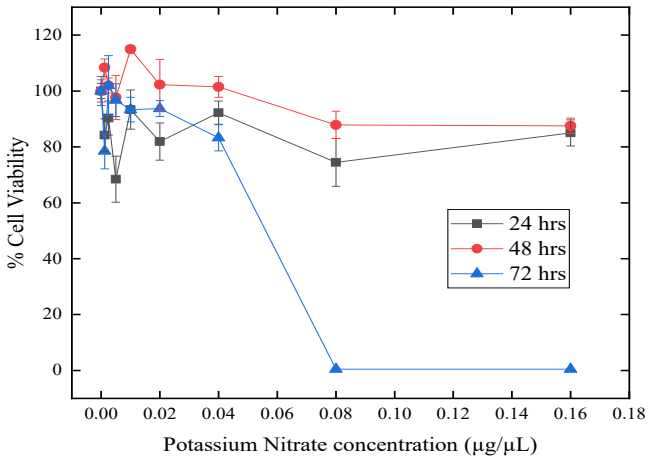

Figure 3.20. Dose-response curve for the growth inhibition activity of potassium nitrate at various incubation times (24, 48, and 72 h) with increasing concentrations of KNO_3. Growth inhibition of AGS cells was assessed by MTT assay. The data presented are depicted as mean ± S.E, n = 3.

Toxic effect or potency of KNO_3 on AGS cell line was measured by finding the half-maximal growth inhibitory concertation (IC_{50}) using non-linear regression, dose-response-inhibition model. The log [inhibitor] vs normalised response curves are shown in Figure 3.21. The estimated IC_{50} values for KNO_3 exposed AGS cell line were 0.012555 µg/µL (R^2 = 0.1246), 0.002063 µg/µL (R^2 = 0.05138) and 0.046433µg/µL (R^2 = 0.9752) for 24, 48 and 72 h, respectively (Figure 3.22.). It was evident from the time evolution of growth inhibition studies for KNO_3 exposure to AGS cells that the 72 h data set was best fitted with the non-linear regression model, and the corresponding IC_{50} value was chosen for further experiments.

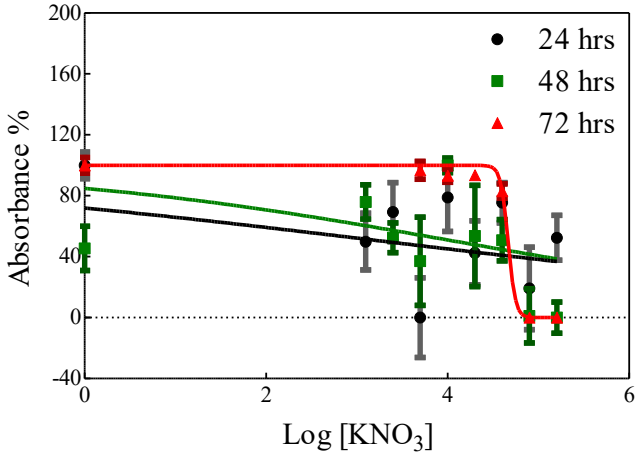

Figure 3.21. Dose-response curve of potassium nitrate exposure to AGS cells with varying incubation periods (24, 48, and 72 h). The data are presented as mean ± S.E, n = 3.

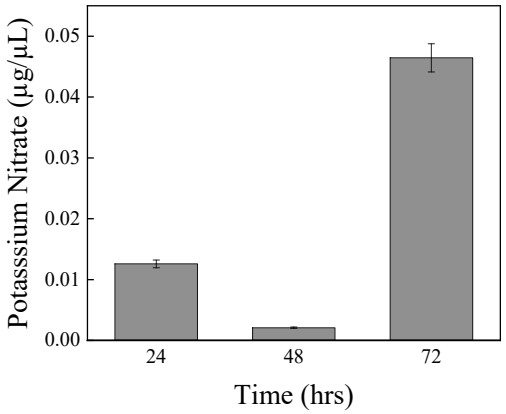

Figure 3.22. Effect of incubation time on IC_{50} values of KNO_3 exposure to AGS cells after 24, 48 and 72 h and MTT assay was applied for calculating the growth inhibition rate of KNO_3. Bars represent mean ± SEM for 3 replicates.

3B.2.5. Sodium Nitrite ($NaNO_2$) cytotoxicity.

Sodium nitrite exposure to AGS cells was evaluated for the putative toxicity effects of $NaNO_2$ by measuring the growth inhibitory effects of $NaNO_2$ using MTT assay (Figure 3.23.). $NaNO_2$ treated AGS cells after 24 h incubation time surprisingly demonstrated a proliferative effect on AGS cells, i.e., the number of viable cells increased to 104 % (SE = 2.07) at 0.01 µg/µL of $NaNO_2$ exposure. Subsequently, with a much higher concentration exposure, a modest growth inhibition of AGS cells (98% at 0.16 µg/µL, SE = 8.04) was detected. More akin to 24 h of incubation, exposure to 0.02 µg/µL of $NaNO_2$ for a 48 h incubation period (% cell viability: 151%, SE = 11.30) as well as 72 h incubation period, NaNO2 exhibited growth stimulatory effects, i.e., at most dosage regimen of $NaNO_2$, the AGS cells were demonstrably proliferated. It was evident from the dose-response curve after 72 h of exposure that initially the cell proliferation was detected with 110% (SE = 12.93) cell growth due to 0.01 µg/µL $NaNO_2$ exposure. Ultimately, growth inhibition to 37 % (SE = 3.50) cell viability was revealed for the highest exposed $NaNO_2$ concentration (0.16 µg/µL). Besides, 72 hrs $NaNO_2$ treatment MTT study also has shown a strong negative correlation between concentration and cell viability ($p<0.01$), whereas Pearson's correlation data showed that a non-significant negative correlation between concentration and cell viability for both the 24 and 48 hrs studies.

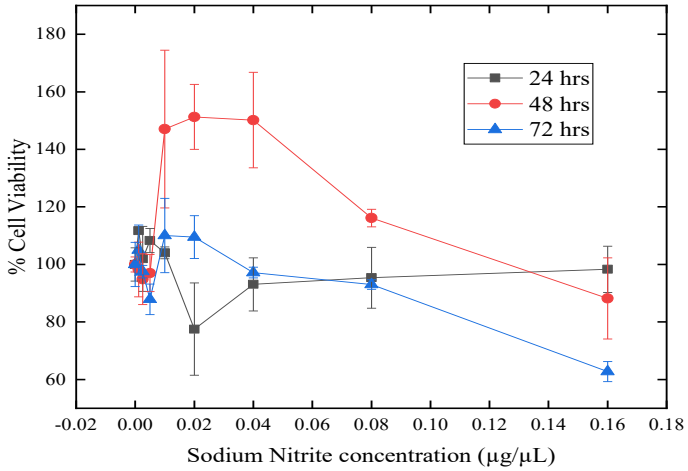

Figure 3.23. Dose-response curve for the putative cytotoxic effects of $NaNO_2$ on AGS cells using MTT assay. The resulting growth inhibition data is represented as mean ± S.E, n = 3.

Using non-linear regression, dose-response-inhibition model, the inhibitory concertation 50 (IC_{50}) was estimated based on the growth modulation potency of $NaNO_2$ with AGS cells exposed to increasing doses of nitrite ions, as shown in Figure 3.24. The IC_{50} values for $NaNO_2$ exposed AGS cell line were 0.058221 µg/µL (R^2 = 0.04201) for 0.006637 µg/µL (R^2 = 0.003024) and 0.081033 µg/µL (R^2 = 0.3066) for 24, 48 and 72 h, respectively (Figure 3.25.). Because of greater variability in the interaction of $NaNO_2$ with AGS cells, there was variations in the IC_{50} values without exhibiting any clear trend, hence none of the data for the time evolution studies fit the non-linear regression model, consequently, the IC_{50} values were not taken into consideration for further experiments.

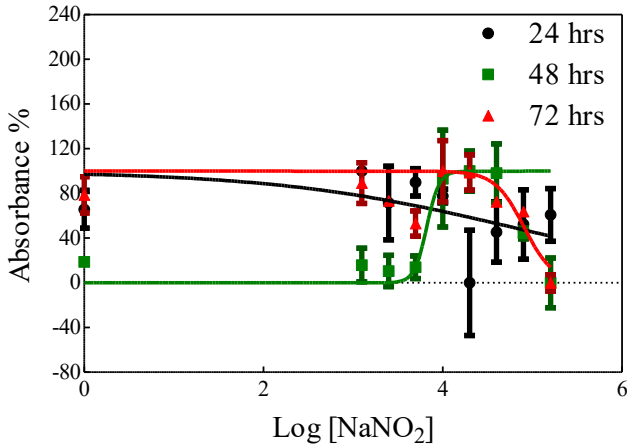

Figure 3.24. Growth altering effects of $NaNO_2$ with AGS cells on exposure to increasing concentrations of $NaNO_2$. Growth modulation(s) were assessed by MTT assay and IC_{50} values were calculated. The data are represented as mean ± S.E, n = 3.

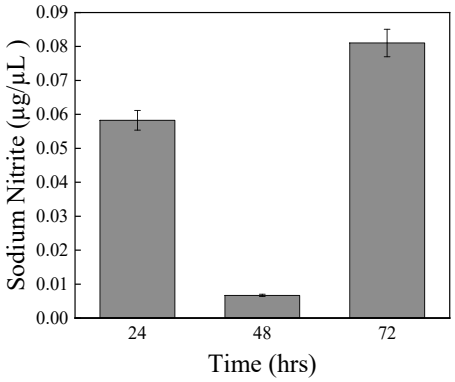

Figure 3.25. Effect of incubation time on IC_{50} (µg/µL) values of $NaNO_2$ exposure to AGS cells using MTT assay. Bars represent mean ± SEM for 3 replicates.

3B.3. Effect of tuibur exposure on Total Antioxidant Capacity (TAC).

AGS cells treated with the effective inhibitory concentrations (IC_{50}) of tuibur, nicotine, hydroquinone and potassium nitrate were evaluated for their total antioxidant capacity. The mean value TAC levels of AGS cells exposed to a polar chemical mixture of as well as 3 chemical constituents of tobacco smoke, viz., tuibur, nicotine, hydroquinone and nitrate ions, respectively, were estimated to be 0.91 ± 0.02, 1.01± 0.0001, 0.82 ± 0.02 and 0.71 ± 0.03 nmole/µL, respectively. The mean TAC level of the AGS cells without any chemical exposure (control) was observed to be 0.94 ± 0.005 nmole/µL. A reduction in the TAC by a factor of 0.03 ± 0.02 nmole/µL in tuibur treated AGS cells was observed when compared to the TAC of untreated cells. In summary, nicotine putatively induced a modest increase in TAC of AGS cells, whereas other tobacco smoke constituents exerted a moderate suppression of antioxidant capacity in AGS cells (Figure 3.26.).

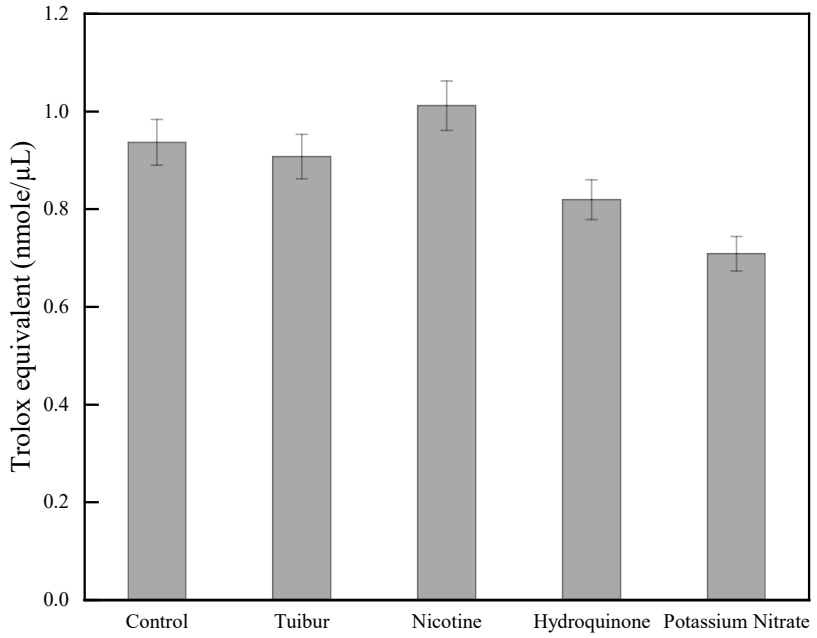

Figure 3.26. Total Antioxidant capacity of tuibur, nicotine, hydroquinone and potassium nitrate treated AGS cells. The data are presented as mean±S.D, n=3.

3B.4. Effect of tuibur treatment on intracellular ROS production.

The intracellular production of reactive oxygen species (ROS) in toxicant treated AGS cell line was further assessed using DCFDA stain with FACS methods. In comparison with fluorescence microscopy methods, Fluorescence-Activated Cell Sorting (FACS) method combines the detection of fluorescent tagged cells with cell sorting to isolate specific cell populations, enabling the rapid assessment of ROS production in live or fixed cells via fluorescent probes like DCFDA which emit fluorescence due to ROS generation after treatment. Figure 3.27. presents the fluorescence intensity shift in control and AGS cells treated with tuibur, nicotine, hydroquinone and KNO_3, in addition to a positive control treatment with H_2O_2. The unstained and untreated AGS cells were used as auto fluorescence control. From the experimental observations, AGS cells treated with nicotine has shown the highest ROS levels with a 79.74 ± 0.0034 % change in the ROS production in comparison with the untreated cells. Relatively higher ROS levels, an increase of 65.59 ± 0.033 % and 49.38 ± 0.019 % were observed in AGS cells treated with tuibur and hydroquinone, respectively. Equivalent ROS production was observed for the positive control hydrogen peroxide treated AGS cells and KNO_3 treated cells with 75.54 ± 0.049 % and 75.23 ± 0.029 %, respectively. The stained untreated control group showed an increased ROS production with 76.94 ± 0.012 %. Among all the control and treated cells, maximum intracellular induced ROS production was seen in AGS cells treated with nicotine followed by the untreated control group. The histogram representing the percentage ROS production in the study groups is shown in figure 3.28.

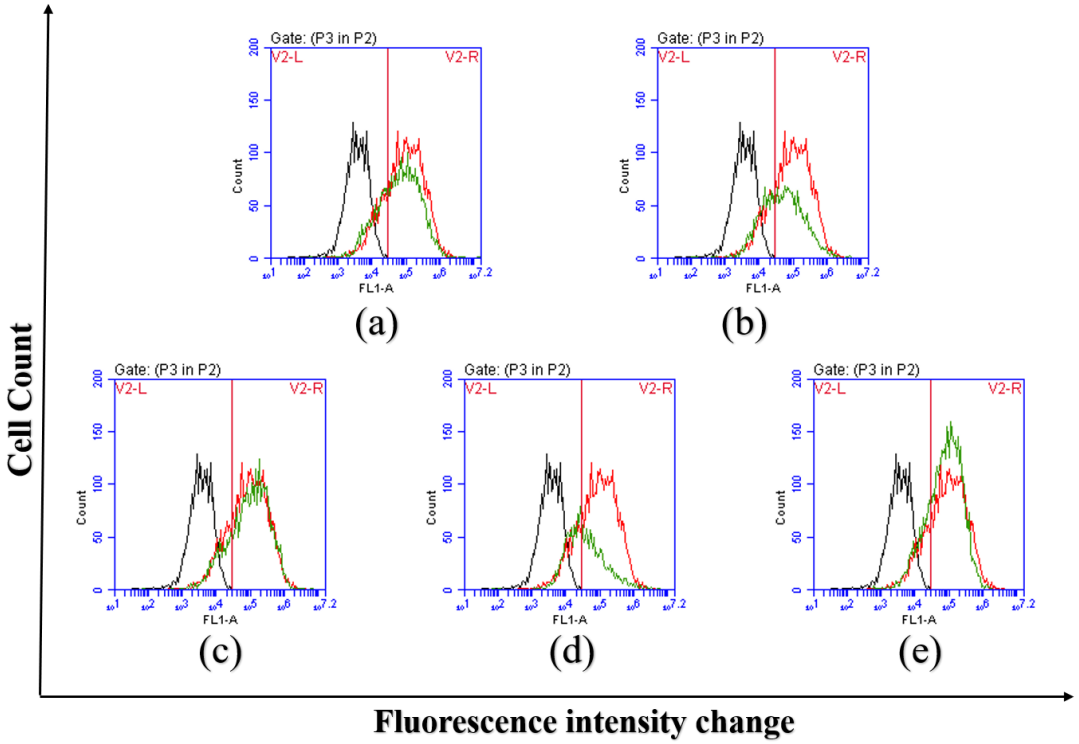

Figure 3.27. Fluorescence intensity change in DCFDA stained cells using FACS; (a) % ROS in H_2O_2 treated cells; (b) % ROS in tuibur treated cells; (c) % ROS in nicotine treated cells; (d) % ROS in hydroquinone treated cells; (e) % ROS in KNO_3 treated cells. (Black indicates unstained control cells, red indicates stained control cells and green indicates stained chemical treated cells).

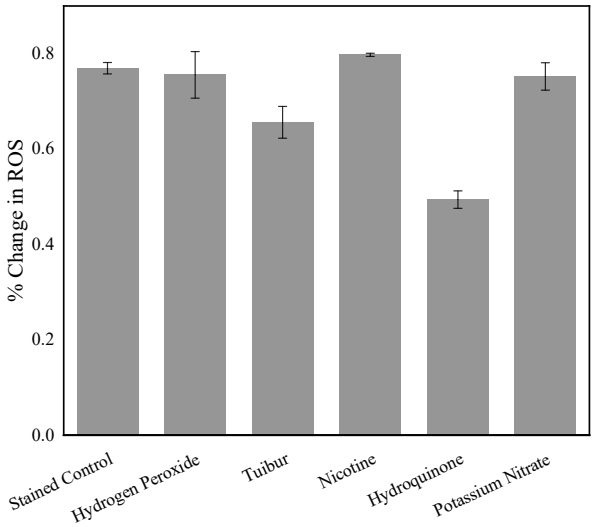

Figure 3.28. Degree of % change in intracellular ROS production in control and treated AGS cells. The data is presented as mean ± S.D., n=2.

3B.5. Effect of tuibur treatment on cellular NO_x level in AGS cell line.

The total cellular NO_x concentration levels (consisting endogenous as well as induced levels) in AGS cells treated with tuibur as well as in nicotine, hydroquinone and potassium nitrate treated AGS cells were determined using Griess Assay Kit. A calibration curve with $R^2 = 0.97$ was obtained by using sodium nitrite standard solution. In the control system, i.e., AGS cells without exposure to any tobacco related chemicals, the nitrite levels were found to be 131.45 ± 0.18 µM, while not surprisingly, the nitrite content of KNO_3 treated cells (128.38 ± 0.004 µM) was more akin to the control system. Interestingly, in tuibur and nicotine treated cells, 126.23 ± 0.03 µM and 120.48 ± 0.03 µM of nitrite levels, respectively, were detected. Whereas, the nitrite concentration in cells treated with hydroquinone was observed to be the lowest at 90.40 ± 0.08 µM. The difference in nitrite concentration with respect to control, for KNO_3 treated cells, 3.07 ± 1.54 µM; for tuibur treated cells, 5.22 ± 2.60 µM; for nicotine treated cells, 10.97± 2.60 µM; and for hydroquinone, 41.05 ± 20.52 µM, respectively. A histogram that summarizes the comparison of nitrite levels in treated AGS cell line is depicted in figure 3.29. The results of in vitro Griess assay for $NO^{\bullet}$ formation in the control and hydroquinone treated cells were consistent with the earlier studies that indicated the NOx levels were modestly supressed in cells treated with hydroquinone (Rao & Snyder, 1995; Snyder & Hedli, 1996). Whereas, no appreciable differences in $NO^{\bullet}$ levels of KNO_3, tuibur, and nicotine treated cells in comparison with the untreated AGS cells (control) were observed.

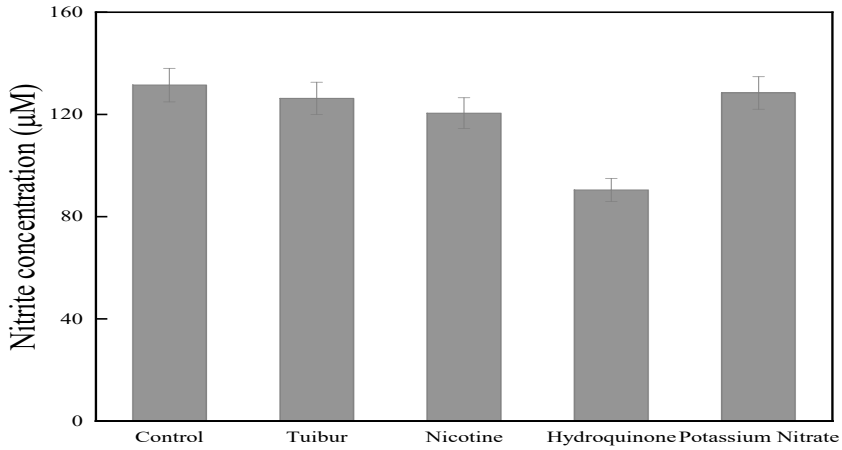

Figure 3.29. Comparison of NO_x levels in AGS cells exposed to tobacco smoke components. NO_x species levels as nitrite ion content was determine by Greiss Assay. The data are presented as mean ± S.D., n = 3.

3B.6. Tuibur treatment induced apoptosis.

The morphological characteristics of AGS cell line treated with the IC_{50} values of tuibur, nicotine, hydroquinone and KNO_3 were assessed by dual fluorescent staining using acridine orange and ethidium bromide (AO/EB) dyes. It is important to note that ethidium bromide is only capable of staining nonviable cells which have obviously lost their membrane integrity, while acridine-orange can stain both viable as well as nonviable cells. The nuclear dye staining experimental results have shown that after incubation of AGS cells with the IC_{50} levels of tobacco smoke chemical constituents as mentioned above, the cells have undergone a series of morphological changes which include condensation of nucleus, formation of early-stage apoptotic and late apoptotic bodies in contrast to untreated AGS cells (control) which have only showed much lower number of early-stage apoptotic cells and revealed the inherent morphology of for the majority of normal viable cells (Figure 3.30.). Early-stage apoptotic cells exhibiting yellowish-green fluorescence as well as late-stage apoptotic cells with orange-red fluorescence with their intact cytoplasm were observed. Table 3.14. displays the apoptotic cell count in the samples. It was observed that >84% cells remained normal in control and all treatment group cells. The AGS cells treated with hydroquinone have displayed the highest frequency of late-stage apoptosis (~ 4%), while in cells treated with nicotine the greatest number of early-stage apoptotic cells were observed. Even though, in tuibur treated AGS cells, there were preponderantly normal (~88%) cells, however, amidst its population ~10% cells with early-stage apoptosis were observed. (Figure 3.31.) From the apoptotic index (%AI) calculated for control and treated cells, nicotine treated cells showed highest % AI followed by tuibur treated AGS cells (Figure 3.32.).

Table 3.14. AGS cell scoring for normal, early-stage and late-stage apoptosis, n=1000 cells/well. The data is presented as mean ± SD, n=3.

Samples	Normal cells	Early-stage apoptosis	Late-stage apoptosis
AGS Control	976.5 ± 0.05	23.5 ± 0.5	0 ± 0.00
AGS treated with Tuibur	880.5 ± 1.50	109.5 ± 0.5	10 ± 1.00
AGS treated with Nicotine	842.5 ± 4.50	126 ± 5.00	31.5 ± 0.5
AGS treated with Hydroquinone	937.5 ± 0.05	24.5 ± 2.50	38 ± 2.00
AGS treated with Potassium Nitrate	926 ± 8.00	38 ± 5.00	36 ± 13.00

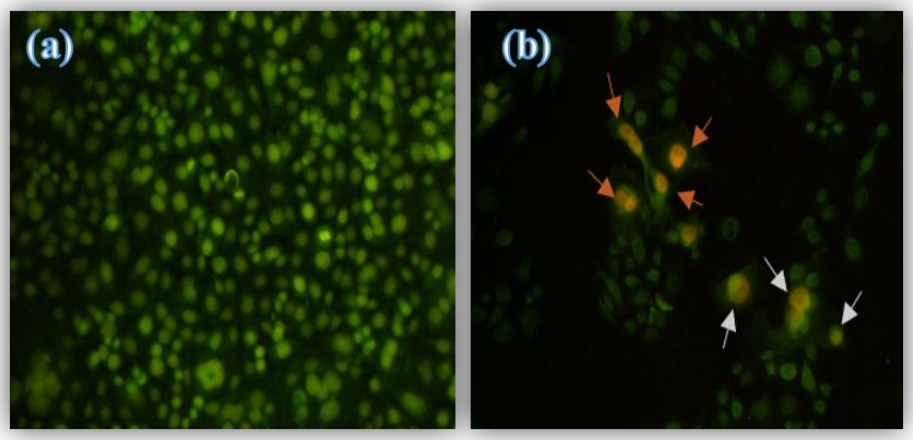

Figure 3.30. (a) Normal AGS cells, (b) early-stage apoptotic (white arrows) and late-stage apoptotic (orange-red arrows) AGS cells. Cells magnified to 16X.

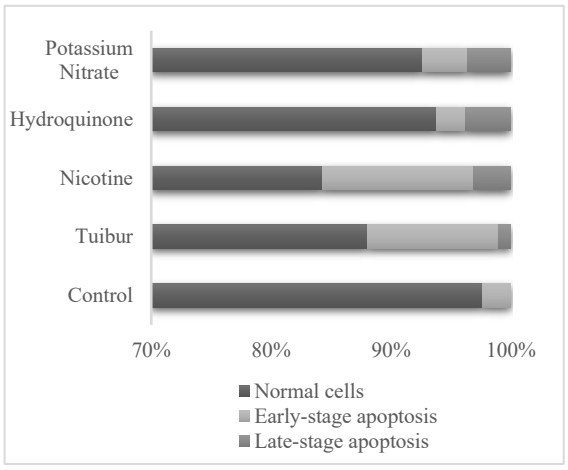

Figure 3.31. Frequency of apoptosis in control and treatment groups of AGS cell line.

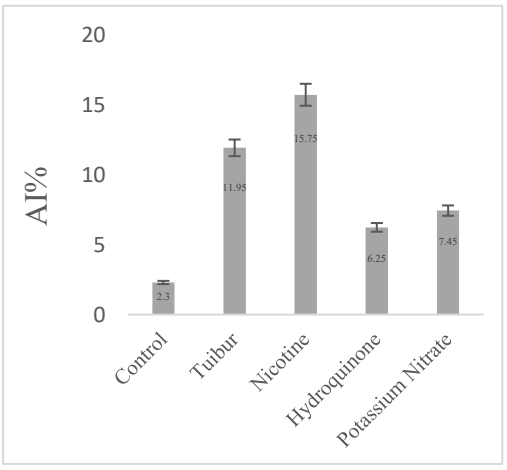

Figure 3.32. Percentage apoptotic index (AI) in control and treatment groups of AGS cell line.

3B.7. Discussion.

Micronuclei (MN) are nuclei-like bodies arising from chromosome fragments or lagging chromosomes persisting into the interphase and are not incorporated into daughter nuclei, indicative of apparent DNA damage. The characteristic features of genetic materials trapped in micronuclei are asynchronous and impaired DNA replication as well as DNA repair defects due to compromised nucleus envelope integrity. Micronuclei detection in exfoliated oral cells has been used as a biomarker for induced chromosomal and/or DNA damage because of genotoxic agents some which are the well-known lifestyle products, viz., tobacco, alcohol and betel nut (Jyoti et al., 2015). Early detection of putative biomarkers such as detection of high frequency of MN or oral lichen planus and/or leukoplakia in the oral cavity of SLT users by virtue of exposure to potent genotoxic and carcinogenic agents of SLT is also one of the prominent and important significant predictors of the preventable adverse health risks pertaining to SLT use (Borse et al., 2020).

This study aimed to investigate the relationship between tuibur and sahdah use related DNA damage in the SLT user population and the assessment of MN frequency in the oral cavity of SLT users. The results of present study have suggested that overall elevated MN frequency levels were detected in tuibur users when compared to both sahdah users and control groups (tobacco unexposed group). No such comparative studies between tuibur users, sahdah users and control group related micronuclei formation have been documented. The results of the present study which examined the oral epithelial cells of SLT users also revealed that all pairwise comparisons between the SLT user groups were statistically significant ($p<0.001$), indicating that both tuibur (alkaline “liquid” SLT) and sahdah (premixed ‘solid’ SLT) use are associated with higher MN frequencies when compared to non-users (control). The development of micronuclei in oral epithelial cells of smokers and SLT users have been well documented (Upadhyay et al., 2019). Earlier studies have documented that micronuclei formation is greater in SLT users as compared to smokers (Bansal et al., 2012) and significantly higher MN frequency in dual or poly-tobacco users (individuals who use frequently both smoke and smokeless tobacco products) (Dash et al., 2018).

Demographic and epidemiologic factors such as age, dietary habits, lifestyle habits and work environments manifest oxidative stress and further exacerbate the micronuclei frequency in individuals (Maldonado et al., 2023; Raimondi et al., 2007; Zhang et al., 2022). For the present study, sampling was performed to exclude the effect of age on the frequency of micronuclei as age has been reported to a major confounding factor as with the progression of senescence, the oxidative stress exasperates (Peace & Succop, 1999). Hence, tuibur user, sahdah user and the control groups' have a mean age of 37.76 ± 9.45, 36.52 ± 8.23 and 39.94 ± 10.81, respectively. From all three group of populations, exfoliated epithelial cell samples were collected. The demographic profile of the sahdah users indicated a mean frequency of use, 10.94 ± 5.23 times per day, which is marginally higher as compared to tuibur users (9.62 ± 5.49/day). The mean duration of tuibur use (in years) by the participants was 18.18 ± 8.84 years while the SLT exposure profile of sahdah users was moderately lower (15.84 ± 9.89 yrs) as summarized in table 3.11. Surprisingly, the correlation between age and MN count, dosage (mean SLT use/day) and MN count besides the duration of SLT use and MN count for both tuibur and sahdah user groups did not show any significant elevated health risk, perhaps due to the limited number of samples. In this study, factors influencing micronuclei formation such as alcohol intake, other tobacco habits etc., were not taken into consideration although Mizo male population tend to indulge in dual or poly-tobacco products (more than two tobacco products) use. In addition, owing to the limited range of variability in the sample set as described above (vide supra), the variability of the data set may not be substantially adequate to depict any significant consequences. However, previous epidemiological studies have demonstrated that virtually all types of SLT use either alone or concurrent use of betel quid with SLT are important causative risk factors of oesophageal and/or stomach cancers (Dhillon et al., 2018; Phukan et al., 2005).

The results of the present study indicated that among the three study groups considered in this study, the formation of micronuclei, a biomarker of DNA damage, was significantly higher in tuibur users when compared to the other two groups. This important finding of the present study is consistent with the earlier studies that have suggested significantly increased cancer risk in tuibur users of Mizoram (Malakar et al., 2012; Phukan et al., 2005). Furthermore, an earlier study on MN formation where

a gradual increase in the frequency of micronuclei in normal oral mucosa portend pre-cancerous lesions and eventually to carcinoma, and thus inferred that the increase in MN frequency more likely linked with the tumorigenic progression (Casartelli et al., 2000). Therefore, investigation of the mechanism of damage of genetic material which may potentially lead to tuibur-related carcinogenesis is required in order to elucidate the harmful effects of tuibur on the user population. Consequently, AGS cell line was chosen as a rudimentary model system *in vitro* to illustrate the putative biological effects that may occur because of the avoidable tuibur exposure in vivo.

Assays designed for *in vitro* toxicological research have been widely used to assess the biological consequences of tobacco products such as cigarette smoke and different types tobacco extracts. Rather very limited studies on the negative health effects of tuibur *in vitro*, *in vivo* or *ex vivo*, were carried out since, it is a 'smokeless' tobacco product predominantly available in Northeast Indian region (Mahanta et al., 1998; Sanjeev, 2019). In the present study, the cytotoxic potential of tuibur on AGS cell line was assessed using MTT assay. The cell viability/toxicity study sheds light on the relationship between concentration of the toxicant, duration of exposure and the rate of induced cell death. Cell proliferation assays are potential tools for gaining an insight into the mechanism of action of certain proteins, genes and pathways involved in the survival or death of cells exposed to toxicants. MTT assay is the gold standard in cytotoxicity testing because it is simple, robust, cost-effective and highly reproducible.

In the present study, a discernible inhibition in the cell growth was observed at rather lower doses of tuibur treatment on the dose- and time-dependent studies, suggesting a most likely tuibur induced cytotoxicity. After 24 h of treatment, tuibur could significantly ($p<0.05$) inhibit the growth and aggregation of adherent AGS cells in a dose-dependent manner. During 24 h, the potency of tuibur is at its maximum, where the polar chemical constituents of the tobacco smoke concentrate (tuibur) have more probably been permeated the cells and induced cytotoxicity. After 48 and 72 h of exposure, an increased cytotoxicity or decreased cell viability is observed at each treatment concentration. This observation has indicated that more likely a gradual uptake of major chemical constituents and their intracellular metabolism may have further augmented the putative cytotoxic potency of polar constituents of tuibur. This

MTT study has demonstrated that tuibur can induce cytotoxicity in a dose-dependent and time-dependent manner in AGS cells indicating the potential negative effects of chronic tuibur use. Similar to this study, tuibur exposed to HPBLs, Hela, V79 and DLA cells were reported to exhibit dose-dependent cytotoxicity (Lalruatfela et al., 2020). Furthermore, aqueous tobacco extracts triggering cell death upon administering increasing dosages of the extract on gingival epithelial cells have been reported (Patil & Baeshen, 2021). Tuibur also exhibited half-maximal inhibitory concentrations of 15.30 µg/µL (24 h), 6.606 µg/µL (48 h) and 6.808 µg/µL (72 h) on AGS cells in this study. While the magnitude of differences in IC_{50} values of tuibur was varied, however the overall order of cytotoxicity was consistent (downward trend). In comparison with other components of tuibur, pure nicotine, hydroquinone and nitrate, tuibur certainly contains various organic/inorganic components whose intermolecular interactions would vary according to the pH and these interactions would further influence the putative cellular functions. Consequently, the fate of tuibur treated cells would be based on the balance of cellular functions. It seems reasonable that the IC_{50} trend for tuibur is plausibly altered by the cellular metabolic activities in the treated cells over the course of time. This set of data provided a measure of putative cell growth inhibitory effect of tuibur demonstrating the cytotoxic potency on immortalised AGS cell line.

Tuibur is an alkaline tobacco smoke concentrate where tobacco smoke was generated using tobacco stalk consisting stem, petiole, and midvein. In tobacco plant, major organic and inorganic mineral chemical constituents preponderantly concentrated in tobacco leaf lamina, while stem and petiole contain moderate to modest levels of majority of chemical constituents. Previous studies have suggested that a wide range of chemical constituents present in tuibur mainly those corresponding to tobacco smoke constituents (Lalmuanpuii et al., 2015). Alkaloids, the principal constituents of tobacco, particularly nicotine, is of µg/mL (ppm) range in different grades of tuibur as observed in this study. The nicotine levels determined in tuibur is approximately three orders lesser than other commercially available SLTs (Stanfill et al., 2023; Stepanov et al., 2005, 2015). In present study, we used a ‘specific’ grade of tuibur for which 500 mg/mL of tobacco stalk is used during the production. Furthermore, taking into account that the tuibur used for treatment (*vide supra*) in

which the evaluated concentration of nicotine was 506 µg/mL, whereas the amount of nicotine concentration we used in our present *in vitro* study ranged between 0.001 – 0.162 µg/µL for treatment, for a positive control group. However, at 100 µM nicotine exposure, normal human endothelial cells and fibroblasts have exhibited an elevated DNA synthesis and altered gene expression patterns (Laytragoon-Lewin et al., 2011). More importantly, considering the heterogeneity of tuibur, the experimentally observed cytotoxicity in vitro cannot be attributed to nicotine alone even though nicotine is the preponderant chemical constituent among many other carcinogenic constituents determined in tuibur (Chang, Muthukumaran, Hu and Chao, 2024, unpublished results). A plethora of other chemical species such as oxidative stress inducing heavy elemental ions, carcinogenic TSNAs, pro-oxidants such as quinones, carbonyl compounds, aromatic amines, along with high levels of nitrosating species such as $(NO_2)^-$, $(NO_3)^-$, etc., could also be other potential contributing factors for the putative cytotoxicity of tuibur.

In order to gain a better understanding of the toxicity of tuibur constituents, independently, the cell viability of selected chemical species present in tuibur were assessed. Subsequently, the cytotoxicity of S-(-) nicotine was examined using MTT assay. The results showed that nicotine induced cell proliferation occurred on exposure at lower concentration of nicotine in AGS cell line. This illustrates the stimulating effects of nicotine on enhanced cell proliferation on gastrointestinal cancer cells. This stimulatory effects of nicotine is in agreement with earlier studies on nicotine exposure augmented cell proliferation in AGS cells because of elevated PGE_2 production and COX-2 activity (Shin et al., 2008). Other *in vitro* and *in vivo* studies have also labelled nicotine as a major risk factor for gastric cancer (K. Jensen, Afroze, et al., 2012). Only with prolonged exposure (72 h) to lower concentration levels of nicotine, the cell viability significantly decreased ($p<0.01$) indicative of the time-dependency of cell growth inhibitory effects of nicotine treatment. Intriguingly, this important finding of the present study is in disagreement with earlier reports on the proliferating effects of low-concentration nicotine. However, there are reports of cytotoxicity of nicotine such as a gradual yet noticeable suppression of cell growth in other immortalised cell lines have been reported (Chioran et al., 2022; Kang et al., 2011). The potency of nicotine

on AGS cell line was demonstrated by evaluating the IC_{50} values in a dose-and time-dependent manner where the agonist activity of nicotine decreased over the period.

Similarly, *in vitro* cytotoxicity of hydroquinone in AGS cells was assessed using MTT assay. Hydroquinone, a chemical constituent of tuibur, is possibly present in modest concentrations, (Lalmuanpuii, 2016), capable of generating free radicals (semi-quinone intermediate) while oxidized to benzoquinone. In this study, the cell viability was found to be supressed by ~50% due to lower concentrations of hydroquinone after 24 h of treatment. The cytotoxic effect of hydroquinone was found to diminish in a dose-dependent manner. The IC_{50} concentration of hydroquinone for AGS cells varied with prolonged exposure duration. Apparently, the cell inhibitory effect of hydroquinone was subdued as the duration of exposure increased. This shows that the inhibitory effect of hydroquinone was diminished in a time-dependent manner. This study coincides with an earlier report of hydroquinone exhibiting negative effects on cell viability in other cell lines (Sharma et al., 2012). Though there are evidences supporting anti-oxidant effects and supplementary data positively associated with hydroquinone, whereas the induction of cancer and tumours in rodents by hydroquinone has also been reported (Byeon et al., 2018). Similarly, various studies have reported the genotoxicity and cell transforming activity of hydroquinone in mammalian cells (Enguita & Leitão, 2013). Furthermore, hydroquinone and catechol, which are arising from the pyrolysis of lignocellulosic content of tobacco matter, were demonstrated to inhibit ribonucleotide reductase and prevent the progression of human T lymphocytes through the S-phase of cell cycle (McCue et al., 2000).

Potassium nitrate (KNO_3) and sodium nitrite ($NaNO_2$) were also assessed using MTT assay, since nitrate and nitrite ions are potential nitrosating agents under different physiological conditions and capable of nitrosating tobacco alkaloids *in situ* leading to the formation of TSNAs. Endogenous TSNA formation have been reported to occur where the major influencing factors are the pH conditions as well as the levels of nitrosating agents which ultimately form NO_x under physiological redox conditions (Nair et al., 1996). When AGS cells were exposed to KNO_3, an elevated cell growth was observed thus demonstrating the proliferating activity in AGS cells after 24 and 48 h treatment regime, respectively. Interestingly, KNO_3 in lower concentrations have been reported to exhibit positive symbiotic effects *in vivo* (Liubertas et al., 2023). After

72 h of exposure to KNO_3, a diminution of cell viability in AGS cells was observed in a dose-dependent manner. Aledwany et al., (2018) also reported in a recent study showing the gradual attenuation of cell growth caused by KNO_3 in a dose-dependent manner in the established human cell lines such as HepG2 and THLE2. At present, the inhibitory effects of KNO_3 on AGS cell growth were modest and was independent of duration of exposure. Similarly, $NaNO_2$ was also assayed with AGS cells by using MTT demonstrating the proliferative effects in a dose-dependent manner. Inhibitory effects of $NaNO_2$ remained insufficiently consistent because of the observed experimental conditions where the data set depicted a low goodness of fit for the logarithmic regression model used for analysis. The inconsistency in the results for $NaNO_2$ may be possibly because of the lower concentration regime that was applied for the in vitro study. The present study was mainly carried out to compare and assess the cellular response towards the preponderant chemical components of tuibur, independently and towards tuibur in order to elucidate the biological effects of tuibut observed. Clearly, additional chemical constituents in the alkaline tobacco smoke concentrate such as heavy element ions, aromatic amines, TSNAs etc., appear to have played a more prominent biological effects over those of nicotine, hydroquinone, $(NO_2)^-$ and $(NO_3)^-$. Besides, common inorganic anionic species such as $(NO_2)^-$, and $(NO_3)^-$ are not known to cause acute cytotoxicity or genotoxicity at lower concentration ranges (Kobayashi, 2018).

From the cytotoxicity experiments in this study, it is evident that tuibur has shown cytotoxic and genotoxic activity *in vitro* more akin to many other SLTs. Tobacco use induced oxidative stress is a potential causative risk factor for the corresponding inflammatory response. In order to assess the extent of oxidative stress induced because of exposure to tuibur and the major chemical constituents of tuibur, independently, total antioxidant capacity was assayed in AGS cells. AGS cell line treated with IC_{50} levels of tuibur showed a decrease in the antioxidant capacity as compared to the untreated control cells. This indicates the reduction of antioxidant potential in the cells which would significantly attenuate the ability of cells to scavenge free radicals, ROS and RNS, and instigate acute oxidative stress in the cells. The purported increase in ROS production due to the tuibur exposure in the AGS cells leads to the depletion of antioxidants and probable suppression of antioxidant enzymes

activities within the cells. This result is also consistent with the cytotoxicity assessment in this present study where cell senescence occurred upon tuibur exposure. Cell death is an inflammatory reaction to oxidative stress. The imbalance of free radicals and antioxidants can lead to the alteration of lipids, proteins and DNA. In a population studies, salivary antioxidant capacity tested in smokers as well as tobacco chewers were reported to be significantly lower than that of non-smokers or non-users. In addition the antioxidant capacity of the saliva of tobacco chewers were the lowest as compare to the other two groups (Ghazi et al., 2020; Shwetha et al., 2018). Cigarette smoke, at the cellular level triggers oxidative stress via ROS, leading to lipid peroxidation, DNA damage and activation of damage-associated molecular patterns (DAMPs) (Roh & Sohn, 2018). Much like the oxidative constituents present in cigarette smoke, tuibur, a variant of tobacco smoke, viz., tobacco stalk smoke, is also likely to consist of similar chemical species capable of intracellular generation of ROS by virtue of disrupted redox status. It is a known fact that, tuibur also contains the polar phenolic species of cigarette smoke, hydroquinone and catechol (Lalmuanpuii, 2016).

Analogous results were observed in cells treated with hydroquinone and KNO_3 similar to the impact of tuibur on the antioxidant capacity of AGS cells. Diminution of antioxidant capacity in the treated cells was more pronounced for the aforementioned chemicals in comparison with tuibur. Hydroquinone is a well-known carcinogen, capable of generating the semi quinone based free radicals besides reactive oxygen species such as superoxide species. The hydroquinone cytotoxicity experiment from this report is also consistent with the TAC. Intracellular metabolism of hydroquinone catalysed by cytochrome-P_{450} results in the production of different concentrations of benzoquinone compounds which has potential to form mono- or poly-glutathione conjugates (IARC, 1987). Polyphenolic-GSH conjugates are known mutagens having cytotoxic and genotoxic properties, which may be a contributory factor for hydroquinone-mediated carcinogenesis (Monks & Lau, 1997). The effect of KNO_3 on AGS cells in terms of antioxidant capacity can be seen as depicted in figure 3. It should be noted that when compared to control and other treatments, KNO_3 treated cells showed significantly diminished antioxidant potential. This reduced antioxidant capacity more likely due to the formation of reactive nitrogen species (RNS) resulting in nitrosative stress. under acidic conditions, nitrite anion, derived from nitrate,

spontaneously decompose to nitrogen dioxide and nitric oxide (Suzuki et al., 2005). The reaction of nitrites with secondary amines lead to the endogenous formation of carcinogenic nitrosamine species. Moreover, the presence of excess intracellular nitrates could also target biomolecules like lipids, proteins and DNA leading to significant toxicity further causing mutagenesis as well as carcinogenesis (Karwowska & Kononiuk, 2020).

In contrast to the previously discussed 3 treatments (tuibur, hydroquinone, and $(NO_3)^-$), nicotine, the preponderant alkaloid of tobacco, showed an elevated total antioxidant capacity in AGS cells. The TAC of control system (untreated cells) was also lower when compared to cells treated with nicotine. This observation commensurate with the enhanced cell proliferation in the nicotine treated cells (vide supra). Studies have suggested low doses of nicotine may exhibit antioxidant properties and have a role in neuroprotective effects. On the contrary, high levels of nicotine have also been reported to induce oxidative stress and toxicity (Zhang et al., 2007). Nicotine's antioxidant properties may be due to the intracellular activation of nicotinic receptors (Newman et al., 2002). An earlier research study by Linert et al., (1999), proposed that antioxidant properties of nicotine may be due to characteristic binding of nicotine with Fe (II) and the concomitant transferrin receptor-mediated reduction of Fe uptake. This study also suggested that the antioxidant properties of nicotine could be tissue-specific. The present investigation observed an enhanced antioxidant capacity in nicotine treated cells although this observation might be possibly due to the type of assay used for this analysis. Resultant data may be affected by the concentration of nicotine used (0.0011 μg/μL) for this study since low levels of nicotine have been documented to exhibit antioxidant effects. Higher concentration levels of nicotine might produce more contrasting results as suggested by Laytragoon-Lewin et al., (2011). Hence, a more in-depth study is warranted to distinguish as well as to gain a better understanding of the antioxidant-oxidative attributes of nicotine.

Reactive oxygen species includes species such as superoxide anion radical ($O_2^{\bullet -}$), , hydroxyl radical($^{\bullet}OH$), hydroperoxide ($^{\bullet}OOH$) and the pro-oxidant species, hydrogen peroxide (H_2O_2). The excess concentrations of these species depicts the state of oxidative stress and thus deleteriously impairing cellular structures by causing the damage to DNA, protein, and the membrane bound lipids (Hayat, 2015). Nicotine is

also known to induce oxidative stress in different types of cells including epithelial, alveolar, hepatocytes, macrophages and mesangial cells both *in vivo* and *in vitro* (Jensen et al., 2012). Nicotine-instigated significant levels of ROS production in mouse proximal tubule cells of the kidney via NADPH oxidase has been reported (Arany et al., 2011). Nicotine is also reported to increase ROS generation in a dose-dependent manner in mesencephalic cells (Barr et al., 2007). Lung epithelial cells also showed an elevated levels of ROS production when treated with nicotine (Zhang et al., 2020). Cigarette smoke has been reported to trigger elevated ROS concentrations and thereby inducing the upregulation of iNOS expression (Zi et al., 2023). Zhao et al., also demonstrated that HUVEC cells treated with an aqueous extract of snus exhibited elevated levels of ROS production which entail cellular damage (J. Zhao et al., 2021). Hydroquinone induced production and the consequent accumulation of elevated ROS levels in different cells is also well documented (Heluany et al., 2021; Y. J. Kim et al., 2009; Hong et al., 2014). Highly reactive $NO^{\bullet}$ and H_2O_2 are likewise well-known ROS responsible for mediating oxidative stress. In the present study, ROS generation was slightly elevated by 2.8 % in AGS cell line on exposure to nicotine as compared to untreated cells. A decrease fluorescence intensity change was observed in AGS cells treated with tuibur, KNO_3 and positive control H_2O_2. Hydroquinone showed lowest degree of ROS production among the treatment groups. The change in ROS for the untreated control cells was observed to be 76.94% which is very high. The reason for this anomaly cannot be explained and hence also affects the outcome for the treatment groups. DCFDA is a widely used dye for ROS detection but has drawbacks. DCFDA is not specific to any ROS, after staining the dye can leak from the cells, the speed of increase in fluorescence intensity is retarded at low concentrations and the occurrence of photo-oxidation of the dye during observation may play a role in any errors that could have occurred, inadvertently, during the experiments (Afzal et al., 2003). Therefore, this assessment of ROS production in our FACS study yielded rather vague and inconclusive results.

Reactive nitrogen species also play a key role in nitrosative/oxidative stress due to tobacco consumption. Griess assay was used for the determination of nitrite levels in AGS cells treated with tuibur, nicotine, hydroquinone and KNO_3. A small but apparent diminution of nitrite levels in tuibur treated AGS cells was observed

when compared to untreated cells. This implies that tuibur more likely inhibit the intracellular production of $NO^{\bullet}$ under the prevailing conditions in AGS cells. A reduction in exhaled nitric oxide levels in smokers when compared to never-smokers have also been reported. Passive smokers have also been reported to exhibit reduced $NO^{\bullet}$ levels upon exhalation (Malinovschi et al., 2006). $NO^{\bullet}$ plays diverse roles in cellular milieu one of which is cell signalling, thus upregulation or downregulation of $NO^{\bullet}$ production may have detrimental effects in various physiological processes. Unregulated production of $NO^{\bullet}$ can cause cell death via oxidative stress and DNA damage (Murphy, 1999). Nicotine treated cells also exhibited lower intracellular nitrite levels than that of both tuibur treated as well as untreated cells in this study demonstrating that nicotine also possibly supresses intracellular nitrite levels. This agrees with the findings of Pisarcik et al., (2008) where reduced nitrite levels in nicotine treated human umbilical artery endothelial cells (HUAECs) was detected when compared to untreated cells. The putative mechanisms of reduction in $NO^{\bullet}$ concentrations in cells treated with nicotine and tuibur were not explored in this study. Nevertheless, studies on superoxide-mediated inactivation of $NO^{\bullet}$ by tobacco smoke and reduction of activity of endothelial nitric oxide synthase (eNOS) by cigarette smoke have been reported (Peluffo et al., 2009; Zhang et al., 2006).

From our results, hydroquinone treated cells have the lowest nitrite levels among the control and treatment group. The reduced levels of $NO^{\bullet}$ production may be due to the ability of hydroquinone to scavenge nitrite via nitration and nitrosation (Lu et al., 2016). Scavenging of peroxynitrite by hydroquinone and suppression of $NO^{\bullet}$ production in RAW264.7 cells have been reported (A. R. Kim et al., 2005). Lipopolysaccharide induced nitric oxide production by neutrophils have likewise been revealed to be quenched by hydroquinone (Enguita & Leitão, 2013). Interestingly, KNO_3 treated AGS cells exhibited slightly reduced but comparable nitrite levels to the untreated cells. The intracellular conversion of nitrate to nitrite seems to be non-existent since nitrate is essentially reduced to nitrite via microbial activity. AGS cells are cultured and maintained in a sterile, controlled environment without contamination. Hence, the presence of microbes responsible for nitrate to nitrite conversion in the cultured AGS cells in the present study can be ruled out entirely. The above results implies that RNS may not be a causative factor of the putative oxidative

stress upon exposure of AGS cells to tuibur and other chemical species studied. Therefore, cytotoxicity in AGS cells treated with tuibur is more likely due to ROS and obviously not by RNS mediated oxidative stress.

The assessment of induced apoptosis in treated AGS cells was performed using AO/EB dual staining probes and fluorescence microscopy. It is well-known fact that AO can penetrate normal cells and early apoptotic cells with normal morphology, and a green or greenish-yellow fluorescent emission can be observed when the dye is bound to DNA. EB on the other hand only enters cells having damaged membranes and emits orange-red fluorescent light when bound to apoptotic bodies. Tuibur and nicotine treated cells displayed greater number of apoptotic cells count, however, the rate of apoptosis in nicotine treated cells were relatively higher than in tuibur. It was experimentally observed in this study that tuibur concentration of 6.81 µg/µL was found to be apoptotic for AGS cells. Hydroquinone and KNO_3 treated cells also showed similar apoptotic cell counts. Apoptosis due to mitochondrial damage via tobacco exposure in A549 epithelial cell line have been reported (Ramage et al., 2006). Mitochondrial-dependent induction of apoptosis in gingival epithelial cells due to tobacco aqueous extract exposure was also reported (Patil & Baeshen, 2021). The present investigation did not probe the putative pathways by which apoptosis induction occurred in tuibur treated cells. There are two type of apoptotic triggering pathways, intrinsic and extrinsic. The intrinsic pathway is regulated by the protein BCL-2. A decreased expression of Bcl-2 genes and an increase in expression of caspase-3 in AGS cell line as a result of tobacco extract exposure have been reported (H. Y. Wang et al., 2003). An overexpression of Bcl-2 was observed in a study on U-937 cells treated with tobacco smoke, though increased Bcl-2 expression was insufficient to prevent apoptosis (Vayssier et al., 1998). Therefore, from the present study and the findings of the earlier studies, it is plausible that the pathway involved in tuibur induced cell death in AGS cell line may be intrinsic, involving the expression of the anti-apoptotic gene Bcl-2.

CHAPTER 4

SUMMARY AND CONCLUSION

CHAPTER 4

SUMMARY AND CONCLUSION

Smokeless tobacco consumption is a rampant epidemic in Mizoram surpassing the frequency of smokers in the state (Indian Council of Medical Research-National Centre for Disease Informatics and Research, 2022). Tuibur, by virtue of the autochthonous manufacturing practices as well as the mode of use, has been a preventable and avoidable habit with negative health consequences as various epidemiological studies have implicated chronic and acute tuibur consumption is injurious to the health of tuibur users (Phukan et al. 2004; Phukan et al. 2005). Determination of different chemical constituents of tuibur and their putative effects in biological systems is either lacking or very much limited. The present research study evaluated and quantitated the preponderant alkaloid – nicotine, and cotinine, besides other components to provide a new insight into the quality of tuibur that is being distributed commercially among the local population. Local grading of tuibur only based on its astringency that essentially reflects its alkalinity and also possibly on the amount of tobacco stalk combusted. Correspondingly, grading of tuibur is individualised as per tuibur cottage personnel who are mostly illiterate laymen and no standard grading procedures exists. This study attempts to systematically grade commercially available tuibur based on its nicotine content.

From the pH measurements, it was ascertained that all tuibur samples were alkaline and their pH ranged between 8.85 to 9.33. This provided a more scientific way of classifying commercial tuibur rather than the local grading system of tuibur which is differentiated as “al” and “al lo”, literally translated as alkaline and non-alkaline, respectively, based on the amount of tobacco combusted. The higher the grade, the greater the amount of tobacco used for generating tobacco smoke, according to the cottage industry. However, the alkalinity of tuibur stems from the preparation of feedstock since ‘feedstock’ is basically stream water percolated through known quantity of plant ash. From this observation, it was hypothesized that the amount of tobacco used for production must have an influence over the overall quantity of chemical constituents, in particular, nicotine. Therefore, the grading of collected tuibur

samples based on the correlations between the amount of combusted tobacco stalk and the determined nicotine content was attempted.

ATR-FTIR spectroscopy in conjunction with chemometrics, a variant of linear regression analysis, was performed to estimate the concentration of nicotine in different grades of tuibur samples. Additional vibrational spectral data on the concentration of carcinogenic hydroquinone and benzoquinone were also collected. The identification of nicotine, hydroquinone and benzoquinone in the IR spectral data of the samples was masked by predominantly broad and intense peaks arising from water (3000-3400 cm^{-1} and ~ 1600 cm^{-1}) which made the spectral data interpretation very difficult in all tuibur samples. Although few distinct vibrational bands in the IR spectral data corresponding to tuibur samples were observed, it could not be discerned as to whether these functional group bands belonged to which molecule since tuibur is a heterogenous mixture. The attempt at the estimation of nicotine using the specific spectral features of mid-IR region selected for the standards and tuibur samples, seemingly unsuccessful. The predicted concentrations of nicotine, hydroquinone and benzoquinone in all the samples, be it in lower or higher grades of tuibur, showed no variability and were similar in all the samples tested. Hence, this method was considered ineffective for the quantification of the chemicals of interest in the tuibur samples, most likely due to the presence of polar solvent water since tuibur is an aqueous tobacco stalk concentrate.

The estimation of nicotine and the possible grading of tuibur samples was further attempted by applying more sensitive SERS methods based on the 'Raman' (inelastic) scattering. The observed characteristic vibrational band at 1031 cm^{-1} corresponding to the C-N stretching vibration band of unionized pyridine moiety of nicotine, allowed us to directly measure the nicotine content in different grades of tuibur samples. This prototype experiment is the first of its kind to measure the nicotine content in different local grades of tuibur by using AuNP-based SERS spectroscopy. The varying size, shape, roughness and ligand chemistry of noble metal nanoparticle may have enabled the detection of vibrational bands corresponding to nicotine which is present in tuibur at trace levels. The nicotine levels, however, were measured by peak intensity and not as actual concentration measurements (by the integration of the area of vibrational band). The absolute concentration of nicotine in tuibur sample could

not be ascertained using this technique. Nevertheless, the applied SERS method could successfully as well as qualitatively observe an increase in the concentration of nicotine corresponding to the increase in amount of tobacco used for the preparation of different local grades of tuibur.

A more accurate quantification of nicotine along with cotinine in the tuibur samples was accomplished by using LC-MS/MS methods based on internal calibration methods also known as isotopic dilution methods. Owing to the specificity of this more rigorous analytical technique, the more precise measurements of nicotine and cotinine concentrations present in the 10 different grades of tuibur samples under investigation could be achieved. The nicotine concentration of the tuibur samples studied ranged between 506 to 1877 μg/mL. Cotinine levels in the different concentrations of tuibur ranged between 6.5 – 44.4 μg/mL. This provides a clear picture of the quality of tuibur being distributed commercially. Grading in terms of nicotine concertation offers a more reliable and scientifically robust approach to the determination of different grades of tuibur enabling the categorization based on the subtle variations in nicotine contents exhibited by the analysed tuibur samples. The assumption that nicotine is present in its unprotonated form owing to the alkalinity of tuibur (pH >8) was also proven by calculating the % unprotonated nicotine in each sample. It was demonstrated that >96% of nicotine determined in tuibur existed in its unionised form. This "free-base" form of nicotine rapidly passes through the hydrophobic biological membranes leading to more rapid absorption in the oral mucosa spiking the blood nicotine level (Mallock et al., 2022). Therefore, with the information provided above, it is most likely that tuibur use can increase the risks of nicotine-dependency and repeated use, also concomitantly instigate the vulnerable people's susceptibility to maintain this insidious lifestyle habit and become addicted. Furthermore, higher alkalinity of tuibur more likely may cause more acute oxidative stress on its own.

Almost 1/3rd of the Mizo population are smokeless tobacco users. Additionally, indigenous and unique tobacco use habits of Mizo tribal population engender a challenging and complex public health problem. Detailed scientific data on the putative 'adverse' effects of tuibur is warranted because rather few experimental studies on the deleterious health effects of chronic tuibur use except some epidemiological studies on smokeless tobacco habits in Mizo population. Tobacco

smoke extracts (mainly cigarette smoke from smoking machine regime) have been reported to mediate cytotoxicity in vitro by using different cell lines. Population based epidemiological studies have also provided evidence on the relationship between chronic tobacco use and various lifestyle disorders including cardiovascular diseases and cancer. Persistent tuibur use has also been linked to the increased risk of developing stomach cancer (Phukan et al., 2005). The current investigation provides the preliminary information on the intracellular toxicity of tuibur using cellular model system study. However, further studies are certainly warranted to quantitatively assess the insidious health effect of tuibur use and to gain a better understanding of the putative biochemical mechanisms of the carcinogenic potential of tuibur.

An easy and efficient mutagenicity test like the micronucleus assay can provide information on chemically induced DNA fragmentation and chromosomal damage. The present study has made an account on the status of this biomarker in the tuibur user population of Mizoram. An increase in micronuclei formation is linked with mutagenesis, chromosome instability and genome rearrangements. Nuclear envelope rupture in micronucleus abruptly exposes DNA inside the micronucleus to the cytoplasm and is thought to be an almost irreversible process (Krupina et al., 2021). Our resultant data on oral epithelial cells of tuibur users indicated the high levels of chromosomal fragmentation and the subsequent nuclear envelop deposition in the form of micronuclei formation among the Mizo populace who consume tuibur frequently. Compared to the micronuclei score of healthy individuals without any tobacco habits, tuibur consumers displayed elevated levels of micronuclei formation. Even when compared with sahdah (coarse tobacco flakes mixed with lime more akin to khaini) user population, significant levels of micronuclei were observed in buccal cells of tuibur consumers. Thus, micronuclei assay has suggested that tuibur use is an important risk factor for the chromosomal instability and DNA damage which also in good agreement with the epidemiological studies (Phukan et al., 2005; Malakar et al. 2014).

The toxicological studies based on relatively simpler model systems have been long practised. Animal models are deemed unethical while the use of cell lines as model systems do not break any ethical codes and are useful tools for the health assessments and the associated clinical studies. Mitochondrial integrity is crucial in

cell survival. An array of diseases, directly or indirectly, stem from mitochondrial dysfunction. The MTT assay is applied for assessing the metabolic or cellular viability in cells. Tuibur mediated cell cytotoxicity on AGS cell lines was illustrated in the present study. AGS cells were also exposed to varying concentrations of tuibur, nicotine, hydroquinone, KNO_3 and $NaNO_2$ solutions. The control cells remained without treatment. These control and treatment groups were incubated for 24, 48 and 72 hrs. The data of these experiments demonstrated the dose-dependent as well as time-dependent attenuation of AGS cells viability when exposed to tuibur and hydroquinone. The cellular proliferation inhibitory capacity of tuibur as well as hydroquinone in AGS cell line was observed in a time-dependent manner. In contrast, nicotine induced proliferative effects on AGS cell lines which qualitatively consistent with earlier studies of this kind. Though at 72 hrs treatment, the cells eventually lost viability in a dose-dependent manner for nicotine also. Thus, the observed AGS cell proliferative effects of nicotine decreased with time. This indicated that at low concentrations, nicotine induced cell proliferation in gastric adenocarcinoma cells. Treatment of AGS cells with KNO_3 demonstrated a concentration and time-dependent proliferative effect on cells. The potency of KNO_3 in inhibiting cell growth was independent of time. The data for the treatment of AGS cells with $NaNO_2$ yielded rather inconclusive results. The results of the MTT studies demonstrated the cytotoxicity of tuibur and hydroquinone even in low concentrations and their potential ability to induce different types of cellular damage. This study also demonstrated the induction of cell proliferation by nicotine and KNO_3 in epithelial cancer cells in low doses indicating the chemicals' ability to promote cellular proliferation.

Reactive nitrogen species (RNS) are types of free radicals which can induce oxidative/nitrosative stress. Evaluation of RNS species in AGS cell line treated with IC_{50} concentrations of tuibur, nicotine, hydroquinone and KNO_3 was carried out by using the Griess assay. In Griess assay, decreased levels of nitrite in each of the treatment groups as compared to that of the control untreated cells were observed. The observed results indicated that RNS formation may not be the cause of oxidative stress within the cell system. Although this may be the case, the suppression of nitric oxide ($NO^{\bullet}$) production, which plays an important role in cell signalling, may also more likely occurred. The reduced $NO^{\bullet}$ levels cause the disruption of cellular signalling

pathways that can prevent the normal cellular functioning. Thus, apparently tuibur promotes the suppression of $NO^{\bullet}$ production within the cell leading to the disruption of normal cellular functions potentially causing damage to the cells.

Fluorescent probes are useful tools in the evaluation of cellular morphology and genotoxicity. Apoptosis upon treatment with IC_{50} concentrations of tuibur, nicotine, hydroquinone and KNO_3 in AGS cells were evaluated. Induced apoptosis however, is a consequence of exposure to genotoxic agents. The outcome of apoptotic assay via AO/EB staining and fluorescence microscopy indicated that apoptosis in the control untreated cells was much lower as compared to the treatment groups. Apoptotic cell score in tuibur and nicotine treated cells were highest among the treatment groups. It is important to note that nicotine has shown non-specific functions as on one hand it has stimulated higher antioxidant levels, however, on the other hand, it also strongly induced apoptosis. This indicates the genotoxicity of tuibur in AGS cells leading to DNA damage as well as cell death. The abovementioned data have suggested that tuibur is a genotoxic agent and is a risk factor for induced cell death and DNA damage.

Antioxidants, small molecule or enzymatic, play a huge role in scavenging free radicals to maintain a state of balance between production and accumulation of oxidative species. With excess of free radicals in the biological milieu, oxidative stress occurs leading to cell and tissue damage. Cell death is an inflammatory response induced by oxidative stress. The MTT assay has demonstrated the cytotoxicity of tuibur via monitoring cell viability which led to a dose-dependent increase in cell death. Oxidative stress was assessed by measuring the total antioxidant capacity (TAC) of AGS cells treated with the IC_{50} concentrations of tuibur, nicotine, hydroquinone and KNO_3. Decreased total antioxidant capacity in AGS cells treated with tuibur, hydroquinone and KNO_3 were observed. Since, hydroquinone is a well-known inducer of oxidative stress and the concomitant apoptosis, our results were in good agreement with earlier studies (Bertram et al. 2009). These results indicated that in these treatment groups, there is an imbalance between free radicals and antioxidants, thus reducing the quantity of antioxidants in the system that could scavenge these species. On the other hand, nicotine showed increased levels of antioxidant capacity suggesting at low concentrations, nicotine could potentially exhibit some antioxidant effects in AGS cells and thus enhance cell proliferation potency of gastrointestinal cancer cells. The

outcome of these experiments thus proved that tuibur upon exposure to cells promotes the formation of free radicals or reactive oxygen species (ROS) thus instigating oxidative stress in the system leading to cellular damage.

Reactive oxygen species (ROS) accumulation is the cause of intracellular oxidative stress when scavenging antioxidant enzymes and small molecule antioxidants such as vitamin c, glutathione etc., are depleted. Assessment of increased ROS generation in AGS cell line treated with IC_{50} concentrations of tuibur, nicotine, hydroquinone and KNO_3 was performed using the nitrite determining DCFDA staining and flow cytometry. It is important to note that for the nicotine treated AGS cells, an increase in ROS levels were observed. Conversely, for the rest of the treatment groups including cells treated with tuibur showed attenuated ROS were observed when compared to untreated 'control' AGS cells. A large body of scientific studies have demonstrated that all types of tobacco products, irrespective of whether smoked or smokeless forms, evoked significantly elevated levels of ROS in various cell line (Bertram et al., 2009; Sobus and Warren, 2014). The results of our FACS assay displayed rather contrasting and inconsistent results in comparison with MTT, TAC and micronuclei assays, and therefore more detailed in vitro studies are certainly required to gain a better understanding of the mode of action of tuibur, a smokeless product with unknown or rarely-studied long-term serious health outcomes.

Tuibur, is an easily accessible, affordable 'smokeless'tobacco product although which is an unwanted, unhealthy and avoidable lifestyle habit among the Mizo population in general, female population more specific. Though there are numerous commercially available SLT products, the cultural nostalgia as well as a relatively lower cost of tuibur entices its users to retain the habit. Tuibur, made from smoldering tobacco stalk in artisanal 'rusted' steel barrels and containers is a major health hazard. Being a heterogenous mixture containing an assortment of trace elements and organic carcinogens are abundant in quantity in tuibur which are capable of inducing oxidative stress, DNA damage and eventually different disorders such as gastritis, cancer, etc. Moreover, the presence of TSAs, TSNAs and other organic and inorganic components in tuibur were identified out of which some are proven group 1 and group 2 carcinogens (IARC, 2004; Lalmuanpuii, 2016). The production process of tuibur is also likely to have a negative environmental impact. The tuibur consuming

populace of Mizoram have much less awareness on the health hazards and consequences of consumption. The present study, as a preliminary study has shed light on the putative detrimental health effects of tuibur consumption which is also qualitatively consistent with the earlier epidemiological studies (Phukan et al. 2005; Phukan et al. 2006; Malakar et al. 2014). The proper hygienic packaging, attachment of suitable health warning labels would improve the awareness among its consumers, especially rural and suburban users. Therefore, pertinent in vitro as well as in vivo research studies are required to spread the awareness, and to enable scientific scrutinization of the chemical constituents and negative health effects of tuibur and its chronic use.

REFERENCES

Afzal, M., Matsugo, S., Sasai, M., Xu, B., Aoyama, K., & Takeuchi, T. (2003). Method to overcome photoreaction, a serious drawback to the use of dichlorofluorescin in evaluation of reactive oxygen species. *Biochemical and Biophysical Research Communications*, *304*(4), 619–624. https://doi.org/10.1016/S0006-291X(03)00641-7

Al-Dahhan, W. H., Kadhom, M., Yousif, E., Mohammed, S. A., & Alkaim, A. (2022). Extraction and Determination of Nicotine in Tobacco from Selected Local Cigarettes Brands in Iraq. *Letters in Applied NanoBioScience*, *11*(1), 3278–3290. https://doi.org/10.33263/LIANBS111.32783290

Aledwany, A., Basal, W., Al-Senosy, N., & Issa, A. (2018). Evaluation of The Cytotoxicity, Cell Cycle Perturbations and Apoptotic Induction in Human Normal and Cancer Liver Cell Lines Exposed to Potassium Nitrate and Sodium Benzoate. *Egyptian Academic Journal of Biological Sciences, B. Zoology*, *10*(1), 105–118. https://doi.org/10.21608/eajbsz.2018.26985

Alfonso, B. F., & Al-Rubeai, M. (2011). Flow Cytometry. In *Comprehensive Biotechnology, Second Edition* (Second Edi, Vol. 1). Elsevier B.V. https://doi.org/10.1016/B978-0-08-088504-9.00065-9

American Type Culture Collection. (2003). *AGS. 11686*, 11686.

Anagu, L. O., & Andoh, N. E. (2022). Vaccine development: from the laboratory to the field. *Vaccinology and Methods in Vaccine Research*, 95–131. https://doi.org/10.1016/B978-0-323-91146-7.00011-1

Arany, I., Grifoni, S., Clark, J. S., Csongradi, E., Maric, C., & Juncos, L. A. (2011). Chronic nicotine exposure exacerbates acute renal ischemic injury. *American Journal of Physiology - Renal Physiology*, *301*(1), 125–133. https://doi.org/10.1152/ajprenal.00041.2011

Asmus, K.-D., & Bonifačić, M. (2000). *Chapter 1 - Free radical chemistry BT - Handbook of Oxidants and Antioxidants in Exercise*. 3–54. http://www.sciencedirect.com/science/article/pii/B9780444826503500018

Balasubramaniam, A., & Arumugham, M. (2022). Salivary oxidative stress level among tobacco chewers and smokers: A comparative Study. *Journal of Advanced Pharmaceutical Technology and Research*, *13*(5), 21–25. https://doi.org/10.4103/japtr.japtr_116_22

Bansal, H., Sandhu, V., Bhandari, R., & Sharma, D. (2012). Evaluation of micronuclei in tobacco users: A study in Punjabi population. *Contemporary Clinical Dentistry*, *3*(2), 184–187. https://doi.org/10.4103/0976-237X.96825

Baranska, M., Dobrowolski, J. C., Kaczor, A., Chruszcz-Lipska, K., Gorz, K., & Rygula, A. (2012). Tobacco alkaloids analyzed by Raman spectroscopy and DFT calculations. *Journal of Raman Spectroscopy*, *43*(8), 1065–1073. https://doi.org/10.1002/jrs.3127

Barber, T. E., List, M. S., Haas, J. W., & Wachter, E. A. (1994). Determination of nicotine by surface-enhanced Raman scattering (SERS). *Applied Spectroscopy*,

48(11), 1423–1427. https://doi.org/10.1366/0003702944027985

Barr, J., Sharma, C. S., Sarkar, S., Wise, K., Dong, L., Periyakaruppan, A., & Ramesh, G. T. (2007). Nicotine induces oxidative stress and activates nuclear transcription factor kappa B in rat mesencephalic cells. *Molecular and Cellular Biochemistry*, *297*(1–2), 93–99. https://doi.org/10.1007/s11010-006-9333-1

Barry Halliwell, J. M. C. G. (1989). Free radicals in biology and medicine. In *International Journal of Radiation Biology*. Clarendon Press.

Baskić, D., Popović, S., Ristić, P., & Arsenijević, N. N. (2006). Analysis of cycloheximide-induced apoptosis in human leukocytes: Fluorescence microscopy using annexin V/propidium iodide versus acridin orange/ethidium bromide. *Cell Biology International*, *30*(11), 924–932. https://doi.org/10.1016/j.cellbi.2006.06.016

Becker, J. M., Caldwell, G. A., & Zachgo, E. A. (1996). Protein Assays. *Biotechnology*, 119–124. https://doi.org/10.1016/B978-012084562-0/50069-2

Begum, S. F., Nagajothi, G., Latha, K. S., Sandeep, G., Sreekanth, B., Kumar, C. S., Rajendra, W., & Maddu, N. (2018). Possible role of nicotine and cotinine on nitroxidative stress and antioxidant content in saliva of smokeless tobacco consumers. *Practical Laboratory Medicine*, *12*(November 2017), 1–10. https://doi.org/10.1016/j.plabm.2018.e00105

Benowitz, N. L., & Gourlay, S. G. (1997). Cardiovascular toxicity of nicotine: Implications for nicotine replacement therapy. *Journal of the American College of Cardiology*, *29*(7), 1422–1431. https://doi.org/10.1016/S0735-1097(97)00079-X

Benowitz, N. L., & Jacob, P. (1994). Metabolism of nicotine to cotinine studied by a dual stable isotope method. *Clinical Pharmacology & Therapeutics*, *56*(5), 483–493. https://doi.org/10.1038/clpt.1994.169

Bhowmick, P., Lalrinhlupuii, Muthukumaran, R, B., &, & Bhattacharjee, P. (2022). *Food Diversity among Northeast Population : Resource of nutraceuticals to Risk Factors for Disease Susceptibility*. *January*.

Biter, A. B., Pollet, J., Chen, W. H., Strych, U., Hotez, P. J., & Bottazzi, M. E. (2019). A method to probe protein structure from UV absorbance spectra. *Analytical Biochemistry*, *587*(June). https://doi.org/10.1016/j.ab.2019.113450

Booker, C. J., Bedmutha, R., Vogel, T., Gloor, A., Xu, R., Ferrante, L., Yeung, K. K. C., Scott, I. M., Conn, K. L., Berruti, F., & Briens, C. (2010). Experimental investigations into the insecticidal, fungicidal, and bactericidal properties of pyrolysis bio-oil from tobacco leaves using a fluidized bed pilot plant. *Industrial and Engineering Chemistry Research*, *49*(20), 10074–10079. https://doi.org/10.1021/ie100329z

Borgerding, M., & Klus, H. (2005). Analysis of complex mixtures - Cigarette smoke. *Experimental and Toxicologic Pathology*, *57*(SUPPL. 1), 43–73. https://doi.org/10.1016/j.etp.2005.05.010

Borse, V., Konwar, A. N., & Buragohain, P. (2020). Oral cancer diagnosis and

perspectives in India. *Sensors International*, *1*(January), 100046. https://doi.org/10.1016/j.sintl.2020.100046

Bryan, N. S., & Grisham, M. B. (2007). Methods to detect nitric oxide and its metabolites in biological samples. *Free Radical Biology and Medicine*, *43*(5), 645–657. https://doi.org/10.1016/j.freeradbiomed.2007.04.026

Bush, L., Hempfling, W. P., & Burton, H. (1999). Biosynthesis of nicotine and related compounds. In *Analytical Determination of Nicotine and Related Compounds and their Metabolites*. Elsevier Science B.V. https://doi.org/10.1016/b978-044450095-3/50003-6

Byeon, S. E., Yi, Y.-S., Lee, J., Yang, W. S., Kim, J. H., Kim, J., Hong, S., Kim, J.-H., & Cho, J. Y. (2018). Hydroquinone Exhibits In Vitro and In Vivo Anti-Cancer Activity in Cancer Cells and Mice. *International Journal of Molecular Sciences*, *19*(3). https://doi.org/10.3390/ijms19030903

Caliri, A. W., Tommasi, S., & Besaratinia, A. (2021). Relationships among smoking, oxidative stress, inflammation, macromolecular damage, and cancer. *Mutation Research - Reviews in Mutation Research*, *787*, 108365. https://doi.org/10.1016/j.mrrev.2021.108365

Carlos Omar Rodríguez-Hernández, Saúl Emmanuel Torres-García, Carlos Olvera-Sandoval, Flor Yazmín Ramírez-Castillo, Abraham Loera Muro, F. J. A.-G. and A. L. G.-B. (2014). Cell Culture: History, Development and Prospects Carlos. *International Journal of Current Research and Academic Review*, *2*(12), 188–200. https://www.researchgate.net/publication/269932638%0ACell

Carlsson, S., Andersson, T., Araghi, M., Galanti, R., Lager, A., Lundberg, M., Nilsson, P., Norberg, M., Pedersen, N. L., Trolle-Lagerros, Y., & Magnusson, C. (2017). Smokeless tobacco (snus) is associated with an increased risk of type 2 diabetes: results from five pooled cohorts. *Journal of Internal Medicine*, *281*(4), 398–406. https://doi.org/10.1111/joim.12592

Cartwright, J. E., Johnstone, A. P., & Whitley, G. S. J. (2000). Endogenously produced nitric oxide inhibits endothelial cell growth as demonstrated using novel antisense cell lines. *British Journal of Pharmacology*, *131*(1), 131–137. https://doi.org/10.1038/sj.bjp.0703539

Caruso, M., Emma, R., Rust, S., Distefano, A., Carota, G., Pulvirenti, R., Polosa, R., & Li Volti, G. (2021). Screening of different cytotoxicity methods for the assessment of ENDS toxicity relative to tobacco cigarettes. *Regulatory Toxicology and Pharmacology*, *125*, 1–35. https://doi.org/10.1016/j.yrtph.2021.105018

Casartelli, G., Bonatti, S., De Ferrari, M., Scala, M., Mereu, P., Margarino, G., & Abbondandolo, A. (2000). Micronucleus frequencies in exfoliated buccal cells in normal mucosa, precancerous lesions and squamous cell carcinoma. In *Analytical and Quantitative Cytology and Histology* (Vol. 22, Issue 6, pp. 486–492).

Census. (2011). Mizoram Population 2022 | Sex Ratio & Literacy rate 2023. In *Population Census Data*. GOI. https://www.census2011.co.in/census/state/jharkhand.html

Cezar-Vaz, M. R., & Cargnin, M. C. D. S. (2019). Use of cotinine biomarker in workers to detect green tobacco sickness. *Revista Latino-Americana de Enfermagem*, *27*. https://doi.org/10.1590/1518-8345.3141.3194

Chandirasekar, R., Murugan, K., Muralisankar, T., Uthayakumar, V., Jayakumar, R., Mohan, K., Vasugi, C., Mathivanan, R., Mekala, S., Jagateesh, A., & Suresh, K. (2019). Genotoxic effects of tobacco use in residents of hilly areas and foot hills of Western Ghats, Southern India. *Scientific Reports*, *9*(1), 1–8. https://doi.org/10.1038/s41598-019-51275-w

Chantzoura, E., & Kaji, K. (2017). Flow Cytometry. In *Basic Science Methods for Clinical Researchers*. Elsevier Inc. https://doi.org/10.1016/B978-0-12-803077-6.00010-2

Chioran, D., Sitaru, A., Macasoi, I., Pinzaru, I., Sarau, C. A., Dehelean, C., Dinu, S., Szuhanek, C., Zetu, I. N., Serafin, A. C., Rivis, M., Poenaru, M., & Dragoi, R. (2022). Nicotine Exerts Cytotoxic Effects in a Panel of Healthy Cell Lines and Strong Irritating Potential on Blood Vessels. *International Journal of Environmental Research and Public Health*, *19*(14). https://doi.org/10.3390/ijerph19148881

Chu, S. , Stoner, . John Oliver , Hurst, . George Samuel and Graybeal, . Jack D. (2023). *Spectroscopy*. Encyclopedia Britannica. https://www.britannica.com/science/spectroscopy

Csonka, C., Páli, T., Bencsik, P., Görbe, A., Ferdinandy, P., & Csont, T. (2015). Measurement of NO in biological samples. *British Journal of Pharmacology*, *172*(6), 1620–1632. https://doi.org/10.1111/bph.12832

Dani, J. A. (2001). Overview of nicotinic receptors and their roles in the central nervous system. *Biological Psychiatry*, *49*(3), 166–174. https://doi.org/10.1016/S0006-3223(00)01011-8

Dani, J. A., & Bertrand, D. (2007). Nicotinic acetylcholine receptors and nicotinic cholinergic mechanisms of the central nervous system. *Annual Review of Pharmacology and Toxicology*, *47*, 699–729. https://doi.org/10.1146/annurev.pharmtox.47.120505.105214

Dash, K. C., Nishat, R., Kumar, H., Mishra, S., Raghuvanshi, M., & Bajoria, A. (2018). Comparative study of micronuclei count in patients with different tobacco-related habits using exfoliated buccal epithelial cells: A tool for assessment of genotoxicity. *Journal of Contemporary Dental Practice*, *19*(9), 1076–1081. https://doi.org/10.5005/JP-JOURNALS-10024-2384

Dhillon, P. K., Mathur, P., Nandakumar, A., Fitzmaurice, C., Kumar, G. A., Mehrotra, R., Shukla, D. K., Rath, G. K., Gupta, P. C., Swaminathan, R., Thakur, J. S., Dey, S., Allen, C., Badwe, R. A., Dikshit, R., Dhaliwal, R. S., Kaur, T., Kataki, A. C., Visweswara, R. N., … Dandona, L. (2018). The burden of cancers and their variations across the states of India: the Global Burden of Disease Study 1990–2016. *The Lancet Oncology*, *19*(10), 1289–1306. https://doi.org/10.1016/S1470-2045(18)30447-9

Dhirendra Narain Sinha, Prakash C. Gupta, S. S. (2006). Carcinogens in tobacco water.

National Medical Journal of India, *19*(2), 110–112.

Drijvers, J. M., Awan, I. M., Perugino, C. A., Rosenberg, I. M., & Pillai, S. (2017). The Enzyme-Linked Immunosorbent Assay: The Application of ELISA in Clinical Research. In *Basic Science Methods for Clinical Researchers*. Elsevier Inc. https://doi.org/10.1016/B978-0-12-803077-6.00007-2

Dwoskin, L. P., Teng, L. H., & Crooks, P. A. (2001). Nornicotine, a nicotine metabolite and tobacco alkaloid: Desensitization of nicotinic receptor-stimulated dopamine release from rat striatum. *European Journal of Pharmacology*, *428*(1), 69–79. https://doi.org/10.1016/S0014-2999(01)01283-3

E-governance, M. S. (2018). History of Mizoram. In *Addiction* (Vol. 113, Issue 3, pp. 577–580). https://doi.org/10.1111/add.14117

Elfein, J. (2022). *Countries with the highest share of smokeless tobacco users 2019*. Statista.

Elmore, S. (2007). Apoptosis: A Review of Programmed Cell Death. *Toxicologic Pathology*, *35*(4), 495–516. https://doi.org/10.1080/01926230701320337

Encyclopedia Britannica. (2018). *Britannica, The Editors of Encyclopaedia. "snuff"*. https://www.britannica.com/topic/snuff. Accessed 27 December 2023

Engstrom PF, Clapper ML, S. R. (2003). *Physiochemical Composition of Tobacco Smoke* (Kufe DW, Pollock RE, Weichselbaum RR, et al. (ed.); 6th Editio). olland-Frei Cancer Medicine. 6th edition. https://www.ncbi.nlm.nih.gov/books/NBK13173/

Enguita, F. J., & Leitão, A. L. (2013). Hydroquinone: Environmental pollution, toxicity, and microbial answers. *BioMed Research International*, *2013*. https://doi.org/10.1155/2013/542168

Ernstsson, M., & Wärnheim, T. D. (2007). Surface Analytical Techniques Applied to Cleaning Processes. *Handbook for Cleaning/Decontamination of Surfaces*, *2*, 747–789. https://doi.org/10.1016/B978-044451664-0/50023-1

F. Sánchez Rojas, J. M. C. P. (2005). SPECTROPHOTOMETRY | Biochemical Applications. In Paul Worsfold and Alan Townshend and Colin Poole (Ed.), *Encyclopedia of Analytical Science* (Second Edi, pp. 366–372). Elsevier. https://doi.org/10.1016/B0-12-369397-7/00722-6

Fant, R. V., Henningfield, J. E., Nelson, R. A., & Pickworth, W. B. (1999). Pharmacokinetics and pharmacodynamics of moist snuff in humans. *Tobacco Control*, *8*(4), 387–392. https://doi.org/10.1136/tc.8.4.387

Fathi, R. M., Fauzantoro, A., Rahman, S. F., & Gozan, M. (2018). Column chromatography isolation of nicotine from tobacco leaf extract (Nicotiana tabaccum L.). *AIP Conference Proceedings*, *1933*(1), 030011-1–6. https://doi.org/10.1063/1.5023958

Fekhar, M., Daghbouche, Y., Bouzidi, N., & El Hattab, M. (2023). ATR-FTIR spectroscopy combined with chemometrics for quantification of total nicotine in Algerian smokeless tobacco products. *Microchemical Journal*, *193*(June),

109127. https://doi.org/10.1016/j.microc.2023.109127

Finkel, T., & Holbrook, N. J. (2000). Oxidants, oxidative stress and the biology of ageing. *Nature*, *408*(6809), 239–247. https://doi.org/10.1038/35041687

Förstermann, U. (2010). Nitric oxide and oxidative stress in vascular disease. In *Pflugers Archiv European Journal of Physiology* (Vol. 459, Issue 6, pp. 923–939). https://doi.org/10.1007/s00424-010-0808-2

Fraga, C. G., Oteiza, P. I., & Galleano, M. (2014). In vitro measurements and interpretation of total antioxidant capacity. *Biochimica et Biophysica Acta (BBA) - General Subjects*, *1840*(2), 931–934. https://doi.org/10.1016/J.BBAGEN.2013.06.030

G.B. Neurath, D. Orth, and F. G. P. (1991). DETECTION OF NORNICOTINE IN HUMAN URINE AFTER INFUSION OF NICOTINE. In K. Adlkofer, F., Thurau (Ed.), *Effects of Nicotine on Biological Systems*. APS Advances in Pharmacological Sciences. Birkhäuser Basel. https://doi.org/10.1007/978-3-0348-7457-1_6

Ganapathy, V., Manyanga, J., Brame, L., McGuire, D., Sadhasivam, B., Floyd, E., Rubenstein, D. A., Ramachandran, I., Wagener, T., & Queimado, L. (2017). Electronic cigarette aerosols suppress cellular antioxidant defenses and induce significant oxidative DNA damage. *PLoS ONE*, *12*(5), 1–20. https://doi.org/10.1371/journal.pone.0177780

Gavilano, L. B., Coleman, N. P., Burnley, L. E., Bowman, M. L., Kalengamaliro, N. E., Hayes, A., Bush, L., & Siminszky, B. (2006). Genetic engineering of Nicotiana tabacum for reduced nornicotine content. *Journal of Agricultural and Food Chemistry*, *54*(24), 9071–9078. https://doi.org/10.1021/jf0610458

Ghazi, A., Pakfetrat, A., Hashemy, S. I., Boroomand, F., & Javan-Rashid, A. (2020). Evaluation of Antioxidant Capacity and Cotinine Levels of Saliva in Male Smokers and Non-smokers. *Addiction & Health*, *12*(4), 244–250. https://doi.org/10.22122/ahj.v12i4.278

Ghiselli, A., Serafini, M., Natella, F., & Scaccini, C. (2000). Total antioxidant capacity as a tool to assess redox status: critical view and experimental data. *Free Radical Biology and Medicine*, *29*(11), 1106–1114. https://doi.org/10.1016/S0891-5849(00)00394-4

GIBCO. (2020). *CELL CULTURE BASICS Handbook*. Invitrogen.

Giustarini, D., Rossi, R., Milzani, A., & Dalle-Donne, I. (2008). Nitrite and Nitrate Measurement by Griess Reagent in Human Plasma: Evaluation of Interferences and Standardization. *Methods in Enzymology*, *440*, 361–380. https://doi.org/10.1016/S0076-6879(07)00823-3

Global adult tobacco Survey 2. (2017). Global adult tobacco survey, India 2016-17. In *February-2014*. https://www.who.int/tobacco/surveillance/survey/gats/GATS_India_2016-17_FactSheet.pdf%0ATata Institute of Social Sciences (TISS), Mumbai and Ministry of Health and Family Welfare, Government of India. Global Adult

Tobacco Survey GATS 2 India 2016-17.%0AIS

Gorrod, J.W., and Warhen, J. (1993). Nicotine and Related Alkaloids. In *Nicotine and Related Alkaloids*. Chapman & Hali. https://doi.org/10.1007/978-94-011-2110-1

Gorrod, J. W., & Schepers, G. (1999). Biotransformation of nicotine in mammalian systems. In *Analytical Determination of Nicotine and Related Compounds and their Metabolites* (pp. 45–67). https://doi.org/10.1016/b978-044450095-3/50004-8

Gould, K. S., Lamotte, O., Klinguer, A., Pugin, A., & Wendehenne, D. (2003). Nitric oxide production in tobacco leaf cells: A generalized stress response? *Plant, Cell and Environment*, *26*(11), 1851–1862. https://doi.org/10.1046/j.1365-3040.2003.01101.x

Gray, J. P., & Hall, G. J. (2014). Cotinine. In *Encyclopedia of Toxicology: Third Edition* (Vol. 1, pp. 1050–1051). https://doi.org/10.1016/B978-0-12-386454-3.00294-3

Guevara, I., Iwanejko, J., Dembińska-Kieć, A., Pankiewicz, J., Wanat, A., Anna, P., Gołąbek, I., Bartuś, S., Malczewska-Malec, M., & Szczudlik, A. (1998). Determination of nitrite/nitrate in human biological material by the simple Griess reaction. *Clinica Chimica Acta*, *274*(2), 177–188. https://doi.org/10.1016/S0009-8981(98)00060-6

Guo, Y., Hiatt, E., Bonnet, C., Kudithipudi, C., Lewis, R. S., Shi, H., Patra, B., Zhao, X., Dorlhac de Borne, F., Gilles, T., Yang, S., Zhang, H., Zhang, M., Lusso, M., Berger, I. J., Xu, D., & Wen, L. (2021). Molecular regulation and genetic manipulation of alkaloid accumulation in tobacco plants. In *Studies in Natural Products Chemistry* (Vol. 70). https://doi.org/10.1016/B978-0-12-819489-8.00006-5

Gupta, A., Gupta, R., Sharma, K. K., Lodha, S., Achari, V., Asirvatham, A. J., Bhansali, A., Gupta, B., Gupta, S., Jali, M. V, Mahanta, T. G., Maheshwari, A., Saboo, B., Singh, J., & Deedwania, P. C. (2014). Prevalence of diabetes and cardiovascular risk factors in middle-class urban participants in India. *BMJ Open Diabetes Research & Care*, *2*(1), e000048. https://doi.org/10.1136/bmjdrc-2014-000048

Gupta, P. C., & Sreevidya, S. (2004). Smokeless tobacco use, birth weight, and gestational age: Population based, prospective cohort study of 1217 women in Mumbai, India. *British Medical Journal*, *328*(7455), 1538–1540. https://doi.org/10.1136/bmj.38113.687882.eb

Gutiérrez, L., Stepien, G., Gutiérrez, L., Pérez-Hernández, M., Pardo, J., Pardo, J., Grazú, V., & de la Fuente, J. M. (2017). Nanotechnology in Drug Discovery and Development. *Comprehensive Medicinal Chemistry III*, *1–8*, 264–295. https://doi.org/10.1016/B978-0-12-409547-2.12292-9

Halliwell, B. (2006). Oxidative stress and neurodegeneration: Where are we now? *Journal of Neurochemistry*, *97*(6), 1634–1658. https://doi.org/10.1111/j.1471-4159.2006.03907.x

Hayat, M. A. (2015). Introduction to Autophagy: Cancer, Other Pathologies, Inflammation, Immunity, Infection, and Aging, Volume 7. *Autophagy: Cancer, Other Pathologies, Inflammation, Immunity, Infection, and Aging*, *7*, 1–53. https://doi.org/10.1016/B978-0-12-801043-3.00001-7

Heluany, C. S., Donate, P. B., Schneider, A. H., Fabris, A. L., Gomes, R. A., Villas-Boas, I. M., Tambourgi, D. V., da Silva, T. A., Trossini, G. H. G., Nalesso, G., Silveira, E. L. V., Cunha, F. Q., & Farsky, S. H. P. (2021). Hydroquinone exposure worsens rheumatoid arthritis through the activation of the aryl hydrocarbon receptor and interleukin-17 pathways. *Antioxidants*, *10*(6), 1–18. https://doi.org/10.3390/antiox10060929

Hoffmann, D., Adams, J. D., Brunnemann, K. D., & Hecht, S. S. (1979). Assessment of Tobacco-Specific N-Nitrosamines in Tobacco Products. In *Cancer Research* (Vol. 39, pp. 2505–2509).

Hole, A., Jadhav, P., Pansare, K., Noothalapati, H., Deshmukh, A., Gota, V., Chaturvedi, P., & Krishna, C. M. (2022). Salivary Raman spectroscopy: Understanding alterations in saliva of tobacco habitués and oral cancer subjects. In *Vibrational Spectroscopy* (Vol. 122). https://doi.org/10.1016/j.vibspec.2022.103414

Hu, R. S., Wang, J., Li, H., Ni, H., Chen, Y. F., Zhang, Y. W., Xiang, S. P., & Li, H. H. (2015). Simultaneous extraction of nicotine and solanesol from waste tobacco materials by the column chromatographic extraction method and their separation and purification. *Separation and Purification Technology*, *146*, 1–7. https://doi.org/10.1016/j.seppur.2015.03.016

Huber, D., Voith von Voithenberg, L., & Kaigala, G. V. (2018). Fluorescence in situ hybridization (FISH): History, limitations and what to expect from micro-scale FISH? *Micro and Nano Engineering*, *1*, 15–24. https://doi.org/10.1016/J.MNE.2018.10.006

Indian Council of Agricultural Research. (2023). *List of Released / Identified Varieties of Various Tobacco Types for Cultivation in India*. https://ctri.icar.gov.in/for_types.php

Indian Council of Medical Research-National Centre for Disease Informatics and Research. (2021). ICMR-NCDIR, Profile of Cancer and Related Health Indicators in the North East Region of India – 2021, Bengaluru, India. In *Angewandte Chemie International Edition, 6(11), 951–952.*

Indian Council of Medical Research-National Centre for Disease Informatics and Research. (2022). *Report on monitoring survey of cancer risk factors and health system response in North East India (NER) Mizoram*.

International Agency for Research on Cancer. (1987). *IARC Monographs Supplement 7* (Vol. 71).

International Agency for Research on Cancer. (2007a). Monographs on the Evaluation of Carcinogenic Risks to Humans - Volume 89. *Smokeless Tobacco and Some Tobacco-Specific N-Nitrosamines*, *89*, 641. http://monographs.iarc.fr/ENG/Monographs/vol89/mono89.pdf

International Agency for Research on Cancer. (2007b). Smokeless tobacco. *Oral Surgery, Oral Medicine, Oral Pathology, Oral Radiology, and Endodontics*, *81*(4), 376. https://doi.org/10.1016/S1079-2104(96)80003-5

International Agency for Research on Cancer. (2020). World Cancer Report : Cancer research for cancer development. In *International Agency for Research on Cancer*.

Iqbal, H. M. N., & Keshavarz, T. (2017). The challenge of biocompatibility evaluation of biocomposites. In *Biomedical Composites, Second Edition* (pp. 303–334). Woodhead Publishing. https://doi.org/10.1016/B978-0-08-100752-5.00014-7

Jabit, M. L., Wahyuni, F. S., Khalid, R., Israf, D. A., Shaari, K., Lajis, N. H., & Stanslas, J. (2009). Cytotoxic and nitric oxide inhibitory activities of methanol extracts of garcinia species. *Pharmaceutical Biology*, *47*(11), 1019–1026. https://doi.org/10.3109/13880200902973787

Jacob, P., Ulgen, M., & Gorrod, J. W. (1997). Metabolism of (-)-(S)-nicotine by guinea pig and rat brain: Identification of cotinine. *European Journal of Drug Metabolism and Pharmacokinetics*, *22*(4), 391–394. https://doi.org/10.1007/BF03190975

Jakubczyk, K., Dec, K., Kałduńska, J., Kawczuga, D., Kochman, J., & Janda, K. (2020). Reactive oxygen species - sources, functions, oxidative damage. *Polski Merkuriusz Lekarski : Organ Polskiego Towarzystwa Lekarskiego*, *48*(284), 124–147. https://pubmed.ncbi.nlm.nih.gov/32352946/#:~:text=Reactive oxygen species (ROS) are,well as free nitrogen radicals.

Jensen, E. C. (2012). Types of Imaging, Part 2: An Overview of Fluorescence Microscopy. *Anatomical Record*, *295*(10), 1621–1627. https://doi.org/10.1002/ar.22548

Jensen, K., Afroze, S., Munshi, M. K., Guerrier, M., & Glaser, S. S. (2012). Mechanisms for nicotine in the development and progression of gastrointestinal cancers. *Translational Gastrointestinal Cancer*, *1*(1), 81–87. https://doi.org/10.3978/j.issn.2224-4778.2011.12.01

Jensen, K., Nizamutdinov, D., Guerrier, M., Afroze, S., Dostal, D., & Glaser, S. (2012). General mechanisms of nicotine-induced fibrogenesis. *FASEB Journal*, *26*(12), 4778–4787. https://doi.org/10.1096/fj.12-206458

Johnson, W.R., Hale, R.W., Nedlock, J.W., Grubbs, H.J., and Powell, D. H. (1973). The distribution mainstream and of products between smoke. *Tobacco Science*, *17*(b), 141–144. https://www.coresta.org/abstracts/distribution-products-between-mainstream-and-sidestream-smoke-34555.html

Johnson, J. (1934). STUDIES ON THE FERMENTATION OF TOBACCO. *Al Research, Washington, D.C.*, *49*(2), 137–160. https://naldc.nal.usda.gov/catalog/IND43968481

Johnson, M. D., Schilz, J., Djordjevic, M. V., Rice, J. R., & Shields, P. G. (2009). Evaluation of in vitro assays for assessing the toxicity of cigarette smoke and smokeless tobacco. *Cancer Epidemiology Biomarkers and Prevention*, *18*(12),

3263–3304. https://doi.org/10.1158/1055-9965.EPI-09-0965

Jyoti, S., Siddique, Y. H., Khan, S., Naz, F., Rahul, & Ali, F. (2015). Effect on micronucleus frequency and DNA damage in buccal epithelial cells of various factors among pan masala and gutkha chewers. *Oral Science International*, *12*(1), 9–14. https://doi.org/10.1016/S1348-8643(14)00030-5

Kang, S. W., Park, H. J., Ban, J. Y., Chung, J. H., Chun, G. S., & Cho, J. O. (2011). Effects of nicotine on apoptosis in human gingival fibroblasts. *Archives of Oral Biology*, *56*(10), 1091–1097. https://doi.org/10.1016/j.archoralbio.2011.03.016

Kannan, K., & Jain, S. K. (2000). Oxidative stress and apoptosis. *Pathophysiology*, *7*(3), 153–163. https://doi.org/10.1016/S0928-4680(00)00053-5

Karwowska, M., & Kononiuk, A. (2020). Nitrates/nitrites in food—risk for nitrosative stress and benefits. *Antioxidants*, *9*(3), 1–17. https://doi.org/10.3390/antiox9030241

Kermanizadeh, A., Jantzen, K., Brown, D. M., Møller, P., & Loft, S. (2018). A Flow Cytometry-based Method for the Screening of Nanomaterial-induced Reactive Oxygen Species Production in Leukocytes Subpopulations in Whole Blood. *Basic and Clinical Pharmacology and Toxicology*, *122*(1), 149–156. https://doi.org/10.1111/bcpt.12845

Khanna, A., Gautam, D., Gokhale, M., & Jain, S. (2014). Tobacco dust induced genotoxicity as an occupational hazard in workers of bidi making cottage industry of central India. *Toxicology International*, *21*(1), 18–23. https://doi.org/10.4103/0971-6580.128785

Kim, A. R., Cho, J. Y., Lee, J. Y., Choi, J. S., & Chung, H. Y. (2005). Hydroquinone modulates reactivity of peroxynitrite and nitric oxide production†. *Journal of Pharmacy and Pharmacology*, *57*(4), 475–481. https://doi.org/10.1211/0022357055731

Kim, Y. J., Woo, H. D., Kim, B. M., Lee, Y. J., Kang, S. J., Cho, Y. H., & Chung, H. W. (2009). Risk Assessment of Hydroquinone: Differential Responses of Cell Growth and Lethality Correlated to Hydroquinone Concentration. *Journal of Toxicology and Environmental Health, Part A*, *72*(21–22), 1272–1278. https://doi.org/10.1080/15287390903212279

Kobayashi, J. (2018). Effect of diet and gut environment on the gastrointestinal formation of N-nitroso compounds: A review. *Nitric Oxide : Biology and Chemistry*, *73*, 66–73. https://doi.org/10.1016/j.niox.2017.06.001

Kozak, K., & Antosiewicz, D. M. (2023). Tobacco as an efficient metal accumulator. *BioMetals*, *36*(2), 351–370. https://doi.org/10.1007/s10534-022-00431-3

Krupina, K., Goginashvili, A., & Cleveland, D. W. (2021). Causes and consequences of micronuclei. *Current Opinion in Cell Biology*, *70*, 91–99. https://doi.org/10.1016/j.ceb.2021.01.004

Kuete, V., Karaosmanoğlu, O., & Sivas, H. (2017). Anticancer Activities of African Medicinal Spices and Vegetables. *Medicinal Spices and Vegetables from Africa: Therapeutic Potential Against Metabolic, Inflammatory, Infectious and Systemic*

Diseases, 271–297. https://doi.org/10.1016/B978-0-12-809286-6.00010-8

Kumar, A., Sharma, R., Sharma, A. K., & Agarwal, A. (2019). A cost-effective identification of tobacco alkaloids using porous Si SERS substrates for forensic and bioanalytical applications. *SN Applied Sciences*, *1*(11), 1–6. https://doi.org/10.1007/s42452-019-1539-4

Kumar, S. B., Chawla, B., Bisht, S., Yadav, R. K., & Dada, R. (2015). Tobacco use increases oxidative DNA damage in sperm - possible eti1ology of childhood cancer. *Asian Pacific Journal of Cancer Prevention*, *16*(16), 6967–6972. https://doi.org/10.7314/APJCP.2015.16.16.6967

Kumar, S. N., Bastia, B., Borgohain, D., Agrawal, U., Raisuddin, S., & Jain, A. K. (2021). Structural changes, increased hypoxia, and oxidative DNA damage in placenta due to maternal smokeless tobacco use. *Birth Defects Research*, *113*(16), 1198–1214. https://doi.org/10.1002/bdr2.1941

Kurrey, R., Saha, A., Sinha, S., Sahu, Y., Khute, M., Sahu, B., & Deb, M. K. (2022). Recent advances on analytical methodologies for screening and detection of biophenols and their challenges: A brief review. *Results in Chemistry*, *4*. https://doi.org/10.1016/j.rechem.2022.100456

Lalmuanpuii, R., and Muthukumaran, R. B. (2016). Vibrational spectroscopic characterization of tuibur: an indigenous nicotine delivery medium. *Sci Vis*, *16*(2), 53–58.

Lalmuanpuii, R. (2016). *RISK FACTORS OF TUMORIGENESIS IN TUIBUR CONSUMERS A Thesis submitted in partial fulfillment of the requirements for the degree of Doctor of Philosophy Department of Chemistry*.

Lalmuanpuii, R., Ghatak, S., Pautu, J. L., & Muthukumaran, R. B. (2015). *Mutation Profiling in Mitochondrial D-Loop Associated with Stomach Cancer Journal of Clinical & Medical Genomics Mutation Profiling in Mitochondrial D-Loop Associated with Stomach Cancer and Tobacco Consumers*. *October*. https://doi.org/10.4172/jcmg.1000122

Lalmuanpuii, R., & Muthukumaran, R. B. (2016). Fourier transform-infrared spectroscopic characterization of the particulate phase of commercial tuibur. *Science Vision*, *16*(2), 68–73.

Lalrammawia, K., Buragohain, A., Kakki, B., Zote, L., Marak, N. K., Lalrinhlupuii, Malsawmtluangi, Lalmuanpuii, R., Kumar, N. S., Jahau, L., Sudarshan, M., Chaligava, O., Yushin, N., Grozdov, D., Nekhoroshkov, P., Vergel, K., Zinicovscaia, I., & Muthukumaran, R. B. (2022). Determination of Multi Elements in Tobacco Plant of Northeast India by Neutron Activation Analysis and Atomic Absorption Spectrometry. *Biological Trace Element Research*, *200*(10), 4534–4549. https://doi.org/10.1007/s12011-021-03040-2

Lalruatfela, B., Zoremsiami, J., A., & Jagetia, C. G. (2020). Evaluation Of The Cytotoxic Effect Of Tuibur (Tobacco Brew) In Different Cultured Cell Lines. In *Journal of Translational Science and Research* (Vol. 2, Issue 1, pp. 1–5). https://doi.org/10.24966/tsr-6899/100005

Laytragoon-Lewin, N., Bahram, F., Rutqvist, L. E., Turesson, I., & Lewin, F. (2011). Direct effects of pure nicotine, cigarette smoke extract, Swedish-type smokeless tobacco (Snus) extract and ethanol on human normal endothelial cells and fibroblasts. *Anticancer Research*, *31*(5), 1527–1534.

Lewis, R. S., Parker, R. G., Danehower, D. A., Andres, K., Jack, A. M., Whitley, D. S., & Bush, L. P. (2012). Impact of alleles at the Yellow Burley (Yb) loci and nitrogen fertilization rate on nitrogen utilization efficiency and tobacco-specific nitrosamine (TSNA) formation in air-cured tobacco. *Journal of Agricultural and Food Chemistry*, *60*(25), 6454–6461. https://doi.org/10.1021/jf2053614

Linert, W., Bridge, M. H., Huber, M., Bjugstad, K. B., Grossman, S., & Arendash, G. W. (1999). In vitro and in vivo studies investigating possible antioxidant actions of nicotine: Relevance to Parkinson's and Alzheimer's diseases. *Biochimica et Biophysica Acta - Molecular Basis of Disease*, *1454*(2), 143–152. https://doi.org/10.1016/S0925-4439(99)00029-0

Liqun Wang, Stephen Stanfill, Liza Valentin-Blasini, Clifford H. Watson, R. B. C. (2019). LC-MS/MS Analysis of Sugars, Alditols, and Humectants in Smokeless Tobacco Products. *Beitr Tab Int.*, *28*(5), 203–213. https://doi.org/10.2478/cttr-2019-0001

Liu, K., Liu, P. cheng, Liu, R., & Wu, X. (2015). Dual AO/EB staining to detect apoptosis in osteosarcoma cells compared with flow cytometry. *Medical Science Monitor Basic Research*, *21*, 15–20. https://doi.org/10.12659/MSMBR.893327

Liubertas, T., Poderys, J. L., Zigmantaite, V., Viskelis, P., Kucinskas, A., Grigaleviciute, R., Jurevicius, J., & Urbonaviciene, D. (2023). The Effect of Potassium Nitrate Supplementation on the Force and Properties of Extensor digitorum longus (EDL) Muscles in Mice. *Nutrients*, *15*(6), 1–13. https://doi.org/10.3390/nu15061489

Lu, Y., Dong, Y., Li, X., & He, Q. (2016). The Nitrite-Scavenging Properties of Catechol, Resorcinol, and Hydroquinone: A Comparative Study on Their Nitration and Nitrosation Reactions. *Journal of Food Science*, *81*(11), C2692–C2696. https://doi.org/10.1111/1750-3841.13535

Lugon-Moulin, N., Martin, F., Krauss, M. R., Ramey, P. B., & Rossi, L. (2006). Cadmium concentration in tobacco (Nicotiana tabacum L.) from different countries and its relationship with other elements. *Chemosphere*, *63*(7), 1074–1086. https://doi.org/10.1016/j.chemosphere.2005.09.005

Mahanta, J., Chetia,M., Hazarika,N. C., Narain, K., and Sharma, S. K. (1998). Toxicity of tuibur, a unique form of tobacco smoke extract used in Mizoram, India. *Current Science*, *75*(4), 381–384.

Malakar, M., Devi, K. R., Phukan, R. K., Kaur, T., Deka, M., Puia, L., Barua, D., Mahanta, J., & Narain, K. (2012). Genetic polymorphism of glutathione s-transferases m1 and t1, tobacco habits and risk of stomach cancer in mizoram, india. *Asian Pacific Journal of Cancer Prevention*, *13*(9), 4725–4732. https://doi.org/10.7314/APJCP.2012.13.9.4725

Maldonado, E., Morales-Pison, S., Urbina, F., & Solari, A. (2023). Aging Hallmarks

and the Role of Oxidative Stress. *Antioxidants*, *12*(3), 1–37. https://doi.org/10.3390/antiox12030651

Malinovschi, A., Janson, C., Holmkvist, T., Norbäck, D., Meriläinen, P., & Högman, M. (2006). Effect of smoking on exhaled nitric oxide and flow-independent nitric oxide exchange parameters. *European Respiratory Journal*, *28*(2), 339–345. https://doi.org/10.1183/09031936.06.00113705

Mallock, N., Schulz, T., Malke, S., Dreiack, N., Laux, P., & Luch, A. (2022). Levels of nicotine and tobacco-specific nitrosamines in oral nicotine pouches. *Tobacco Control*, *33*(2), 193–199. https://doi.org/10.1136/tc-2022-057280

Marclay, F., & Saugy, M. (2010). Determination of nicotine and nicotine metabolites in urine by hydrophilic interaction chromatography-tandem mass spectrometry: Potential use of smokeless tobacco products by ice hockey players. *Journal of Chromatography A*, *1217*(48), 7528–7538. https://doi.org/10.1016/j.chroma.2010.10.005

María-Teresa Arango, Paula Quintero-Ronderos, John Castiblanco, and G. M.-O. (2013). Cell culture and cell analysis. In et al. Anaya JM, Shoenfeld Y, Rojas-Villarraga A (Ed.), *Autoimmunity: From Bench to Bedside*. El Rosario University Press. https://doi.org/10.1007/978-3-642-54596-2_200813

McCue, J. M., Link, K. L., Eaton, S. S., & Freed, B. M. (2000). Exposure to cigarette tar inhibits ribonucleotide reductase and blocks lymphocyte proliferation. *Journal of Immunology (Baltimore, Md.: 1950)*, *165*(12), 6771–6775. https://doi.org/10.4049/jimmunol.165.12.6771

McIlwain, D. R., Berger, T., & Mak, T. W. (2015). Caspase functions in cell death and disease. *Cold Spring Harbor Perspectives in Biology*, *7*(4). https://doi.org/10.1101/cshperspect.a026716

McKinney, D. L., & Vansickel, A. R. (2016). Nicotine Chemistry, Pharmacology, and Pharmacokinetics. In *Neuropathology of Drug Addictions and Substance Misuse Volume 1: Foundations of Understanding, Tobacco, Alcohol, Cannabinoids and Opioids* (Vol. 1). Elsevier Inc. https://doi.org/10.1016/B978-0-12-800213-1.00009-2

McKinnon, K. M. (2019). Flow cytometry: An overview. *Curr Protoc Immunol.*, *120*, 5.1.1–5.1.11. https://doi.org/10.1002/cpim.40.

Mesaik, M. A., Khalid, A., Abdalla, A. N., Sultana, S., Youssef, A. R., Ahmed, I. E., Mohammed, Y. I., Mirghani, H. O., Rehman, Z. U., Alhazmi, H. A., & Al Bratty, M. (2022). GC-MS and Cellular Toxicity Studies on Smokeless-Tobacco Show Alerting Cytotoxic effect on Human Gingiva and Lung Fibroblasts. *Journal of Spectroscopy*, *2022*. https://doi.org/10.1155/2022/4005935

Milnerowicz, H., Ściskalska, M., & Dul, M. (2015). Pro-inflammatory effects of metals in persons and animals exposed to tobacco smoke. In *Journal of Trace Elements in Medicine and Biology* (Vol. 29, pp. 1–10). Urban & Fischer. https://doi.org/10.1016/j.jtemb.2014.04.008

Mirabelli, P., Coppola, L., & Salvatore, M. (2019). Cancer cell lines are useful model

systems for medical research. *Cancers*, *11*(8). https://doi.org/10.3390/cancers11081098

Mizoram State E-Governance Society. (2021). History of Mizoram. In *A Government of Mizoram Undertaking* (pp. 1–14). https://rajbhavan.mizoram.gov.in/page/history-of-mizoram

Monks, T. J., & Lau, S. S. (1997). Biological Reactivity of Polyphenolic−Glutathione Conjugates. *Chemical Research in Toxicology*, *10*(12), 1296–1313. https://doi.org/10.1021/tx9700937

Murphy, M. P. (1999). Nitric oxide and cell death. *Biochimica et Biophysica Acta - Bioenergetics*, *1411*(2–3), 401–414. https://doi.org/10.1016/S0005-2728(99)00029-8

Muthukrishnan, A., & Warnakulasuriya, S. (2018). *Oral health consequences of smokeless tobacco use*. *July*, 35–40. https://doi.org/10.4103/ijmr.IJMR

Nair, J., Ohshima, H., Nair, U. J., & Bartsch, H. (1996). Endogenous formation of nitrosamines and oxidative DNA-damaging agents in tobacco users. *Critical Reviews in Toxicology*, *26*(2), 149–161. https://doi.org/10.3109/10408449609017928

National Center for Biotechnology Information. (2022a). *PubChem Compound Summary for CID 134694222*. PubChem. https://pubchem.ncbi.nlm.nih.gov/compound/5352425%0Ahttps://pubchem.ncbi.nlm.nih.gov/compound/134694222.

National Center for Biotechnology Information. (2022b). *PubChem Compound Summary for CID 25245913*. PubChem [Internet]. Bethesda (MD): National Library of Medicine (US). https://pubchem.ncbi.nlm.nih.gov/compound/Nornicotine

National Center for Biotechnology Information. (2023). *PubChem Compound Summary for CID 89594, Nicotine*.

Neal L. Benowitz, Janne Hukkanen, and P. J. I. (2009). Nicotine Chemistry, Metabolism, Kinetics and Biomarkers. *Handb Exp Pharmacol.*, *192*, 29–60. https://doi.org/10.1007/978-3-540-69248-5_2

Newman, M. B., Arendash, G. W., Shytle, R. D., Bickford, P. C., Tighe, T., & Sanberg, P. R. (2002). Nicotine's oxidative and antioxidant properties in CNS. *Life Sciences*, *71*(24), 2807–2820. https://doi.org/10.1016/S0024-3205(02)02135-5

NFHS5. (2021). *Fact Sheets Key Indicators, 22 STATES/UTs FROM PHASE - I National Family Health Survey (NFHS-5) 2019-20*.

Novotny, T. E., Bialous, S. A., Burt, L., Curtis, C., da Costa, V. L., Iqtidar, S. U., Liu, Y., Pujari, S., & D'Espaignet, E. T. (2015). Impacts environnementaux et sanitaires de la culture du tabac, de la fabrication de cigarettes et de leur consummation. *Bulletin of the World Health Organization*, *93*(12), 877–880. https://doi.org/10.2471/BLT.15.152744

Pang, T., Bai, C., Xu, Y., Xu, G., Yuan, Z., Su, Y., & Peng, L. (2006). Determination

of sugars in tobacco leaf by HPLC with evaporative light scattering detection. *Journal of Liquid Chromatography and Related Technologies*, *29*(9), 1281–1289. https://doi.org/10.1080/10826070600598993

Papke, R. L., Dwoskin, L. P., & Crooks, P. A. (2007). The pharmacological activity of nicotine and nornicotine on nAChRs subtypes: Relevance to nicotine dependence and drug discovery. *Journal of Neurochemistry*, *101*(1), 160–167. https://doi.org/10.1111/j.1471-4159.2006.04355.x

Park, S. J., Lim, H. S., Lee, K., & Yoo, S. J. (2018). Green Tobacco Sickness Among Tobacco Harvesters in a Korean Village. *Safety and Health at Work*, *9*(1), 71–74. https://doi.org/10.1016/j.shaw.2017.06.007

Patil, S., & Baeshen, H. A. (2021). Aqueous extract of tobacco induces mitochondrial potential dependent cell death and epithelial-mesenchymal transition in gingival epithelial cells. *Saudi Journal of Biological Sciences*, *28*(8), 4613–4618. https://doi.org/10.1016/j.sjbs.2021.04.068

Peace, B. E., & Succop, P. (1999). Spontaneous micronucleus frequency and age: what are normal values? *Mutation Research/Fundamental and Molecular Mechanisms of Mutagenesis*, *425*(2), 225–230. https://doi.org/10.1016/S0027-5107(99)00030-5

Peluffo, G., Calcerrada, P., Piacenza, L., Pizzano, N., & Radi, R. (2009). Superoxide-mediated inactivation of nitric oxide and peroxynitrite formation by tobacco smoke in vascular endothelium: Studies in cultured cells and smokers. *American Journal of Physiology - Heart and Circulatory Physiology*, *296*(6). https://doi.org/10.1152/ajpheart.00930.2008

Perfetti, T. A., & Rodgman, A. (2011). The complexity of Tobacco and Tobacco Smoke. *Beitrage Zur Tabakforschung International/ Contributions to Tobacco Research*, *24*(5), 215–232. https://doi.org/10.2478/cttr-2013-0902

Phukan, R. K., Zomawia, E., Narain, K., Hazarika, N. C., & Mahanta, J. (2005). Tobacco use and stomach cancer in Mizoram, India. *Cancer Epidemiology Biomarkers and Prevention*, *14*(8), 1892–1896. https://doi.org/10.1158/1055-9965.EPI-05-0074

Pinzaru, I., Chioibas, R., Marcovici, I., Coricovac, D., Susan, R., Predut, D., Georgescu, D., & Dehelean, C. (2021). Rutin exerts cytotoxic and senescence-inducing properties in human melanoma cells. *Toxics*, *9*(9). https://doi.org/10.3390/toxics9090226

Pisarcik, S., Luke, T., Nelin, L. D., & Shimoda, L. A. (2008). Nicotine causes depolarization, decreased intracellular calcium concentration ([Ca2+]i) and reduced nitric oxide (NO) production in human umbilical artery endothelial cells (HUAECs). *The FASEB Journal*, *22*(S1), 1196.6-1196.6. https://doi.org/https://doi.org/10.1096/fasebj.22.1_supplement.1196.6

Pizzino, G., Irrera, N., Cucinotta, M., Pallio, G., Mannino, F., Arcoraci, V., Squadrito, F., Altavilla, D., & Bitto, A. (2017). Oxidative Stress: Harms and Benefits for Human Health. *Oxidative Medicine and Cellular Longevity*, *2017*. https://doi.org/10.1155/2017/8416763

Planchet, E., Gupta, K. J., Sonoda, M., & Kaiser, W. M. (2005). Nitric oxide emission from tobacco leaves and cell suspensions: Rate limiting factors and evidence for the involvement of mitochondrial electron transport. *Plant Journal*, *41*(5), 732–743. https://doi.org/10.1111/j.1365-313X.2005.02335.x

Pollio, A., Zarrelli, A., Romanucci, V., Mauro, A. Di, Barra, F., Pinto, G., Crescenzi, E., Roscetto, E., & Palumbo, G. (2016). Polyphenolic profile and targeted bioactivity of methanolic extracts from mediterranean ethnomedicinal plants on human cancer cell lines. *Molecules*, *21*(4). https://doi.org/10.3390/molecules21040395

Pyror, W. A. (1992). Biological effects of cigarette smoke, wood smoke, and the smoke from plastics: The use of electron spin resonance. *Free Radical Biology and Medicine*, *13*(6), 659–676. https://doi.org/10.1016/0891-5849(92)90040-N

Raimondi, S., Garte, S., Sram, R. J., Binkova, B., Kalina, I., Lyubomirova, K., Taioli, E., Singh, R., & Farmer, P. B. (2007). Effects of diet on biomarkers of exposure and effects, and on oxidative damage. *Mutation Research - Fundamental and Molecular Mechanisms of Mutagenesis*, *620*(1–2), 93–102. https://doi.org/10.1016/j.mrfmmm.2007.02.027

Ramage, L., Jones, A. C., & Whelan, C. J. (2006). Induction of apoptosis with tobacco smoke and related products in A549 lung epithelial cells in vitro. *Journal of Inflammation*, *3*, 1–11. https://doi.org/10.1186/1476-9255-3-3

Rao, N. R., & Snyder, R. (1995). Oxidative modifications produced in HL-60 cells on exposure to benzene metabolites. *Journal of Applied Toxicology*, *15*(5), 403–409. https://doi.org/10.1002/jat.2550150511

Regassa, G., & Chandravanshi, B. S. (2016). Levels of heavy metals in the raw and processed Ethiopian tobacco leaves. *SpringerPlus*, *5*(1), 1–9. https://doi.org/10.1186/s40064-016-1770-z

Riss, T. L., Moravec, R. A., Niles, A. L., Duellman, S., Benink, H. A., Worzella, T. J., & Minor, L. (2004). Cell Viability Assays. In *Assay Guidance Manual* (Issue Md, pp. 1–25). http://www.ncbi.nlm.nih.gov/pubmed/23805433

Robert M. Silverstein, F. X. W. and D. J. Ki. (2005). *Spectrometric Identification of Organic Compounds* (Vol. 7, p. 72). https://doi.org/10.1021/jm00342a059

Robertson, G. S., LaCasse, E. C., & Holcik, M. (2009). Programmed Cell Death. In *Pharmacology: Principles and Practice* (pp. 455–473). Academic Press. https://doi.org/10.1016/B978-0-12-369521-5.00018-X

Roh, J. S., & Sohn, D. H. (2018). Origin and List of DAMPS. *Immune Network*, *18*(4), 1–14.

Sachin S Devi and Harihara M Mehendale. (2005). Quinone. In *Encyclopedia of Toxicology* (Second Edi, Issue April). Elsevier. https://doi.org/10.1016/B0-12-369400-0/00827-9

Saeidnia, S., & Abdollahi, M. (2013). Toxicological and pharmacological concerns on oxidative stress and related diseases. *Toxicology and Applied Pharmacology*, *273*(3), 442–455. https://doi.org/10.1016/j.taap.2013.09.031

Sanchez-Ramos, J. R. (2020). The rise and fall of tobacco as a botanical medicine. In *Journal of Herbal Medicine* (Vol. 22, Issue January). https://doi.org/10.1016/j.hermed.2020.100374

Sanderson, M. J., Smith, I., Parker, I., & Bootman, M. D. (2014). Fluorescence microscopy. *Cold Spring Harbor Protocols*, *2014*(10), 1042–1065. https://doi.org/10.1101/pdb.top071795

Sanjay Gupta, Ruchika Gupta, Dhirendra N. Sinha, R. M. (2018). Relationship between type of smokeless tobacco & risk of cancer: A systematic review. *Indian Journal of Medical Research*, *148*, 56–76. https://doi.org/10.4103/ijmr.IJMR_2023_17

Sanjeev, S. (2019). *Evaluation of diosgenin and tobacco smoke infused water on ovarian function in mice*. Mizoram university.

Schorderet Weber, S., Kaminski, K. P., Perret, J. L., Leroy, P., Mazurov, A., Peitsch, M. C., Ivanov, N. V., & Hoeng, J. (2019). Antiparasitic properties of leaf extracts derived from selected Nicotiana species and Nicotiana tabacum varieties. *Food and Chemical Toxicology*, *132*(June), 110660. https://doi.org/10.1016/j.fct.2019.110660

Shahbandeh, M. (2023). *World tobacco production by country 2021 | Statista*. Statista. https://www.statista.com/statistics/261173/leading-countries-in-tobacco-production/

Sharifi-Rad, M., Anil Kumar, N. V., Zucca, P., Varoni, E. M., Dini, L., Panzarini, E., Rajkovic, J., Tsouh Fokou, P. V., Azzini, E., Peluso, I., Prakash Mishra, A., Nigam, M., El Rayess, Y., Beyrouthy, M. El, Polito, L., Iriti, M., Martins, N., Martorell, M., Docea, A. O., … Sharifi-Rad, J. (2020). Lifestyle, Oxidative Stress, and Antioxidants: Back and Forth in the Pathophysiology of Chronic Diseases. *Frontiers in Physiology*, *11*(July), 1–21. https://doi.org/10.3389/fphys.2020.00694

Sharma, A., Patil, J. A., Gramajo, A. L., Seigel, G. M., Kuppermann, B. D., & Kenney, C. M. (2012). Effects of hydroquinone on retinal and vascular cells in vitro. *Indian Journal of Ophthalmology*, *60*(3), 189–193. https://doi.org/10.4103/0301-4738.95869

Shen, C.-H. (2023). Quantification and analysis of proteins. *Diagnostic Molecular Biology*, 231–257. https://doi.org/10.1016/B978-0-323-91788-9.00002-8

Shin, V. Y., Jin, H. C., Ng, E. K. O., Yu, J., Leung, W. K., Cho, C. H., & Sung, J. J. Y. (2008). Nicotine and 4-(methylnitrosamino)-1-(3-pyridyl)-1-butanone induce cyclooxygenase-2 activity in human gastric cancer cells: Involvement of nicotinic acetylcholine receptor (nAChR) and β-adrenergic receptor signaling pathways. *Toxicology and Applied Pharmacology*, *233*(2), 254–261. https://doi.org/10.1016/j.taap.2008.08.012

Shwetha, S., Chandra Sekhara Reddy, V., Sudhir, K. M., Krishna Kumar, R. V. S., & Srinivasulu, G. (2018). Influence of tobacco chewing and smoking on the salivary total antioxidant power-a clinical comparative study. *Journal of Clinical and Diagnostic Research*, *12*(6), ZC09-ZC12.

https://doi.org/10.7860/JCDR/2018/30278.11677

Sies, H. (2019). Oxidative stress: Eustress and distress in redox homeostasis. In *Stress: Physiology, Biochemistry, and Pathology Handbook of Stress Series, Volume 3* (pp. 153–163). Academic Press. https://doi.org/10.1016/B978-0-12-813146-6.00013-8

Sies, H. (2020). Oxidative stress: Concept and some practical aspects. *Antioxidants*, *9*(9), 1–6. https://doi.org/10.3390/antiox9090852

Sigma-Aldrich and ECACC. (2018). Cell Types & Culture Characteristics. In *Fundamental Techniques in Cell Culture, Laboratory Handbook* (pp. 12–14). https://www.sigmaaldrich.com/GB/en/technical-documents/technical-article/cell-culture-and-cell-culture-analysis/mammalian-cell-culture/cell-types-culture%0Ahttps://www.sigmaaldrich.com/technical-documents/protocols/biology/cell-types-culture.html

Siminszky, B., Gavilano, L., Bowen, S. W., & Dewey, R. E. (2005). Conversion of nicotine to nornicotine in Nicotiana tabacum is mediated by CYP82E4, a cytochrome P450 monooxygenase. *Proceedings of the National Academy of Sciences of the United States of America*, *102*(41), 14919–14924. https://doi.org/10.1073/pnas.0506581102

Sinha, D. N., Suliankatchi, R. A., Gupta, P. C., Thamarangsi, T., Agarwal, N., Parascandola, M., & Mehrotra, R. (2018). Global burden of all-cause and cause-specific mortality due to smokeless tobacco use: Systematic review and meta-analysis. *Tobacco Control*, *27*(1), 35–42. https://doi.org/10.1136/tobaccocontrol-2016-053302

Sisson, V., & Severson, R. (1990). Alkaloid Composition of the Nicotiana Species. *Contributions to Tobacco & Nicotine Research*, *14*(6), 327–339. https://doi.org/10.2478/cttr-2013-0610

Snyder, R., & Hedli, C. C. (1996). An overview of benzene metabolism. *Environmental Health Perspectives*, *104*(SUPPL. 6), 1165–1171. https://doi.org/10.1289/ehp.96104s61165

Stanfill, S. B., Connolly, G. N., Zhang, L., Jia, L. T., Henningfield, J. E., Richter, P., Lawler, T. S., Ayo-Yusuf, O. A., Ashley, D. L., & Watson, C. H. (2011). Global surveillance of oral tobacco products: Total nicotine, unionised nicotine and tobacco-specific N-nitrosamines. *Tobacco Control*, *20*(3), 1–10. https://doi.org/10.1136/tc.2010.037465

Stanfill, S. B., Croucher, R. E., Gupta, P. C., Lisko, J. G., Lawler, T. S., Kuklenyik, P., Dahiya, M., Duncan, B., Kimbrell, J. B., Peuchen, E. H., & Watson, C. H. (2018). Chemical characterization of smokeless tobacco products from South Asia: Nicotine, unprotonated nicotine, tobacco-specific N′-Nitrosamines, and flavor compounds. *Food and Chemical Toxicology*, *118*, 626–634. https://doi.org/10.1016/j.fct.2018.05.004

Stanfill, S. B., Hecht, S. S., Joerger, A. C., González, P. J., Maia, L. B., Rivas, M. G., Moura, J. J. G., Gupta, A. K., Le Brun, N. E., Crack, J. C., Hainaut, P., Sparacino-Watkins, C., Tyx, R. E., Pillai, S. D., Zaatari, G. S., Henley, S. J., Blount, B. C.,

Watson, C. H., Kaina, B., & Mehrotra, R. (2023). From cultivation to cancer: formation of N-nitrosamines and other carcinogens in smokeless tobacco and their mutagenic implications. *Critical Reviews in Toxicology*, *53*(10), 658–701. https://doi.org/10.1080/10408444.2023.2264327

Stedman, R. L. (1968). The chemical composition of tobacco and tobacco smoke. *Chemical Reviews*, *68*(2), 153–207. https://doi.org/10.1021/cr60252a002

Stepanov, I., Gupta, P. C., Dhumal, G., Yershova, K., Toscano, W., Hatsukami, D., & Parascandola, M. (2015). High levels of tobacco-specific N-nitrosamines and nicotine in Chaini Khaini, a product marketed as snus. *Tobacco Control*, *24*(e4), e271–e274. https://doi.org/10.1136/tobaccocontrol-2014-051744

Stepanov, I., Hecht, S. S., Ramakrishnan, S., & Gupta, P. C. (2005). Tobacco-specific nitrosamines in smokeless tobacco products marketed in India. *International Journal of Cancer*, *116*(1), 16–19. https://doi.org/10.1002/ijc.20966

Stephen B. Stanfill, André Luiz Oliveira da Silva, Joseph G. Lisko, Tameka S. Lawler, Peter Kuklenyik, Robert E. Tyx, Elizabeth H. Peuchen, P. R. and C. H. W. (2015). Comprehensive Chemical Characterization of Rapé Tobacco Products: Nicotine, Un-ionized Nicotine, Tobacco-specific N'- Nitrosamines, Polycyclic Aromatic Hydrocarbons, and Flavor Constituents. *Food Chem Toxicol.*, *82*, 50–58. https://doi.org/10.1016/j.fct.2015.04.016.

Sun, J., Zhang, X., Broderick, M., Fein, H., Instruments, W. P., & International, S. (2003). Measurement of Nitric Oxide Production in Biological Systems by Using Griess Reaction Assay. *Sensors*, *3*, 276–284. http://www.mdpi.net/sensors

Supriya, K., Chaudhary, J., & Shamal, S. N. (2017). Oxidative stress in cigarette smoker and smokeless tobacco user among ethnic group north-eastern population of Uttar Pradesh, India. *International Journal of Research in Medical Sciences*, *5*(4), 1439. https://doi.org/10.18203/2320-6012.ijrms20171242

Suzuki, H., Iijima, K., Scobie, G., Fyfe, V., & McColl, K. E. L. (2005). Nitrate and nitrosative chemistry within Barrett's oesophagus during acid reflux. *Gut*, *54*(11), 1527–1535. https://doi.org/10.1136/gut.2005.066043

Tan, X., Vrana, K., & Ding, Z. M. (2021). Cotinine: Pharmacologically Active Metabolite of Nicotine and Neural Mechanisms for Its Actions. *Frontiers in Behavioral Neuroscience*, *15*(October), 1–15. https://doi.org/10.3389/fnbeh.2021.758252

Thuy le, T. T., Thuy, T. T. V., Hai, H., & Kawada, N. (2017). Role of Oxidative and Nitrosative Stress in Hepatic Fibrosis. *Liver Pathophysiology: Therapies and Antioxidants*, 213–224. https://doi.org/10.1016/B978-0-12-804274-8.00016-3

Trédaniel, J., Boffetta, P., Buiatti, E., Saracci, R., & Hirsch, A. (1997). Tobacco smoking and gastric cancer: Review and meta-analysis. *International Journal of Cancer*, *72*(4), 565–573. https://doi.org/10.1002/(SICI)1097-0215(19970807)72:4<565::AID-IJC3>3.0.CO;2-O

Tricker, A. R., Haubner, R., Spiegelhalder, B., & Preussmann, R. (1988). The occurrence of tobacco-specific nitrosamines in oral tobacco products and their

potential formation under simulated gastric conditions. *Food and Chemical Toxicology*, *26*(10), 861–865. https://doi.org/10.1016/0278-6915(88)90027-0

Tsikas, D. (2007). Analysis of nitrite and nitrate in biological fluids by assays based on the Griess reaction: Appraisal of the Griess reaction in the l-arginine/nitric oxide area of research. *Journal of Chromatography B*, *851*(1–2), 51–70. https://doi.org/10.1016/J.JCHROMB.2006.07.054

Tso, T. C. (1972). Physiology and biochemistry of tobacco plants. In *Plant Biotechnology Journal* (Vol. 13, Issue 8). Stroudsburg, Pa., USA, Dowden, Hutchinson & Ross, Inc.

U.S. Department of Health and Human Services. (2010). How Tobacco Smoke Causes Disease: The Biology and Behavioral Basis for Smoking-Attributable Disease. In *How Tobacco Smoke Causes Disease: The Biology and Behavioral Basis for Smoking-Attributable Disease: A Report of the Surgeon General*.

Upadhyay, M., Verma, P., Sabharwal, R., Subudhi, S., Jatol-Tekade, S., Naphade, V., Choudhury, B., & Sahoo, P. (2019). Micronuclei in exfoliated cells: A biomarker of genotoxicity in tobacco users. *Nigerian Journal of Surgery*, *25*(1), 52. https://doi.org/10.4103/njs.NJS_10_18

Uriarte, I., Pérez, C., Caballero-Mancebo, E., Basterretxea, F. J., Lesarri, A., Fernández, J. A., & Cocinero, E. J. (2017). Structural Studies of Nicotinoids: Cotinine versus Nicotine. *Chemistry - A European Journal*, *23*(30), 7238–7244. https://doi.org/10.1002/chem.201700023

Valavanidis, A., Vlachogianni, T., & Fiotakis, K. (2009). Tobacco smoke: Involvement of reactive oxygen species and stable free radicals in mechanisms of oxidative damage, carcinogenesis and synergistic effects with other respirable particles. *International Journal of Environmental Research and Public Health*, *6*(2), 445–462. https://doi.org/10.3390/ijerph6020445

Vayssier, M., Banzet, N., François, D., Bellmann, K., & Polla, B. S. (1998). Tobacco smoke induces both apoptosis and necrosis in mammalian cells: Differential effects of HSP70. *American Journal of Physiology - Lung Cellular and Molecular Physiology*, *275*(4 19-4), 771–779. https://doi.org/10.1152/ajplung.1998.275.4.l771

Vermes, I., & Haanen, C. (1994). Apoptosis and Programmed Cell Death in Health and Disease. *Advances in Clinical Chemistry*, *31*(C), 177–246. https://doi.org/10.1016/S0065-2423(08)60336-4

Wald, N. J., & Hackshaw, A. K. (1996). Cigarette smoking: an epidemiological overview. *British Medical Bulletin*, *52*(1), 3–11. https://doi.org/10.1093/oxfordjournals.bmb.a011530

Wang, H. Y., Shin, V. Y., Leung, S. Y., Yuen, S. T., & Cho, C. H. (2003). Involvement of bcl-2 and Caspase-3 in Apoptosis Induced by Cigarette Smoke Extract in the Gastric Epithelial Cell. *Toxicologic Pathology*, *31*(2), 220–226. https://doi.org/10.1080/01926230390183715

Wang, J., Yang, H., Shi, H., Zhou, J., Bai, R., Zhang, M., & Jin, T. (2017). Nitrate and

Nitrite Promote Formation of Tobacco-Specific Nitrosamines via Nitrogen Oxides Intermediates during Postcured Storage under Warm Temperature. *Journal of Chemistry*, *2017*. https://doi.org/10.1155/2017/6135215

Wolk, R., Shamsuzzaman, A. S. M., Svatikova, A., Huyber, C. M., Huck, C., Narkiewicz, K., & Somers, V. K. (2005). Hemodynamic and autonomic effects of smokeless tobacco in healthy young men. *Journal of the American College of Cardiology*, *45*(6), 910–914. https://doi.org/10.1016/j.jacc.2004.11.056

World Health organisation. (2017). Tobacco and its environmental impact: an overview. In *International Review of Psychiatry* (Vol. 34, Issue 1). http://dx.doi.org/10.1016/j.ccm.2013.09.011

World Health Organisation. (2013). *Word No Tobacco Day: Fact Sheet*. *August*, 2011–2013. https://www.who.int/docs/default-source/campaigns-and-initiatives/world-no-tobacco-day-2020/wntd-tobacco-fact-sheet.pdf

World Health Organisation. (2021). *WHO global report on trends in prevalence of tobacco use Fourth edition* (Fourth edi). Geneva: World Health Organization; 2021. Licence: CC BY-NC-SA 3.0 IGO.

World Health Organization. (2024). *WHO global report on trends in prevalence of tobacco use 2000 – 2030* (Licence: C).

Worsfold, P. (2005). SPECTROPHOTOMETRY / Overview SPECTROPHOTOM. In *Encyclopedia of Analytical Science (Second Edition)* (pp. 318–321). https://doi.org/10.1016/B0-12-369397-7/00714-7

Wu, J., Rickert, W. S., Masters, A., & Joza, P. (2012). Determination of N-nitrososarcosine in tobacco and smokeless tobacco products using isotope dilution liquid chromatography tandem mass spectrometry. *Analytical Methods*, *4*(10), 3448–3452. https://doi.org/10.1039/c2ay25540e

Xu, E. G., Richardot, W. H., Li, S., Buruaem, L., Wei, H. H., Dodder, N. G., Schick, S. F., Novotny, T., Schlenk, D., Gersberg, R. M., & Hoh, E. (2019). Assessing Toxicity and in Vitro Bioactivity of Smoked Cigarette Leachate Using Cell-Based Assays and Chemical Analysis. *Chemical Research in Toxicology*, *32*(8), 1670–1679. https://doi.org/10.1021/acs.chemrestox.9b00201

Yajima, T., Yu, Y., & Futamata, M. (2012). Flocculation and SERS activation of au nanoparticles using cationic and neutral cresyl violet molecules. *E-Journal of Surface Science and Nanotechnology*, *10*(August), 417–425. https://doi.org/10.1380/ejssnt.2012.417

Yamamoto, H., Shibuya, K., Fukushima, T., & Hashizume, T. (2022). Effects of antioxidant capacity on micronucleus induction by cigarette smoke in mammalian cells. *Mutation Research/Genetic Toxicology and Environmental Mutagenesis*, *873*, 503427. https://doi.org/10.1016/J.MRGENTOX.2021.503427

Yao, W., Yu, L., Fan, W., Shi, X., Liu, L., Li, Y., Qin, X., Rao, C., & Wang, J. (2019). A cell-based strategy for bioactivity determination of long-acting Fc-fusion recombinant human growth hormone. *Molecules*, *24*(7). https://doi.org/10.3390/molecules24071389

Yu Chun Hong, Suriguga, Li Yang, Li Yi Ran, Tang Ke Ya, Jiang Liang, and Y. Z. C. (2014). *The Role of ROS in Hydroquinone-induced Inhibition of K562 Cell Erythroid Differentiation*. *27*(3), 212–214. https://doi.org/10.3967/ bes2014.043

Zaini, R., Clench, M. R., & Le Maitre, C. L. (2011). Bioactive chemicals from carrot (daucus carota) juice extracts for the treatment of leukemia. *Journal of Medicinal Food*, *14*(11), 1303–1312. https://doi.org/10.1089/jmf.2010.0284

Zenkner, F. F., Margis-Pinheiro, M., & Cagliari, A. (2019). Nicotine Biosynthesis in Nicotiana : A Metabolic Overview . *Tobacco Science*, *56*(1), 1–9. https://doi.org/10.3381/18-063

Zhang, H., Pang, Y., Luo, Y., Li, X., Chen, H., Han, S., Jiang, X., Zhu, F., Hou, H., & Hu, Q. (2018). Enantiomeric composition of nicotine in tobacco leaf, cigarette, smokeless tobacco, and e-liquid by normal phase high-performance liquid chromatography. *Chirality*, *30*(7), 923–931. https://doi.org/10.1002/chir.22866

Zhang, L., Liu, B., Zhou, L., Cai, Y., Guo, W., Huang, W., Yan, X., & Chen, H. (2022). Analysis of occupational stress and its correlation with oxidative-antioxidant levels among employees of a power grid enterprise in Guangdong. *BMC Psychiatry*, *22*(1), 1–14. https://doi.org/10.1186/s12888-022-04226-1

Zhang, Q., Ganapathy, S., Avraham, H., Nishioka, T., & Chen, C. (2020). Nicotine exposure potentiates lung tumorigenesis by perturbing cellular surveillance. *British Journal of Cancer*, *122*(6), 904–911. https://doi.org/10.1038/s41416-020-0730-0

Zhang, W. Z., Venardos, K., Chin-Dusting, J., & Kaye, D. M. (2006). Adverse effects of cigarette smoke on no bioavailability: Role of arginine metabolism and oxidative stress. *Hypertension*, *48*(2), 278–285. https://doi.org/10.1161/01.HYP.0000231509.27406.42

Zhang, X. Y., Tan, Y. L., Zhou, D. F., Haile, C. N., Wu, G. Y., Cao, L. Y., Kosten, T. A., & R. Kosten, T. (2007). Nicotine dependence, symptoms and oxidative stress in male patients with schizophrenia. *Neuropsychopharmacology*, *32*(9), 2020–2024. https://doi.org/10.1038/sj.npp.1301317

Zhao, J., Qiao, L., Shang, P., Hua, C., Xie, Y., Li, X., Ding, M., Liu, K., Guo, J., Zhao, G., Wang, S., Liu, H., & Xie, F. (2021). Effects of smokeless tobacco on cell viability, reactive oxygen species, apoptosis, and inflammatory cytokines in human umbilical vein endothelial cells. *Toxicology Mechanisms and Methods*, *31*(5), 349–358. https://doi.org/10.1080/15376516.2021.1876800

Zhao, S., Smith, K. S., Deveau, A. M., Dieckhaus, C. M., Johnson, M. A., Macdonald, T. L., & Cook, J. M. (2002). Biological activity of the tryprostatins and their diastereomers on human carcinoma cell lines. *Journal of Medicinal Chemistry*, *45*(8), 1559–1562. https://doi.org/10.1021/jm0155953

Zhu, A. Z. X., Renner, C. C., Hatsukami, D. K., Swan, G. E., Lerman, C., Benowitz, N. L., & Tyndale, R. F. (2013). The ability of plasma cotinine to predict nicotine and carcinogen exposure is altered by differences in cyp2a6: The influence of genetics, race, and sex. *Cancer Epidemiology Biomarkers and Prevention*, *22*(4), 708–718. https://doi.org/10.1158/1055-9965.EPI-12-1234-T

Zi, Y., Wang, X., Zi, Y., Yu, H., Lan, Y., Fan, Y., Ren, C., Liao, K., & Chen, H. (2023). Cigarette smoke induces the ROS accumulation and iNOS activation through deactivation of Nrf-2/SIRT3 axis to mediate the human bronchial epithelium ferroptosis. *Free Radical Biology and Medicine*, *200*, 73–86. https://doi.org/10.1016/J.FREERADBIOMED.2023.03.002

BIO-DATA

1. NAME : Lalrinhlupuii

2. DATE OF BIRTH : 4th May, 1990

3. FATHER'S NAME : Vanlalchama

4. PERMANENT ADDRESS : Châltlâng, Aizawl, Mizoram

5. EMAIL ADDRESS : crisralte@gmail.com

6. EDUCATIONAL QUALIFICATIONS :

Examination passed	Year of Passing	Board/University	Division	% of marks	Subjects
HSLC	2007	Mizoram Board of School Education	D	80.6	Linguistics, Mathematics, Science, Social Sciences
HSSLC	2009	Mizoram Board of School Education	I	63.8	Linguistics, Biology, Physics, Chemistry, Mathematics
B.Sc (Chemistry)	2012	Mizoram University	I	72.6	Chemistry, Botany, Zoology
M. Sc (Chemistry)	2014	North-Eastern Hill University	I	61.55	Chemistry

List Of Publications

(A) Journals:

1. Dharaben J. Joshi, **Lalrinhlupuii**, Naved I. Malek, Rajendra Bose Muthukumaran and Suresh Kumar Kailasa (2022). Microwave-Assisted Synthesis of Red Emitting Copper Nanoclusters Using Trypsin as a Ligand for Sensing of Pb^{2+} And Hg^{2+} Ions in Water and Tobacco Samples. *Applied Spectroscopy*, 76(10), 1234-1245. DOI: 10.1177/00037028221100544.
2. Priya Bhowmick[#], **Lalrinhlupuii**[#], Rajendra Bose Muthukumaran, Pritha Bhattacharjee (2021). Food Diversity among Northeast Population: Resource of nutraceuticals to Risk factors for Disease Susceptibility. Food Culture, Health and Sustainability: A New Paradigm. 15. *Upanayan Publications, Delhi*. Madhurima Chowdhury and Animesh Manna. ISBN: 978-93-91467-30-2. *([#] share equal first author contribution).*
3. L Zote, K Lalrammawia, A Buragohain, **Lalrinhlupuii**, B Kakki, R Lalmuanpuii, Z Pachuau, J Vanlalhruaia, Rajendra B Muthukumaran*****, N Senthil Kumar, L Jahau, M Sudarshan, N Yushin, P Nekhoroshkov, D Grozdov, A Sergeeva, Inga Zinicovscaia (2021). Macro-, micro-, and trace element distributions in arecanut, husk, and soil of northeast India, *Enviro. Monit. Assess*. 193(2):65. DOI: 10.1007/s10661-021-08859-9. PMID: 33449210
4. K Lalrammawia, A Buragohain, B Kakki, L Zote, N K Marak, **Lalrinhlupuii**, Malsawmtluangi, R Lalmuanpuii, RB Muthukumaran, N Senthil Kumar, L Jahau, M Sudarshan, O Chaligava, N Yushin, D Grozdov, P Nekhoroshkov, K Vergel, I Zinicovscaia, (2021). Determination of Multi Elements in Tobacco Plant of Northeast India by Neutron Activation Analysis and Atomic Absorption Spectrometry. *Biol. Trace Elem. Res*. DOI: 10.1007/s12011-021-03040-2. PMID: 34820780

(B) Conferences/Symposiums:

1. **Lalrinhlupuii** and Rajendra Bose Muthukumaran. Evaluation of Adverse Oral Health Effects of Indigenous Smokeless Tobacco Products Use. *Proceedings of The International Conference on Chemistry and Environmental Sustainability* (ICCES – 2019), 19th to 22nd February, 2019, Department of Chemistry, Mizoram University, Aizawl, Mizoram, India.
2. **Lalrinhlupuii.** Characterization of Indigenous Tobacco Product (Tuibur) of Mizoram. *Proceedings of School on "Know Your Elements"* (KYE – 2019), 4th to 10th August, 2019, Chemical Sciences Division, Saha Institute of Nuclear Physics, Kolkata, West Bengal, India.
3. **Lalrinhlupuii,** Lalbiaktluanga, Rajendra Bose Muthukumaran, H. H. Thanga. Multivariate Analysis of Selected Chemical Constituents in Tuibur using ATR-FTIR Spectroscopy. *Proceedings of The National Symposium on "Recent Trends in Chemistry* (RTC – 2019), 31st October to 1st November, 2019, Department of Chemistry, Centre for Advanced Studies, North Eastern Hill University, Shillong, Meghalaya, India.
4. **Lalrinhlupuii**, S. Sarathbabu, N. Senthil Kumar, M. Vabeiryureilai, R. Muthukumaran. In vitro exposure to tuibur: A cytotoxicity Study. *Proceedings of The International Conference on Recent Advances in Animal Sciences* (ICRAAS-2019), 6th to 8th November, 2019, Department of Zoology, Pachhunga University College, Aizawl, Mizoram, India.

PARTICULARS OF THE CANDIDATE

NAME OF CANDIDATE : Lalrinhlupuii

DEGREE : Doctor of Philosophy (Ph.D.)

DEPARTMENT : Chemistry

TITLE OF THESIS : Oxidative stress effects of an indigenous tobacco product (*Tuibur*): An *in vitro* study.

DATE OF ADMISSION : 11th August, 2016

APPROVAL OF RESEARCH PROPOSAL :

1. BOS : 2nd May, 2017

2. SCHOOL BOARD : 15th May, 2017

3. MZU REGN. NO. : 1506941

4. Ph.D. REGN. NO. & DATE : MZU/Ph.D./1007 of 15.05.2017

5. EXTENSION : 1) No.16-2/MZU(Acad)/21/70-71
Dt. 25th February, 2022
2) No.16-2/ MZU(Acad)/24/14-15
Dt. 3rd July, 2024

Head

Department of Chemistry

ABSTRACT

OXIDATIVE STRESS EFFECTS OF AN INDIGENOUS TOBACCO PRODUCT (*TUIBUR*): *AN IN VITRO STUDY*

AN ABSTRACT SUBMITTED IN PARTIAL FULFILLMENT OF THE REQUIREMENTS FOR THE DEGREE OF DOCTOR OF PHILOSOPHY

LALRINHLUPUII

MZU REGISTRATION NO. : 1506941

Ph.D. REGISTRATION NO. : MZU/Ph.D./1007 OF 15.05.2017

DEPARTMENT OF CHEMISTRY

SCHOOL OF PHYSICAL SCIENCES

FEBRUARY, 2025

OXIDATIVE STRESS EFFECTS OF AN INDIGENOUS TOBACCO PRODUCT (*TUIBUR*): *AN IN VITRO STUDY*

BY

LALRINHLUPUII

Department of Chemistry

Under the supervision of

Prof. MUTHUKUMARAN R.

and joint-supervision of

Prof. G. GURUSUBRAMANIAN

Department of Zoology

Submitted

In partial fulfillment of the requirement of the Degree of Doctor of Philosophy in Chemistry of Mizoram University, Aizawl.

ABSTRACT

Originating from the Northeastern state of Mizoram, India, traditionally tuibur is a part of the cultural heritage of the Mizo people. As a tobacco-smoke infused liquid preparation, tuibur lacks comparable analogous products. Tobacco stalk, petioles, vein and lamina considered otherwise as tobacco waste is imported from Myanmar and serves as the raw material. A makeshift hydro-powered aspirator allows for dispensing tobacco smoke into an alkaline feedstock (water percolated through ash) and thereby generating the resultant product, tuibur. Depending on the amount of tobacco used as well as alkalinity of tuibur, it is locally graded into 'Al' and 'Al lo'. Normally tuibur is sipped, retained in the lower buccal space of the mouth (yet occasionally unintentionally also swallowed) and discarded after its alkalinity has been spent. There are numerous quality and health concerns related to tuibur use, aside from tobacco-related health impacts.

Characterization of and grading tuibur based on nicotine contents in tuibur was attempted by performing three different kinds of analytical methods. Firstly, the use of Attenuated Total Reflectance Fourier-transform Infrared Spectroscopy (ATR - FTIR) paired with multivariate analysis using chemometrics enables the assessment of target analytes present in a mixture. Using this semi-quantitative method, three chemical constituents of tobacco smoke varying polarities, viz., nicotine, hydroquinone and benzoquinone, were analysed in tuibur samples to discern the variance of different grades of tuibur. Though this method could predict the probable concentrations of each chemical within the tuibur samples, it was incapable of qualitatively differentiating the grades of tuibur based on the amount of nicotine present in each sample more likely due to the inherent limitations of FTIR methods for the evaluation of a mixture of constituents with similar polarities present in the aqueous solutions.

Secondly, Surface-enhanced Raman Spectroscopy (SERS) is an analytical technique complementary to ATR-FTIR with high sensitivity in molecule detection owing to its signal enhancement ability in presence of nanoscale metallic particles. Gold nanoparticles were synthesized and utilized for the semi-quantitative evaluation of nicotine in different grades of tuibur samples using SERS methods. The SERS peak

intensity of the purchased standard S(-)-nicotine sample displayed a characteristic vibrational band at 1030 cm^{-1} (for a pyridine-based alkaloid) which was selected to assess the nicotine concentrations, the predominant alkaloid present in tobacco products like tuibur. The same peak was observed with different intensities in each of the analysed tuibur samples. The peak intensities for each sample were determined and the grade of tuibur was categorized based on nicotine concentration levels with respect to the amount of tobacco used during preparation. The SERS method could evidently differentiate various grades of tuibur in a semi-quantitative manner, wherein nicotine concentrations (or nicotine peak intensity) were observed to be increasing corresponding to the amount of tobacco used for tuibur samples. This method provided a better classification to assess different grades of tuibur albeit in a semi-quantitative manner, by probing the nicotine contents in tuibur.

In order to gain a better understanding of the grading of tuibur, for the determination of tobacco alkaloids, nicotine and cotinine in various grades of tuibur samples, Liquid-Chromatography tandem Mass Spectrometry (LC-MS/MS) methods were utilised. In general, LC-MS/MS methods are aptly suitable for determining selected target analytes in a heterogenous mixture. Multiple reaction monitoring (MRM) allows for the identification and quantification of chemical compounds with high accuracy owing to its' better selectivity and high sensitivity aspects, both the parent and daughter ions for the quantification of desired polar chemical constituents in an alkaline solution. The determination of concentration levels of nicotine ranged between 569 to 1877 µg/mL and the concentration of cotinine ranged between 6.5 to 44.4 µg/mL in different grades of tuibur was successfully accomplished by using internal calibration LC-MS/MS methods. This robust and sensitive analysis also revealed that the concentration of both nicotine and cotinine increased as the amount of tobacco increased for the preparation of tuibur. Therefore, the analysed tuibur samples could be categorized into specific grades, in a more reliable and convincing manner, depending on their nicotine concentration levels.

To examine the biological activity of tuibur, a variety of biological assays were performed. For the preliminary assessment of DNA damage due to tuibur use, micronuclei formation in buccal cells of tuibur consumers, sahdah consumers and tobacco non-user was assessed within the Mizo population. This study revealed that

tuibur consumers have increased micronuclei formations as compared to that of sahdah users as well as tobacco non-users. These results indicated that chronic tuibur exposure via repeated tuibur use can be a major risk factor for DNA damage with signs of chromosomal instability.

To study the toxicological effects of tuibur at the cellular level, gastric adenocarcinoma (AGS) cell lines was chosen as a model system. 3-(4, 5-dimethylthiazol -2-yl)-2',5'-diphenyltetrazolium bromide (MTT) test was performed to assess the purported cytotoxicity of tuibur on AGS cells. AGS cells were exposed to varying concentrations of tuibur, nicotine, hydroquinone, KNO_3 and $NaNO_2$ and incubated for 24, 48 and 72 hrs. Tuibur and hydroquinone were observed to inflict a dose and time-dependent diminished cell viability as well as proliferation of AGS cells. Low concentrations of nicotine exposure displayed moderate proliferative effects on AGS cell lines indicating induced cell proliferation. KNO_3 was observed to stimulate a concentration and time-dependent proliferative effect on AGS cells. The data for the treatment of AGS cells with $NaNO_2$ produce non-specific and inconclusive results. MTT studies revealed that tuibur and hydroquinone are highly cytotoxic even at low doses.

Apoptosis was assessed in AGS cells by exposure of IC_{50} concentrations of tuibur, nicotine, hydroquinone and KNO_3 via dual acridine orange and ethidium bromide staining and the associated fluorescence microscopy studies. The results indicated a lower degree of apoptosis in untreated cells when compared to the treatment groups. Tuibur and nicotine exposed AGS cells showed highest apoptotic cell counts among the treatment groups indicating the genotoxicity of tuibur in AGS.

Reactive nitrogen species (RNS) were evaluated in AGS cell line exposed to IC_{50} concentrations of tuibur, nicotine, hydroquinone and KNO_3 by Griess assay. The oxidative assay revealed a decrease in nitrite levels for all the treatment groups in comparison to untreated cells indicating that RNS formation may not be inducing the purported oxidative stress. Nevertheless, a decrease in nitrite level may indicate tuibur-related suppression of nitric oxide (NO) production, disrupting normal cellular functions plausibly causing potential damage to the cellular functions.

Oxidative stress was evaluated by the total antioxidant capacity (TAC) assay on AGS cells exposed to IC_{50} concentrations of tuibur, nicotine, hydroquinone and KNO_3. When treated with tuibur, hydroquinone and KNO_3 a decreased TAC was observed, demonstrating an 'induced' imbalance of free radicals and antioxidants in the AGS cells. However, nicotine showed increased TAC, insinuating nicotine's potential antioxidant effects at low concentrations that corroborate with the cell proliferation on AGS cells due to nicotine exposure. Therefore, tuibur exposure on AGS cells promotes free radicals or reactive oxygen species (ROS) formation imposing unpleasant side effects of oxidative stress that engender the cellular damage.

The assessment of relative ROS levels in AGS cells treated with IC_{50} concentrations of tuibur, nicotine, hydroquinone and KNO_3 was performed by using DCF-DA fluorescent dye combined with flow cytometry methods. However, according to the flow cytometry study, in contrast to the TAC assay methods, an increase in ROS for nicotine exposed AGS cells whereas in other treatment groups a decrease in ROS generation relative to untreated AGS cells were observed. Though a large body of scientific studies implicate the elevation of ROS levels in cells due to the aqueous extracts of tobacco products (smoked or smokeless), our results failed to explain the observed results that needed more detailed investigations.

Tuibur's cultural nostalgia and cost factor are compelling determinants for its users to retain the habit though less convincing health warnings are displayed on its packages, recently. As a heterogenous mixture, tuibur is comprised of heavy element species (factors for oxidative stress and DNA damage), tobacco specific alkaloids (TSAs), tobacco-specific nitrosamines (TSNAs) and other organic and inorganic constituents of which some are proven group 1 and group 2 carcinogens. Indigenous and unique tobacco use habits of Mizo tribal population engender a challenging and complex public health problem. The present research highlights the detrimental health effects of tuibur consumption and demands for devising proper regulatory standard protocols in order to spread and maintain an improved awareness among its consumers, especially the relatively less-literate rural as well as suburban populace.